

# **Investigation of upstream and downstream events in CERK1-mediated signaling in plant immunity**

**Dissertation**

der Mathematisch-Naturwissenschaftlichen Fakultät  
der Eberhard Karls Universität Tübingen  
zur Erlangung des Grades eines  
Doktors der Naturwissenschaften  
(Dr. rer. nat.)

vorgelegt von  
Xiao Kun Liu  
aus  
Anhui, China

Tübingen

2015

Tag der mündlichen Qualifikation:

16.07.2015

Dekan:

Prof. Dr. Wolfgang Rosenstiel

1. Berichterstatter:

Prof. Dr. Thorsten Nürnberger

2. Berichterstatter:

Dr. Andrea Gust

## Table of contents

<b>1. Introduction.....</b>	<b>1</b>
<b>1.1 Origin and evolution of plant immunity concepts.....</b>	<b>1</b>
1.1.1 Plant and microbe interactions.....	1
1.1.2 Immunity in animals and plants.....	1
1.1.3 History of plant immunity.....	3
<b>1.2 The plant immune system.....</b>	<b>4</b>
1.2.1 The three-layer-defence in plants.....	4
1.2.2 Plant PTI: PAMPs and pattern-recognition receptors.....	5
1.2.3 Plant ETI.....	7
1.2.4 Signal transduction in plant immunity.....	8
<b>1.3 Chitinases in plant immunity.....</b>	<b>9</b>
1.3.1 Chitinases.....	9
1.3.2 Role of chitinases in plant defence.....	10
<b>1.4 Peptidoglycan and its receptors as example for a PAMP-PRR pair.....</b>	<b>11</b>
1.4.1 Peptidoglycan.....	11
1.4.2 PGN perception systems.....	12
<b>1.5 From microbial complex structures to PAMPs.....</b>	<b>14</b>
1.5.1 Generation of PAMPs through spontaneous release.....	15
1.5.2 Generation of PAMPs through host hydrolytic enzymes.....	15
<b>1.6 Aims of the thesis.....</b>	<b>16</b>
<b>2. Materials and Methods.....</b>	<b>17</b>
<b>2.1. Materials.....</b>	<b>17</b>
2.1.1. Plants.....	17
2.1.1.1. <i>Arabidopsis thaliana</i> .....	17
2.1.1.2. <i>Nicotiana benthamiana</i> and <i>Oryza sativa</i> .....	17
2.1.2. Microbes.....	18
2.1.3. Media and buffers.....	19
2.1.4. Vectors.....	20
2.1.5. Enzymes and antibodies.....	21
2.1.6. Chemicals and solutions.....	21
2.1.7. Oligonucleotides.....	22
2.1.8. PAMPs.....	22
<b>2.2. Methods.....</b>	<b>22</b>
2.2.1. Plant growth.....	22
2.2.1.1. Growth conditions.....	22
2.2.1.2. Seed sterilization.....	23

2.2.1.3. Cell cultures.....	23
2.2.2. Microbe cultivation.....	23
2.2.2.1. Growth of <i>Escherichia coli</i> .....	23
2.2.2.2. Growth of <i>Pseudomonas syringae</i> .....	23
2.2.2.3. Growth of <i>Agrobacterium tumefaciens</i> .....	23
2.2.3. Molecular biology.....	24
2.2.3.1. Isolation of plasmid DNA from <i>E.coli</i> .....	24
2.2.3.2. Genomic DNA isolation from plant.....	25
2.2.3.3. Total RNA isolation from <i>Arabidopsis</i> seedling.....	25
2.2.3.4. Complementary DNA synthesis.....	26
2.2.3.5. Standard PCR.....	26
2.2.3.6. DNA agarose gel electrophoresis.....	26
2.2.3.7. Sequencing.....	26
2.2.3.8. Quantitative fluorescent real time PCR.....	27
2.2.3.9. Restriction endonuclease digestion.....	27
2.2.3.10. Isolation of DNA fragments from agarose gels.....	27
2.2.3.11. DNA ligation.....	27
2.2.3.12. Gateway cloning.....	27
2.2.3.13. Preparation and transformation of chemically competent <i>E.coli</i> cells.....	28
2.2.3.14. Preparation and transformation of electrical competent cells of <i>A. tumefaciens</i> .....	29
2.2.4. Plant methods.....	30
2.2.4.1. Isolation of mesophyll protoplasts from <i>Arabidopsis</i> .....	30
2.2.4.2. Stable transformation of <i>Arabidopsis thaliana</i> .....	30
2.2.4.3. Transient transformation of <i>Nicotiana benthamiana</i> .....	30
2.2.4.4. Generation of knock-down lines.....	31
2.2.4.5. Genotyping analysis of T-DNA insertion lines.....	31
2.2.5. Protein biochemistry.....	32
2.2.5.1. Protein extraction from plant tissue.....	32
2.2.5.2. Immunoprecipitation.....	32
2.2.5.3. LYS1 purification.....	33
2.2.5.4. Transient expression and co-immunoprecipitation.....	33
2.2.5.5. Determination of protein concentration.....	34
2.2.5.6. SDS-PAGE.....	34
2.2.5.7. Coomassie Brilliant Blue staining.....	34
2.2.5.8. Western blot analysis.....	34
2.2.5.9. CTAB western blotting.....	35
2.2.5.10. MAPK kinase assay.....	35
2.2.5.11. Turbidity assay (PGN-hydrolysis assay).....	35

2.2.5.12. 4-MUC cellulose assay.....	36
2.2.5.13. 4-MUCT assay (Chitin-hydrolysis assay).....	36
2.2.5.14. Zymogram.....	36
2.2.5.15. HPLC analysis of PGN fragments.....	37
2.2.6. Bioassay.....	37
2.2.6.1. Infection with <i>Pseudomonas syringae</i> .....	37
2.2.6.2. Elicitation assays in leaves or seedlings.....	38
2.2.6.3. Medium alkalization assay.....	39
2.2.6.4. Oxidative burst assay.....	39
2.2.7. Microscopy.....	39
2.2.8. Statistical analysis.....	39
<b>3. Results.....</b>	<b>41</b>
<b>3.1 Identification of an <i>Arabidopsis</i> PGN hydrolase.....</b>	<b>41</b>
3.1.1 An induced PGN-degrading activity is not due to PGN receptors LYM1 and LYM3 in <i>Arabidopsis</i> .....	41
3.1.2 Identification of LYS1 as a potential PGN hydrolase.....	43
3.1.3 Expression of epitope-tagged LYS1 and identification of active LYS1.....	45
3.1.4 Purification of active LYS1 using FPLC.....	55
<b>3.2 Characterization of LYS1.....</b>	<b>56</b>
3.2.1 LYS1 is a bifunctional enzyme with lysozyme- and chitinase-activity.....	56
3.2.2 Enzyme Kinetics of LYS1.....	58
3.2.3 LYS1 localizes to the apoplast.....	59
<b>3.3 Role of LYS1 in the generation of immunogenic PGN fragments.....</b>	<b>60</b>
3.3.1 LYS1 generates plant immunogenic PGN fragments.....	60
3.3.2 LYS1-overdigested PGN induces weaker immunity responses.....	62
<b>3.4 LYS1 is required for immune responses to PGN.....</b>	<b>63</b>
3.4.1 Characterization of <i>LYS1</i> <sup>KD</sup> lines.....	63
3.4.2 Lack of LYS1 PGN-degrading activity dampens plant immunity.....	66
3.4.3 LYS1 is able to decompose <i>PtoDC3000</i> cells but does not inhibit their growth.....	68
<b>3.5 Identification of a CERK1-interacting calcium-dependent protein kinase.....</b>	<b>70</b>
3.5.1 Identification of putative CERK1 interactors from a Y2H database.....	70
3.5.2 Analysis of M.I.N.D.-interactors for CERK1.....	72
<b>3.6 CPK15 is involved in the CERK1-mediated PTI pathway.....</b>	<b>74</b>
3.6.1 Characterization of <i>CPK15</i> T-DNA insertion lines.....	74
3.6.2 <i>cpk15-1</i> produces less ROS in response to complex or soluble chitin.....	75
3.6.3 Chitin-induced activation of MAPK is not affected in <i>cpk15-1</i> .....	76
3.6.4 CPK15 localizes to the plasma membrane.....	77
3.6.5 CERK1 physically interacts with CPK15.....	79

<b>3.7 Characterization of knockdown lines of <i>CPK15</i> and <i>CPK15/21/23</i>.....</b>	<b>80</b>
3.7.1 Structure and classification of Arabidopsis CDPKs.....	80
3.7.2 Characterization of artificial microRNA lines of <i>CPK15</i> , <i>CPK21</i> and <i>CPK23</i> .....	81
<b>4. Discussion.....</b>	<b>83</b>
4.1 <i>LYS1</i> is involved in the apoplastic battle between plants and pathogens.....	83
4.2 <i>LYS1</i> is involved in plant inducible defence.....	86
4.3 <i>LYS1</i> is a bifunctional Lysozyme/chitinase.....	88
4.4 How does <i>LYS1</i> contribute to defence: direct killing or generating PAMPs?.....	90
4.5 Dynamics of <i>LYS1</i> protein levels are related to immunity performance.....	92
4.6 Known signaling components in CERK1-mediated immunity.....	94
4.7 CDPKs in plant immunity.....	95
<b>5. Summary.....</b>	<b>98</b>
<b>6. Zusammenfassung.....</b>	<b>99</b>
<b>7. Reference.....</b>	<b>100</b>
<b>8. Appendix.....</b>	<b>113</b>
<b>9. Acknowledgement .....</b>	<b>115</b>
<b>10. Curriculum vitae.....</b>	<b>116</b>

List of figures

Figure 1 Bacterial PAMPs induce lysozyme-like activities in *Arabidopsis*.....42

Figure 2 LYM1 and LYM3 do not possess PGN hydrolytic activity.....43

Figure 3. Protein sequence alignment of the 24 *Arabidopsis* chitinases and cartoon diagram of the 3D structure of LYS1.....44

Figure 4. Analysis of LYS1 protein levels in *LYS1<sup>OE</sup>* lines.....46

Figure 5. Isolation and analysis of LYS1-GFP via immunoprecipitation (IP).....47

Figure 6. CTAB-PAGE zymography and immunoblot analysis of extracts of *LYS<sup>OE</sup>* plants and *N. benthamiana* transiently expressing LYS1-GFP.....49

Figure 7. Transiently expressed LYS1 is a glucan hydrolase.....50

Figure 8. Analysis of the activity of transiently expressed LYS1.....52

Figure 9. Isolation and identification of active LYS1 transiently expressed in *N. benthamiana*.....53

Figure 10. Isolation and analysis of LYS1-myc and LYS1-HA via immunoprecipitation (IP).....54

Figure 11. FPLC purification of active LYS1 from *LYS1<sup>OE</sup>* .....56

Figure 12. Purified LYS1 from *LYS1<sup>OE</sup>* has glucan-hydrolase activity.....57

Figure 13. LYS1 is devoid of cellulose hydrolytic activity.....58

Figure 14. LYS1 is localized to the apoplast.....59

Figure 15. Purified LYS1 generates immunogenic PGN fragments.....61

Figure 16. Analysis of *LYS1* knockdown lines.....64

Figure 17. Determination of putative *LYS1* amiRNA off-targets.....65

Figure 18. Manipulation of *LYS1* levels causes a loss of PGN-triggered immune responses.....66

Figure 19. *LYS1* overexpression does not affect PGN receptor expression.....67

Figure 20. Impact of weak *LYS1* overexpression.....68

Figure 21. LYS1 can digest bacteria cells and inhibit bacterial growth.....69

Figure 22. Gene models and genotyping of T-DNA insertion mutants of three putative CERK1 interactors.....72

Figure 23. Screening analysis of T-DNA mutants of *PK*, *CIPK7* and *CPK15* in a ROS oxidative burst assay.....74

Figure 24. Morphological phenotypes of *cpk15-1* T-DNA insertion lines.....75

Figure 25. Determination of ROS accumulation in *cpk15-1* mutant plants.....76

Figure 26. Chitin induced MAPK activation is not impaired in the *cpk15-1* mutant.....77

Figure 27. Subcellular localization of the CPK15-YFP fusion protein.....78

Figure 28. CERK1 physically interacts with CPK15.....79

Figure 29. Structure and subfamilies of *Arabidopsis* CDPKs.....80

Figure 30. Generation of *CPK15* single and *CPK15/21/23* triple knockdown lines.....82

**List of tables**

Table 1. *Arabidopsis* mutantS and transgenic lines used in this study.....17

Table 2. Bacterial strains used in this work.....18

Table 3. Media used in this study.....19

Table 4. Antibiotics used in this study.....20

Table 5. Vectors in this study.....20

Table 6. Antibodies used in this study.....21

Table 7. Putative CERK1 interacting proteins identified from the Membrane-based Interactome Network Database (M.I.N.D. 0.5).....71

Table 8. Oligonucleotides used in this study.....113

## Abbreviations

<b>amiRNA</b>	Artificial micro RNA
<b>At</b>	<i>Arabidopsis thaliana</i>
<b>AtDORN1</b>	Arabidopsis does not respond to nucleotides 1
<b>AtWAK1</b>	Arabidopsis wall-associated kinase 1
<b>Avr gene</b>	Avirulence gene
<b>BAK1</b>	BRI1-associated kinase 1
<b>BRI1</b>	Brassinosteroid insensitive 1
<b>BiFC</b>	Bimolecular fluorescence complementation
<b>cDNA</b>	Complementary DNA
<b>C(D)PK</b>	Calcium-dependent protein kinase
<b>Cfu</b>	Colony forming unit
<b>DAMP</b>	Damage-associated molecular pattern
<b>DNA</b>	Deoxyribonucleic acid
<b>ECD</b>	Extracellular domain
<b>EF1a</b>	Elongation factor 1a
<b>EFR</b>	Elongation factor-Tu receptor
<b>EGF</b>	Epidermal growth factor
<b>EF-TU</b>	Elongation factor-Tu
<b>ETI</b>	Effector triggered immunity
<b>ETS</b>	Effector-triggered susceptibility
<b>FLS2</b>	Flagellin-sensing 2
<b>FPLC</b>	Fast protein liquid chromatography
<b>FRK1</b>	Flagellin responsive kinase 1
<b>GFP</b>	Green fluorescent protein
<b>GlcNAc</b>	N-acetylglucosamine
<b>GNBP1</b>	Gram-negative bacteria-derived binding protein 1

<b>HPLC</b>	High performance liquid chromatography
<b>HR</b>	Hypersensitive response
<b>HRP</b>	Horseradish peroxidase
<b>KD</b>	Kinase domain
<b>kDa</b>	KiloDalton
<b>LORE</b>	Lipooligosaccharide-specific reduced elicitation
<b>LPS</b>	Lipooligosaccharide
<b>LRR</b>	Leucine rich repeat
<b>LYS1</b>	Lysozyme-like enzyme 1
<b>LysM</b>	Lysin motif
<b>MAPK</b>	Mitogen-activated protein kinase
<b>MbSUS</b>	Mating-based split ubiquitin system
<b>MDP</b>	Muramyl dipeptide
<b>MIMP</b>	Microbe-associated molecular patterns
<b>MIND</b>	Membrane-based interactome network database
<b>MurNAc</b>	N-Acetylmuramic acid
<b>NASC</b>	Nottingham Arabidopsis stock center
<b>NOD</b>	Nucleotide-binding oligomerization domain-containing protein
<b>PAMP</b>	Pathogen-associated molecular pattern
<b>Peptidoglycan</b>	PGN
<b>PGRP</b>	PGN-recognition protein
<b>PR protein</b>	Pathogenesis-related protein
<b>PRR</b>	Pattern recognition receptor
<b>PTI</b>	PAMP-triggered immunity
<b>Pto</b>	<i>Pseudomonas syringae</i> pv. <i>tomato</i>
<b>R gene</b>	Resistance gene
<b>RFP</b>	Red fluorescent protein

<b>RLK</b>	Receptor-like kinases
<b>RLP</b>	Receptor-like protein
<b>RNA</b>	Ribonucleic acid
<b>ROS</b>	Reactive oxygen species
<b>RT-qPCR</b>	Reverse transcription quantitative PCR
<b>SAR</b>	Systemic acquired resistance
<b>SOBIR1</b>	Suppressor of <i>bir1</i>
<b>T-DNA</b>	Transfer DNA
<b>TLR2</b>	Toll-like receptor 2
<b>WT</b>	Wild type
<b>YFP</b>	Yellow fluorescent protein

# 1. Introduction

## 1.1 Origin and evolution of plant immunity concepts

### 1.1.1 Plant and microbe interactions

The advent of the earliest land plants around 480 million years ago is one of the most important evolutionary events in the history of life on Earth (Gehrig et al., 1996). During their establishment in terrestrial ecosystems, land plants have had to adapt to an environment that houses a large variety of microbes such as fungi, oomycetes, bacteria, and viruses. From then on, if not earlier, plants and microbes have had continual interaction, and this interplay has been influencing the evolution of both plants and microbes (Wang et al., 2010).

The interplay of plants and microbes has led to a wide range of relationships in which one or both of the organisms may have a beneficial, neutral or negative effect on the other partner. These diverse plant-microbe interactions have been broadly classified into three categories from the plant perspective: beneficial, detrimental or neutral interaction (Schenk et al., 2012).

Most plant-microbe interactions have neutral effects on plants. These “neutral” microbes often utilize plant derived organic compounds as energy sources, and thus play important roles in nutrient cycling and modification of environments. Many microbes are beneficial for plants and promote growth or suppress diseases via a number of mechanisms, including improved nutrient acquisition, production of growth regulators, and biosynthesis of pathogen-inhibiting compounds (Schenk et al., 2012). Microbes that are harmful to plants are much fewer, although more noticeable, such as plant pathogenic fungi, oomycetes, bacteria and viruses that can potentially cause diseases in plants. The outcome of these plant–microbe interactions are further influenced by wounding, herbivores and abiotic stress factors such as salinity, drought, temperature (Thaler et al., 1999; Cheong et al., 2002; Berg, 2009).

### 1.1.2 Immunity in animals and plants

To respond appropriately to diverse microbes, plants have evolved abilities to distinguish self from non-self and friends from enemies. With this distinction, plants can adapt to

their environment by either activating immune responses to defend against pathogens or initiating symbiosis signaling to facilitate the accommodation of symbionts.

The last common ancestor of plants and animals is thought to have lived approximately one billion years ago, which may explain dramatic differences in structures and lifestyles between plants and animals. The differences made biologists initially believe that plants and animals defend against microbial pathogens in separate and distinct ways (Ronald and Beutler, 2010). For example, vertebrates have developed two types of immunity, innate and adaptive immunity, to defend against microbial invaders (Medzhitov and Janeway, 2002; McGuinness et al., 2003). Adaptive immunity in vertebrate animals is mediated by a clonal system of T lymphocytes and B lymphocytes, and is characterized by the creation of antigen-specific receptors through somatic recombination in maturing lymphocytes, and this system does not exist in plants. Moreover, specialized cell types such as macrophages, neutrophils, and dendritic cells, which as parts of a circulatory blood system are the key players of the animal immune system, are not found in plants either. In contrast, each plant cell is autonomously capable of sensing the presence of microbial infection and of mounting defence responses (Nürnberger et al., 2004).

Despite the well-documented differences, increasing evidences over the past twenty years have revealed striking structural and strategic similarities in the immune systems of plants and animals (Nürnberger and Brunner, 2002b). For instance, both are able to respond to microbial signature molecules using analogous regulatory modules. Pathogen-associated molecular patterns (PAMP) that are similar to those activating innate immune responses in animals have been shown to trigger the activation of plant defence. Moreover, recognition complexes that are structurally related to animal PAMP receptors are now being discovered in plants (Nürnberger and Brunner, 2002a).

The remarkable similarities of the innate immune systems between animal and plant raise an intriguing issue: Did an ancient ancestor common to plants and animals evolve a basic innate immune system, one that began to differ in the two lineages once they split (divergent evolution)? Or did plants and animals evolve innate immunity independently but ended up with similar mechanisms (convergent evolution)? Comparative analyses of innate immune systems in plants and animals, based on

significantly broad data sets, may provide a basis to address this issue more precisely in the future.

### 1.1.3. History of plant immunity

Although plant diseases were mentioned as early as 750 BCE in the Hebrew Bible, it was not until 1853 that De Bary discovered that rust and smut fungi were causal agents of certain diseases in cereal crops (Agrios, 2005). The first description of a genetic relationship between host plants and their pathogens was in the early 1940s by Harold Flor, based on genetic investigation of flax and the flax rust fungus, and the investigation lead to the “gene-for-gene hypothesis” in 1946 (Flor, 1971). The hypothesis proposed that the ability of fungal pathogens to cause disease was controlled by two matching genes: an avirulence (Avr) gene from the pathogen and a matching resistance (R) gene from the host. This hypothesis was a theoretical breakthrough in plant pathology and led to practical advances in plant breeding.

Flor’s model presumed that specific sensors for microbial molecules, termed elicitors, or Avr gene products, were present in immunocompetent hosts. In the 1980s an intense hunt for the genes encoding these receptors and their corresponding elicitors, based on biochemical approaches, identified specific binding sites for elicitors in intact plant cells and on isolated plasma membranes, but failed to purify the expected receptors (Boller, 1995).

In the 1990s, an avalanche of genetic experiments led to the isolation of the first R genes and, subsequently, more R genes from multiple plant species (Martin et al., 1993). These discoveries established that diverse molecules and mechanisms govern the resistance phenotypes described by Flor, and that the resistance response was more complex than previously realized.

A philosophical divergence between geneticists, who isolated R genes, and biochemists, who identified general elicitors, lead to two schools of thought: microbial elicitor-induced plant non cultivar-specific defence and microbial avirulence factor-induced plant cultivar-specific defence. The divergence raised a debate whether the elicitor-induced defence responses were physiologically relevant to plant immunity and what the relationship

between the gene-for-gene resistance and the elicitor-induced defence would be. Since the first elicitor receptor (Gomez-Gomez and Boller, 2000) was identified, the debate has given way to the idea that two types of defence both contribute to plant immunity in an integrated fashion. A simple and elegant view of innate immunity in plant pathogen interactions is depicted by the so-called zigzag model, introduced by Jones and Dangl, providing an integrated model for plant disease resistance (Jones and Dangl, 2006).

### **1.2 The plant immune system**

Plants, unlike animals, are sessile organisms and cannot escape from environmental threats such as biotic and abiotic stresses. Instead, plants have evolved a wide range of mechanisms to cope with these biotic and abiotic stresses for survival. Biotic stresses result from surrounding living organisms such as microbes, parasites, herbivores and other plants. Of these biotic stress factors, phytopathogenic microbes frequently and seriously threaten food security and thus are overwhelmingly focused on by scientists.

#### **1.2.1 The three-layer-defence in plants**

Resistances of plants to phytopathogens have been described as three broad layers relevant to pathogens' foliar infection strategies and plant counter-defensive responses (Senthil-Kumar and Mysore, 2013). Upon landing on the surface of a plant, a potential microbial pathogen initially encounters the first plant defence layer that restricts pathogen entry. This step usually involves preformed defence, such as a wax layers, rigid cell walls, cuticular lipids (Reina-Pinto and Yephremov, 2009), antimicrobial enzymes or secondary metabolites (Ahuja et al., 2012; Bednarek, 2012), as well as inducible defence, such as stomatal closure (Melotto et al., 2006). Pathogens that overcome this surface defence layer encounter a second layer of defence in the apoplastic region. This step also involves preformed defence, such as the presence of antimicrobial compounds, coupled with overall apoplastic physiological incompatibility and induced defence, such as phytoalexin production (Dixon et al., 2002; Ham et al., 2007; Hann and Rathjen, 2007; Huckelhoven, 2007). The pathogens that successfully break through the first two layers of defence must finally face a third layer of defence at and inside the plant cell. This defence layer involves two inducible interconnected

mechanisms: pathogen-associated molecular pattern (PAMP)-triggered immunity (PTI) and effector-triggered immunity (ETI). Both PTI and ETI are induced by pathogen-generated stimuli and regulate the protective responses of plants against pathogens in synergistic and antagonistic ways (Jones and Dangl, 2006).

### **1.2.2 Plant PTI: PAMPs and pattern-recognition receptors**

Activation of plant PTI depends on the perception of invariant structures of mostly pathogen surfaces, formerly known as “general elicitors” (Boller, 1995). These invariant pathogen structures are named as pathogen-associated molecular patterns (PAMPs) (Medzhitov and Janeway, 1997). PAMPs are highly conserved molecular patterns across a wide range of pathogens but are not present in the host and thus enable hosts to distinguish self and non-self (Medzhitov and Janeway, 2002; Akira et al., 2006). PAMPs include (poly)peptides, glycoproteins, lipids, and oligosaccharides, which are essential for microbial fitness and survival (Nürnbergger et al., 2004). Classical PAMPs are exemplified by eubacterial flagellin, elongation factor-Tu (EF-Tu), peptidoglycans (PGNs), oomycete glucans, and fungal chitin (Sharp et al., 1984; Cheong et al., 1991; Felix et al., 1993; Felix et al., 1999; Zipfel et al., 2004; Zipfel et al., 2006; Gust et al., 2007). As PAMP molecules are found not only in pathogenic microbes but also non-pathogenic microorganisms (Ausubel, 2005), in the recent literature more correct terms have therefore been introduced, such as MAMPs (microbe-associated molecular patterns) (Ausubel, 2005) or MIMPs (microbe-induced molecular patterns) (Mackey and McFall, 2006). While these terms have their merits and justification, using the ‘historical’ term PAMPs allows for better understanding among researchers in animal and plant immunity (Nürnbergger and Kemmerling, 2009), and therefore in this thesis I will follow this suggestion.

In addition to microbial PAMPs, the structural barriers of plant tissues can be degraded by the lytic enzymes of plant pathogens, releasing products such as plant cell wall fragments (Darvill and Albersheim, 1984), cutin monomers (Kauss et al., 1999) and peptides (Boller, 2005; Huffaker et al., 2006), all of which can function as endogenous elicitors called damage-associated molecular patterns (DAMPs). These DAMPs

characteristically emerge in the apoplast and serve as danger signals to induce innate immunity similar to PAMPs (Henry et al., 2012).

Plant PTI relies on the perception of PAMPs by plant cell surface-localized pattern recognition receptors (PRRs). All known plant PRRs are plasma membrane-localized receptor-like kinases (RLKs) or receptor-like proteins (RLPs) with modular functional domains. RLKs contain an extracellular domain (ECD), a single-pass transmembrane (TM) domain, and an intracellular kinase domain (KD), whereas RLPs include an ECD and a TM but lack the intracellular KD (Monaghan and Zipfel, 2012). Typically, small epitopes within PAMPs provide ligands for PRR receptors. Various receptor types mediate pattern recognition that differ in extracellular ligand-binding domains, membrane embedding and intracellular cytoplasmic domains (Böhm et al., 2014). Structural biochemistry has recently highlighted ligand induced immune receptor complex formation as a common principle in pattern binding and cytoplasmic signal transduction (Böhm et al., 2014).

The first major class of PRRs is leucine-rich repeat receptor kinases/proteins (LRR-RLKs/RLPs). LRR-RLKs contain a leucine-rich repeat (LRR) ectodomain, which can bind to proteinaceous immunogenic patterns (Zhang and Thomma, 2013). For example, flagellin-sensing 2 (FLS2) recognizes a 22-amino acid epitope (flg22) conserved in bacterial flagellins (Zipfel et al., 2004) and EF-Tu receptor (EFR) perceives the first 18 amino acids (elf18) of bacterial EF-Tu (Zipfel et al., 2006). These LRR-RLKs form heterodimeric complexes with the Brassinosteroid-insensitive 1 (BRI1)-associated kinase 1 (BAK1), a LRR-RLK, in a ligand dependent manner. Likewise, LRR-RLP receptors that lack intracellular kinase domains also form heteromeric complexes with different LRR-RK-type co-receptors such as BAK1 or suppressor of bir1 (SOBIR1), in a ligand-dependent manner as well (Jehle et al., 2013; Zhang et al., 2013; Zhang et al., 2014).

Lysin motif (LysM)-type immune receptor, a second major class of PRRs, mediates recognition of N-acetylglucosamine (GlcNAc)-containing carbohydrate ligands. For example, bacterial PGN recognition in *Arabidopsis* involves two LysM-RLPs (AtLYM1/3) and one LysM-RLK (Chitin elicitor receptor-like kinase 1, CERK1) (Gust et al., 2007).

Similarly, the chitin perception in *Arabidopsis* also involves one LysM-RLK (CERK1) and one kinase-inactive LysM-RLK (LYK5) (Miya et al., 2007; Liu et al., 2012b; Cao et al., 2014) and in rice similar perception systems for PGN and chitin have been described (Kaku et al., 2006; Liu et al., 2012a; Hayafune et al., 2014).

Additional PRRs include an epidermal growth factor (EGF)-like domain-containing receptor kinase AtWAK1 (*Arabidopsis* wall-associated kinase 1) (Brutus et al., 2010), a DAMP receptor implicated in resistance to fungal infection, and a lectin receptor kinase I.9 /AtDORN1 (*Arabidopsis* Does not Respond to Nucleotides 1) that binds extracellular ATP likely released during wounding, herbivory or microbial infection (Choi et al., 2014). Recently, the bulb-type lectin S-domain-1 receptor-like kinase LORE (lipooligosaccharide-specific reduced elicitation) was identified as a potential receptor to recognize the lipid A moiety of lipooligosaccharides (LPS) (Ranf et al., 2015).

With the expansion of plant post-genomic tools, many more PRRs are likely to be identified in the future.

Although it is not fully understood, accumulating evidences support the idea that plant PRRs likely appear as central components of multiprotein complexes in the plasma membrane, which links the detection of PAMPs to the activation of downstream signaling components under tight control by regulatory proteins such as phosphatases or E3 ligases (Böhm et al., 2014; Macho and Zipfel, 2014).

### 1.2.3 Plant ETI

As basal immunity, PTI is sufficient for plants to defend against non-adapted pathogens. In response, some would-be pathogens have successfully evolved the capability to avoid PTI by secreting a collection of effectors into the host apoplast or directly inside the host cell to interfere with PTI (Hogenhout et al., 2009; Bozkurt et al., 2012; Feng and Zhou, 2012). These effectors suppress PTI either upstream of PAMP recognition by targeting PRRs directly (de Jonge et al., 2010; Mentlak et al., 2012), or downstream by blocking signaling events (Zhang et al., 2007a; Göhre et al., 2008; Navarro et al., 2008), and finally result in the effector-triggered susceptibility (ETS). To counteract ETS, some plants have further evolved additional resistance (R) proteins that specifically recognize

the pathogen-secreted effectors, establishing a second layer of immunity known as the effector-triggered immunity (ETI) (Jones and Dangl, 2006).

Although the PTI-ETI nomenclature unarguably has its merits in illustrating how co-evolution of microbes and their hosts has shaped the plant immune system, the distinction between PAMPs and effectors, between PAMP receptors and resistance proteins, and therefore, also between PTI and ETI, cannot strictly be maintained. Some examples support a continuum between PTI and ETI, and therefore it has been suggested that plant immune activation is generally determined by immune receptors or PRRs that mediate pattern recognition (Thomma et al., 2011; Böhm et al., 2014).

### 1.2.4 Signal transduction in plant immunity

Perception of PAMPs (during PTI) or effectors (during ETI) rapidly activates a set of common defence responses, which are usually sufficient to defend against most non-adapted pathogens. These often include a rapid influx of calcium ions from external stores (Lee et al., 2001; Jeworutzki et al., 2010), a burst of active oxygen species (Apel and Hirt, 2004), activation of mitogen-activated protein kinases (MAPKs) and calcium ( $\text{Ca}^{2+}$ )-dependent protein kinases (CDPKs) (Tena et al., 2011), activation of WRKY transcription factors (Asai et al., 2002), reprogramming of gene expression and transcription of defence-related genes (Zipfel et al., 2004), deposition of callosic cell wall appositions at sites of attempted infection (Lazarovits and Higgins, 1976), phytoalexin accumulation (Nürnberg, 1999; Zipfel et al., 2006; Chinchilla et al., 2007) and plant hormonal responses (Denance et al., 2013). These responses also play important roles in defence against adapted pathogens (Bittel and Robatzek, 2007) and might lead to ETI-associated cell death (hypersensitive response, HR) (Beers and McDowell, 2001), often followed by the establishment of systemic acquired resistance (SAR) which is a long lasting and broad-spectrum resistance mechanism (Durrant and Dong, 2004).

One of the important early responses following PAMP perception is the activation of CDPKs, resulting in an expression of defence-related genes (Tena et al., 2011). Perception of PAMPs induces an immediate  $\text{Ca}^{2+}$  influx that contributes to immune signaling through the activation of  $\text{Ca}^{2+}$ -binding proteins such as CDPKs (Romeis and

Herde, 2014). Several CDPKs are involved in plant immune signaling, mostly as positive regulators (Boudsocq and Sheen, 2013) and rarely as negative regulators (Monaghan et al., 2014). For example, CPK5, CPK4, CPK6, and CPK11 participate in immunity as early transcriptional regulators (Boudsocq and Sheen, 2013). In contrast, CPK28 negatively regulates immune signaling through controlling BIK1 turnover (Monaghan et al., 2014).

Although PTI and ETI share many signaling components, it has been proposed that immune responses in ETI occur more quickly, are more prolonged, and are more robust than those in PTI, suggesting that PTI is a weak variant of ETI (Thomma et al., 2011).

One of the big gaps in our understanding of plant immunity is in the signaling pathways that operate immediately downstream of PRR and R protein activation. Genetic screens have had very limited success in identifying signaling components, and thus the components of these pathways remain mostly elusive (Dodds and Rathjen, 2010).

### **1.3 Chitinases in plant immunity**

As mentioned above, recognition of PAMPs leads to a transcriptional reprogramming within the plant cell, resulting in expression of immunity-related proteins. In fact, a group of plant-coded proteins induced by different stresses, named pathogenesis-related (PR) proteins, has been assigned an important role in plant defence against pathogens. This group of proteins has been defined as ‘proteins encoded by the host plant but induced only in pathological or related situations’ (Antoniw et al., 1980), and are historically classified into 17 PR protein families on the basis of their characteristics and biological activity (van Loon et al., 2006). Four PR protein families are classified as chitinases and are thought to play a role in defence through their hydrolytic activities towards major components of fungal cell walls (van Loon et al., 2006).

#### **1.3.1 Chitinases**

Chitinases (EC 3.2.1.14) catalyze the hydrolysis of the  $\beta$ -1,4-glycosidic bonds between the GlcNAc residues of chitin (Collinge et al., 1993). Chitin, the second most abundant

biopolymer on the planet (Shahidi and Abuzaytoun, 2005), is found in the outer skeleton of insects, fungi, yeasts, algae, crabs, shrimps, and lobsters, and in the internal structures of other invertebrates (Hamid et al., 2013). Interestingly, chitinases are present not only in chitin-containing organisms, like fungi and insects, but also appear in organisms that do not contain chitin, such as bacteria, higher plants and animals, and play important physiological and ecological roles (Nagpure et al., 2014).

Apart from chitin, chitinases can also hydrolyze chitin derivatives. For example, one of the chitinase substrates is chitosan, the deacetylated form of chitin (Tanabe et al., 2000). Likewise, lipochitooligosaccharides produced by rhizobia and functioning as nodulation factors during root nodule formation (Mergaert et al., 1997), essentially consist of an acylated chitin oligomeric backbone with various substitutions at the (non)reducing-terminal and/or nonterminal residues (den Hartog et al., 2003), and are also hydrolyzed by chitinases (Goormachtig et al., 1998). Moreover, bacterial peptidoglycan, a polymer of  $\beta$ -1,4-linked GlcNAc and N-acetylmuramic acid (MurNAc) residues, can be cleaved by plant chitinases (Collinge et al., 1993). Plant cell wall glycoproteins containing GlcNAc are considered to be the endogenous substrate for plant chitinases (Dyachok et al., 2002).

As far as the amino acid similarity of chitinases from various organisms is considered, 5 classes of chitinases have been proposed (Passarinho and de Vries, 2002), and have been categorized into 2 families, which include families 18 and 19 of glycosyl hydrolases (GH) based on the catalytic domain of chitinases (Henrissat, 1991). The GH18 chitinases include class III and V plant chitinase members (Takenaka et al., 2009). GH19 family is exclusively composed of chitinases of classes I, II, and IV (Santos et al., 2008). The chitinases of the 2 different families do not share amino acid sequence similarity, and have completely different 3-dimensional (3D) structures and molecular mechanisms. Therefore, they are likely to have evolved from different ancestors (Tyler et al., 2010).

### 1.3.2 Role of chitinases in plant defence

Bacterial and fungal chitinases often function in nutrition processes or in morphogenesis of the cell wall (Cohen-Kupiec and Chet, 1998). In contrast, the plant and animal chitinases mainly play a role in the host defence against pathogen attack (Kasprzewska, 2003), which can be confirmed by that fact that four PR protein families are plant chitinases (von Dach, 2006).

Plant chitinases have been shown to contribute to defence against fungi in two distinct manners. Exochitinases reside in the apoplast and are not considered directly detrimental to fungal growth, but are presumed to release fungal chitin oligosaccharides, which in turn trigger downstream defence responses (Kombrink et al., 2011). These responses include the production of endochitinases that accumulate in the vacuole and are released to directly inhibit the growth of the fungal hyphae during the infection process, when hyphae penetrate and affect cell integrity (Collinge et al., 1993).

In order to avoid plant chitinase-mediated defence, plant pathogens have evolved several counteracting strategies, including modification of carbohydrate chains (Ride and Barber, 1990), cell wall remodeling (Fujikawa et al., 2009), and secretion of effectors to inhibit chitinase activity (Marshall et al., 2011), scavenge chitin (van den Burg et al., 2006), or compete for receptor binding (de Jonge et al., 2010; Sanchez-Vallet et al., 2013).

In addition to biotic stress, chitinases are also involved in plant abiotic stress responses such as osmotic, salt, cold, wounding, and heavy metal stresses (Grover, 2012).

### **1.4 Peptidoglycan and its receptors as example for a PAMP-PRR pair**

#### **1.4.1 Peptidoglycan**

Most eubacteria are entirely surrounded by a strong cell wall, usually namely a sacculus, to maintain the bacterial shape and counteract the internal pressure of the bacterial cell (Weidel and Pelzer, 1964). Besides its protective function and shape formation, the cell

wall also provides an interface for interaction with the surrounding environment and potential hosts.

The most important component of the bacterial cell wall conferring strength and rigidity is the heteropolymeric macromolecule peptidoglycan (PGN), firm glycan chains that are interlinked either directly or via short peptide bridges (Glauner et al., 1988). PGN is composed of three main building blocks: glycan strand, peptide subunit or stem peptide, and the inter-peptide bridge. The glycan strand is composed of alternating  $\beta$  (1,4) linked GlcNAc and MurNAc, which is cross-linked by short peptides attached by an amide linkage to the lactyl group of MurNAc.

The most common sequence of the stem peptide is L-Ala-D-iso-Glu-mDAP/L-Lys-D-Ala-D-Ala, with a dibasic amino acid (mostly either meso-diaminopimelic acid (mDAP) or L-Lys) residing at position three, hence distinguishing Dap-type from Lys-type PGN. DAP-type PGN is present in most Gram-negative bacteria as well as in *Bacilli* and *Mycobacteria* compared to the Lys-type in most Gram-positives (Schleifer and Kandler, 1972). Gram-positive and Gram-negative bacteria differ not only in the type of PGN they harbor, but also in the PGN amount. Gram-positive cell walls contain a thick PGN sacculus of up to forty layers (20 - 80 nm), which is embedded with teichoic and lipoteichoic acids and proteins. Instead, Gram-negative cell walls mostly consist of a single layered PGN macromolecule (1-7 nm) and an additional membrane, the outer membrane (Cabeen and Jacobs-Wagner, 2005).

The PGN of bacteria is steadily remodeled and degraded during cell growth and differentiation as well as in response to changing environmental conditions. Up to 50% of the PGN is shed from the cell wall in one generation by cell wall turnover (Park and Uehara, 2008; Reith and Mayer, 2011). Thus it was proposed that particular PGN fragments can be exploited as signaling molecules for bacteria themselves, reflecting the status of their cell wall (Bertsche et al., 2015).

### 1.4.2 PGN perception systems

As signaling molecules, PGNs can be sensed by not only bacteria themselves but also by their host. PGNs have the features that are shared among all PAMPs. For instance, PGNs, as major building blocks of the bacterial cell walls, are highly conserved and exposed at the bacterial cell surface, and hence they constitute excellent targets for recognition by the innate immune system of potential host organisms that contain no PGNs. In fact, PGN has been known for a long time to promote innate immune responses in vertebrates, insects and plants (Dziarski and Gupta, 2005a; Gust et al., 2007; Erbs et al., 2008). PGN can be recognized in mammals by two intracellular receptors: Nucleotide-binding oligomerization domain-containing protein 1 (NOD1) and NOD2, which both contain an N-terminal caspase recruitment domain (CARD), a C-terminal LRR domain for ligand sensing, and a central nucleotide oligomerisation domain (NOD) (Tanabe et al., 2004; Inohara et al., 2005). NOD2 detects Lys-type PGN and muramyl dipeptide (MDP) as the minimal recognition structure, whereas NOD1 preferentially senses the mDAP-containing muramyl tripeptide found mostly in Gram-negative PGN (Chamaillard et al., 2003; Girardin et al., 2003).

In addition, PGN can also be perceived by so called PGN-recognition proteins (PGRPs, PGLYRPs), highly conserved pattern-recognition receptors of the innate immune system present in insects and mammalian cells (Lu et al., 2006; Guan and Mariuzza, 2007; Dziarski and Gupta, 2010; Kurata, 2014). Mammalian PGRPs bind bacterial PGN and might even kill Gram-positive bacteria by directly interacting with PGN, thereby interfering with PGN maturation (Cho et al., 2007). Some structurally known PGRPs are able to bind PGN, but unable to hydrolyze it due to a lack of zinc-coordinating residues in the active site (Reiser et al., 2004; Guan et al., 2005). It was proposed that these non-lytic PGRPs may inhibit bacterial growth by enclosing parts of the PGN layer and thereby preventing further crosslinking (Bertsche et al., 2015). In contrast, there are also PGN-hydrolysing PGRPs in insects and mammals that have at least one C-terminal PGRP domain, which is homologous to bacteriophage and bacterial type 2 amidases such as the *Drosophila* PGRP-LB (Kim et al., 2003). Although it is not yet clear what role exactly PGN-hydrolysing PGRPs have during infection, it has been proposed that degradation of PGN might contribute to boosting the innate immune system and

coordinating the inflammation response by multiplication of PGN molecules recognized by NOD2 (Schaffler et al., 2014).

In addition to intracellular receptors of PGNs, mammals have also extracellular PGN receptors like membrane-bound Toll-like receptor 2 (TLR2) (Dziarski and Gupta, 2005b). The role of TLR2 as a specific PGN receptor has been heavily debated (Muller-Anstett et al., 2010). Recently, it has been shown that the NOD2 mediated activation of dendritic cells with polymeric PGN is dependent on a TLR2 co-stimulation. In other words, signaling via both receptors, NOD2 and TLR2, leads to a more potent activation of the immune system compared to stimulation of each receptor alone (Schaffler et al., 2014).

In plants, LysM proteins have been shown recently to act as receptors for PGN. The lysin motif (LysM), typically from 44 to 65 amino acids in length, is an ancient and ubiquitous protein domain (Pfam PF01476) found in all living organisms except for *Archaea* (Bateman and Bycroft, 2000). The LysM has a  $\beta\alpha\alpha\beta$  secondary structure with the two  $\alpha$ -helices packing onto the same side of an antiparallel  $\beta$ -sheet (Zhang et al., 2007b). In prokaryotes, LysMs were found in bacterial lysins or chitinases, which hydrolyze glycosidic bonds of PGN or chitin (Buist et al., 2008). Thus, the GlcNAc moiety is generally thought to be the LysM ligand. Indeed, the plant LysM proteins characterized are implicated in recognition of GlcNAc-containing substrates such as chitin and PGN. For example, in *Arabidopsis* PGN can be recognized by a tripartite recognition system, composed of the two membrane-tethered LysM receptor proteins LYM1 and LYM3, and one transmembrane LysM receptor kinase CERK1 (Willmann et al., 2011). All three proteins are indispensable for PGN sensitivity and immunity to bacterial infection (Willmann et al., 2011). Similarly, the PGN perception system in rice is made of the two LysM receptor proteins LYP4 and LYP6 (Liu et al., 2012a). LYP4 and LYP6 were shown to physically interact with OsCERK1, which is also required for PGN perception (Kouzai et al., 2014).

### **1.5 From microbial complex structures to PAMPs**

Plants are able to detect non-self via sensing microbial-derived PAMPs by PRRs. The efficient activation of PRRs relies on the form, amount, concentration, and size of PAMP ligands. It is generally little known how microbial patterns are released from complex

extracellular structures such as microbial cell walls. Two possible scenarios as to how soluble PAMP fragments might be generated from macromolecular assemblies of microbes are described below.

### 1.5.1 Generation of PAMPs through spontaneous release

During bacterial growth large amounts of PGN building blocks are steadily shed into the extracytoplasmic space. For example, *B.subtilis* releases about 50% of its PGN in one generation during growth (Goodell and Schwarz, 1985). It also been found that flagellin monomers are shed into the supernatant of *P.aeruginosa* cultures (Bardoel et al., 2011). Likewise, LPS is shed into liquid culture when *E.coli* grows *in vitro* (Mackowiak, 1984). Upon infection, these building blocks are shed into space surrounding cells and can serve as PAMPs for the activation of PTI signaling. For instance, culture supernatants from *Bacillus sp.* were shown to cause immune responses through activation of the NOD1 signaling cascade in response to mDAP containing cell wall peptides (Fujimoto and Fukase, 2011). *P.aeruginosa aprA* mutants induced an activation of TLR5 signaling via shedding monomeric flagellin into their environment (Bardoel et al., 2011). Similarly, fungal cells also shed chitin into the environment when growing (Bueter et al., 2013).

### 1.5.2 Generation of PAMPs through host hydrolytic enzymes

Upon infection, hosts often secrete hydrolytic enzymes to harm the invader and to either deliberately or incidentally produce soluble PAMPs. Eukaryotic PGN recognition proteins (PGRPs), which are conserved from insects to mammals, bind PGN and function in antibacterial immunity (Bertsche et al., 2015). Non-enzymatic PGN sensors such as PGRP-SA depend on fragmented PGN for perception and immune stimulation, which is delivered by the PGN-hydrolytically active Gram-negative bacteria-derived binding protein 1 (GNBP1) (Wang et al., 2006). Apart from PGRPs, other PGN-hydrolytic enzyme activities such as lysozymes have been reported to functions in generating soluble PGN fragments a ligands for PRRs (Callewaert and Michiels, 2010).

Similarly, plants have also been reported to produce PAMPs through secreted hydrolytic enzymes. For instance, upon infection of fungal pathogens plant chitinases are often

induced to target fungal cell walls, releasing chitin as PAMPs (Sanchez-Vallet et al., 2015). Soluble PGN fragments have previously been shown to stimulate plant immune responses in *Arabidopsis* (Gust et al., 2007; Erbs et al., 2008). However, it is unknown how PGN PAMPs are generated, and if so, which host protein is involved in PGN hydrolysis in *Arabidopsis*.

### 1.6 Aims of the thesis

Overwhelming focus has been put on PTI studies since the innate immunity concept was first described in 1997 (Medzhitov and Janeway, 1997), but there are still many big gaps in our understanding of PTI, such as the molecular events pre- and post-recognition via the plasma-membrane located PRR complexes. For instance, although PGN and LYM1/LYM3/CERK1 have been identified as one PAMP-PRR pair in *Arabidopsis* (Gust et al., 2007; Willmann et al., 2011), upstream and downstream events of PGN perception remain largely elusive.

This thesis therefore focuses on the investigation of upstream and downstream molecular events of CERK1-mediated perception in plants.

It was generally proposed that soluble PAMPs derived from complex microbial cell walls serve as ligands for host PRRs and subsequent immune activation in plants. For example, macromolecular chitin was presumed to be hydrolyzed by exo-chitinases and released chitin oligomers can then act as PAMPs in PTI (Kombrink et al., 2011). However, it is unknown whether, and if so, how PGN is hydrolyzed prior to PGN-perception in *Arabidopsis*. The first aim of this thesis was thus to identify potential PGN hydrolases in *Arabidopsis* and afterwards characterize this enzyme(s), and finally to examine how the enzyme(s) might contribute to PGN recognition and thus to PGN-triggered immunity in plants.

CERK1 mediates both PGN- and chitin-induced immune responses (Miya et al., 2007; Willmann et al., 2011). But it is still unknown how the plant cell accomplishes the differentiation between bacterial PGN and fungal chitin by employing the same CERK1 receptor. Therefore, the second aim of the thesis was to decipher downstream signaling

components of CERK1, which might be the basis for differentiation of these two PAMP-mediated signaling pathways.

## 2. Materials and Methods

### 2.1 Materials

#### 2.1.1 Plants

##### 2.1.1.1 *Arabidopsis thaliana*

The experiments in this study were conducted using the *Arabidopsis thaliana* ecotypes Columbia-0 (Col-0), or Landsberg erecta (Ler) and transgenic lines generated in these ecotypes. The knock-out or knockdown lines used in this study, if not stated otherwise, were obtained from the Nottingham Arabidopsis Stock Centre (NASc) or received from other labs, and are listed in Table 1.

**Table 1. *Arabidopsis* mutant and transgenic lines used in this study.**

AGI	Gene	Mutant(type)	stock	reference
At5g24090	<i>LYS1/CHIA</i>	<i>lys1-kd/chia-kd</i> (amiRNA)		This study and Grabherr, 2011
At3g21630	<i>CERK1</i>	<i>cerk1-2</i> (T-DNA)	GABI_096F09	(Miya et al., 2007)
At1g77630	<i>LYM3</i>	<i>lym3-1</i> (T-DNA)	SALK_111212	(Willmann et al., 2011)
At1g21880	<i>LYM1</i>	<i>lym1-1</i> (T-DNA)	GABI_419G07	(Willmann et al., 2011)
At1g69910	<i>PK</i>	<i>pk-1</i> (T-DNA)	SALK_085634	This study
At1g69910	<i>PK</i>	<i>pk-2</i> (T-DNA)	GABI_109A12	This study
At3g23000	<i>CIPK7</i>	<i>cipk7-1</i> (T-DNA)	CS307124	This study
At3g23000	<i>CIPK7</i>	<i>cipk7-2</i> (T-DNA)	SALK_124117	This study
At4g21940	<i>CPK15</i>	<i>cpk15-1</i> (T-DNA)	CS879228	This study
At4g21940	<i>CPK15</i>	<i>cpk15-2</i> (T-DNA)	WiscDsLoxHs_12H	This study
At4g21940	<i>CPK15</i>	<i>cpk15-kd1</i> (amiRNA)		This study
At4g21940	<i>CPK15</i>	<i>cpk15-kd2</i> (amiRNA)		This study

**2.1.1.2 *Nicotiana benthamiana* and *Oryza sativa***

The proteins were transiently expressed in *Nicotiana benthamiana* to study protein interaction and protein activity. The pH assay was conducted using *Oryza sativa* and *Arabidopsis thaliana* cell cultures.

**2.1.2 Microbes**

**Table 2. Bacterial strains used in this work**

Species	Strain	Genotype
<i>Escherichia coli</i>	DH5 $\alpha$	<i>supE44</i> $\Delta$ <i>lacU169</i> ( $\Phi$ 80 <i>lacZM15</i> ) <i>hsdR17 recA1 endA1 gyrA96 thi-1 relA1</i>
	TOP10	<i>mcrA</i> , delta ( <i>mrr-hsdRMS-mcrBC</i> ), $\phi$ 80delta <i>lac</i> delta M15, delta <i>lacX74, deoR, recA1, araD139</i> delta ( <i>ara, leu</i> ),7697, <i>galU, galK, lambda-</i> , <i>rpsL, endA1, mupG</i>
	BL21AI	F- <i>ompT hsdSb(rb-mb-)</i> <i>gal dcm</i> <i>araB::T7RNAP-tetA</i>
<i>Pseudomonas syringae</i>	<i>Pto</i> DC3000	Rif <sup>r</sup>
<i>Agrobacterium tumefaciens</i>	GV3101:: <i>pMP90</i>	T-DNA <sup>-</sup> <i>vir</i> <sup>+</sup> <i>rif</i> <sup>r</sup> , <i>pMP90 gen</i> <sup>r</sup>
	GV3101:: <i>pMP90RK</i>	T-DNA <sup>-</sup> <i>vir</i> <sup>+</sup> <i>rif</i> <sup>r</sup> , <i>pMP90 gen</i> <sup>r</sup> , <i>kan</i> <sup>r</sup>
	C58C1	T-DNA <sup>-</sup> <i>vir</i> <sup>+</sup> <i>rif</i> <sup>r</sup> , <i>carb</i> <sup>r</sup>

**2.1.3 Media and buffer**

The media used in this study were sterilized by autoclaving for 20 minutes at 121°C and are summarized in Table 3. All buffers were prepared according to (Molecular cloning, 3<sup>rd</sup> edition, Sambrook and Russell). Antibiotics were added, if necessary, to the sterilized medium in appropriate final concentrations as listed in Table 4.

**Table 3. Media used in this study**

Media	Ingredients(1 liter)	Species
Luria-Bertani broth(LB)	10 g Bacto-Tryptone, 5 g NaCl, 5 g Yeast extract (YE)	<i>Escherichia coli</i>
Kings Medium B (King's B)	20 g glycerol, 40 g Proteose Pepton 3, after autoclaving addition of 0.1 % (v/v) MgSO <sub>4</sub> and KH <sub>2</sub> PO <sub>4</sub>	<i>Pseudomonas syringae</i>
½ Murashige-Skoog Medium (½ MS)	2.2 g MS (Duchefa), pH 5.7 (KOH)	<i>Arabidopsis thaliana</i>

**Table 4. Antibiotics used in this study**

Antibiotics	Working concentration(µg/ml)	solvent
Carbenicillin	50-100	Water
Cycloheximid	50	Water
Kanamycin	50	Water
Rifampicin	50	Methanol
Spectinomycin	100	Water
Tetracyclin	50	Ethanol
Ampicillin	50-100	Water
Gentamycin	25	Water
Hygromycin	50	Water

### 2.1.4 Vectors

**Table 5. Vectors in this study**

Vector	Characteristics	Reference
pDONR201	Ori Puc, rrnB, T2, rrnB,T1, attP1, attP2, ccdB,Cm <sup>r</sup> , Kan <sup>r</sup>	Invitrogen
pDONR207	Ori Puc, rrnB, T2, rrnB,T1, attP1, attP2, ccdB,Cm <sup>r</sup> , Gent <sup>r</sup>	Invitrogen
pK7FWG2.0	P35S, T35S, eGFP, attR1, attR2, ccdB, Cm <sup>r</sup> , Kan <sup>r</sup>	VIB
pDEST17	PT7, RBS, His <sub>6</sub> -tag, attR1, attR2, ccdB, Cm <sup>r</sup> , PT7, bla, Promotor, Amp <sup>r</sup> , pBR322 origin, ROP, orf	Invitrogen
miR319a pBSK (pRS300)	B reverse, T3 promotor, miR319a, T7 promotor, A forward, Amp <sup>r</sup>	Weigelworld.org
pCR8/GW/TOPO	Entry vector for the Gateway system	Invitrogen
pGWB5/14/17	Binary gateway destination vector	(Nakagawa et al., 2007)

### 2.1.5 Enzymes and antibodies

Restriction enzymes, ligase and DNA modification enzymes were purchased from Fermentas (St. Leon-Rot) and New England Biolabs (Beverly, USA). Mutanolysin was purchased from Sigma-Aldrich. Antibodies were purchased from the companies Sigma-Aldrich (Taufkirchen), New England Biolabs (Beverly, USA) and Acris Antibodies GmbH (Herford) and are listed in Table 6. The antibody against tobacco class III chitinases from rabbit and the antibody against YFP from rabbit were kind gifts from Dr. Frédéric Brunner and Dr.Sara Mazzotta, respectively. The antibody against AtCERK1 was kindly provided by Dr.Gary Stacey (University of Missouri, USA).

**Table 6. Antibodies used in this study**

	Antibody	Host	Dilution	Reference
Primary antibodies	α-p42/44 MAPK	rabbit	1:3000	Sigma-Aldrich
	α-HA	rabbit	1:3000	Sigma-Aldrich
	α-MYC	mouse	1:3000	Sigma-Aldrich
	α-GFP	goat	1:3000	Sigma-Aldrich
Secondary	α-mouse IgG HRP	rabbit	1:10000	Sigma-Aldrich

antibodies	conjugated			
	$\alpha$ -goat IgG HRP conjugated	rabbit	1:10000	Sigma-Aldrich
	$\alpha$ -rabbit IgG HRP conjugated	goat	1:10000	Sigma-Aldrich
	Anti-goat IgG-AP	rabbit	1:3000	Sigma
	Anti-rat IgG-AP	goat	1:3000	Sigma
	Anti-mouse IgG-AP	rabbit	1:3000	Sigma
	Anti-rabbit IgG-AP	goat	1:3000	Sigma

### 2.1.6 Chemicals and solutions

Laboratory grade chemicals and reagents were purchased from Sigma-Aldrich (Taufkirchen), Carl Roth (Karlsruhe), Merck (Darmstadt), Qiagen (Hilden), Invitrogen (Karlsruhe), Duchefa (Haarlem, Niederlande), Molecular Probes (Leiden, Niederlande), Fluka (Buchs, Schweiz) and BD (Sparks, USA), unless noted otherwise in the text. All buffers and solutions were prepared, if not stated otherwise, with milli-Q water. Sterilization was conducted by autoclaving or filter sterilization.

### 2.1.7 Oligonucleotides

The oligonucleotides used in this study were synthesized by Eurogins MWG Operon. The sequences of these oligonucleotides are listed in the Appendix Table 7.

### 2.1.8 PAMPs

*Bacillus subtilis* PGN was purchased from Invivogen (San Diego, CA). *Micrococcus luteus* cells were purchased from Sigma-Aldrich (Hamburg, Germany). Chitin hexamer was purchased from Carbosynth (UK), chitin octamer was purchased from Seikagaku (Japan), and crab chitin was purchased from Sigma-Aldrich. All PAMPs, unless stated otherwise, are dissolved or resuspended in ddH<sub>2</sub>O.

Flg22 peptide QRLSTGSTINSAKDDAAGLQIA was purchased from Selleckchem company and was dissolved in ddH<sub>2</sub>O at high concentration (1 M) and in 1mg/mg BSA

and 0.1M NaCl at low concentration (1mM). Elf18 peptide SKEKFERTKPHVNVGTIG was a gift from George Felix.

## 2.2 Methods

### 2.2.1 Plant growth

#### 2.2.1.1 Growth conditions

*A. thaliana* seeds were sown on steam-sterilized GS90-soil (Gebr. Patzer GmbH) mixed with vermiculite or after surface-sterilization with chlorine gas on sterile ½ MS plates. After stratification of the seeds for two days at 4°C in the dark, the plants were grown in either long-day (16 h light, 8 h darkness) or short-day (8 h light, 16 h darkness) environmental chambers under standard conditions (150µmol/cm<sup>2</sup>s light, 40-60 % humidity, 22°C). *N. benthamiana* plants were cultivated in a mixture of soil and sand containing 0.1 % (v/v) Confidor in the greenhouse (13 h light, 11 h darkness).

#### 2.2.1.2 Seed surface sterilization

*Arabidopsis* seeds were sterilized by chlorine gas treatment. Seeds were transferred to Eppendorf tubes and placed in a desiccator. In a glass beaker placed in the desiccator, 2 ml of 37 % HCl were added to 50 ml of 12 % sodium hypochloride solution forming the chlorine gas. The lid of the desiccator was immediately closed and a vacuum was generated to get an airtight seal. The seeds were incubated for 4 h.

#### 2.2.1.3 Cell suspension cultures

*Arabidopsis* and *Oryza sativa* suspension cell cultures were grown in MS medium (4.41g/l MS salt, 6% sucrose, 50 mg/l MES, 2mg/l 2, 4-D) at 150 rpm and sub-cultured every week.

## 2.2.2 Microbe cultivation

### 2.2.2.1 Growth of *Escherichia coli*

*E. coli* strains were cultivated overnight at 37°C either on LB-plates in oven or in liquid LB medium at 230 rpm in shaker. Antibiotics were added into the media according to the resistance cassettes of each strains.

### **2.2.2.2 Growth of *Pseudomonas syringae***

*P. syringae* pv. *tomato* DC3000 were grown for 24-48 hours at 28°C either on King's B-plates in an oven or in liquid King's B medium at 180 rpm in a shaker. For the determination of bacterial growth in infection assays the *Pseudomonas* strains were re-isolated from plant material and plated on LB plates containing cycloheximide in addition to other antibiotics.

### **2.2.2.3 Growth of *Agrobacterium tumefaciens***

*A. tumefaciens* strains were cultivated for 48 hours at 28°C on LB-plates in an oven or in liquid LB medium at 230 rpm in a shaker. Additional antibiotics were added into the media according to the plasmid-DNA the strains were carrying.

## **2.2.3 Molecular biology**

### **2.2.3.1 Isolation of plasmid DNA from *E.coli***

For alkaline lysis, a bacterial pellet from a 2 ml overnight culture was resuspended in 100 µl lysis buffer (50 mM Tris/HCl pH 8.0, 50 mM EDTA pH 8.0, 15 % Saccharose), and lysed with 200 µl alkaline SDS-buffer (200 mM NaOH, 1 % (w/v) SDS) for a maximum of 5 min and finally 150 µl Potassium acetate buffer (3 M Potassium acetate, 11.5 % (v/v) acetic acid) was added. The mix was centrifuged and the aqueous phase containing plasmid DNA was precipitated with 0.6 Vol Isopropanol. The pellet was washed with 70 % ethanol and dissolved in TE-buffer (10 mM Tris/HCl, 1 mM EDTA, pH 8) or deionized water.

Alternatively to the classical alkaline lysis, for mini scale isolation, plasmid DNA was extracted from 3 ml overnight culture using the MiniPrep Kit (Thermo Scientific) according to the manufacturer's instructions.

For midi scale isolation, plasmid DNA was extracted from 25 ml (high copy plasmid) or 100 ml (low copy plasmid) overnight culture using the PureLink HiPure kit (Invitrogen) according to the manufacturer's instructions.

For large scale plasmid isolation, a manual protocol was used as described below. A single colony was pre-cultured in 2.5 ml LB for 3 hours and was enlarged with pre-warmed 500 ml LB culture for overnight growing at 37°C. Cells were collected by centrifuging for 30 minutes at 5000 rpm and manipulated from this step onward on ice or at 4°C. Bacterial pellets were suspended in 2.5 ml freshly-prepared lysozyme solution (10 mg/ml), mixing them by up-and-down pipetting followed by 5 minutes incubation on ice. 2 ml of 0.5 M EDTA pH 8 was added, mixed and incubated for 5 minutes on ice. The solution was mixed with 100 µl RNAase A (20 mg/ml) and 150 µl of 10% Triton X-100 and topped up to 1 ml with 0.02xTE. The mixture was then incubated for 60 minutes on ice. The supernatant was separated by centrifugation at 18000 rpm for 60 minutes and then transferred to a new tube and mixed 1:1 with phenol (equilibrated with 0.1% 8-hydroxyquinoline pH 8) and shaken vigorously for 1 minute. The solution was centrifuged for 20 min. The upper aqueous phase was carefully recovered and transferred to a new tube containing 1 volume chloroform, followed by shaking and spinning as before. The aqueous phase was recovered to a 30 ml corex tube, adding 10% 5M NaClO<sub>4</sub> of water volume and 80% isopropanol of water volume. The tube was sealed with parafilm and mixed by turning upside down. Then the tube was centrifuged at 10000 rpm for 15 minutes. The pellet was air-dried, and re-suspended in 500 µl TE by incubation overnight. The DNA was checked by agarose gel electrophoresis (2.2.3.6).

### **2.2.3.2 Genomic DNA isolation from plant material**

Leaf pieces were ground in a 1.5 ml Eppendorf tube with 200 µl Edwards buffer (200 mM Tris/HCl pH 7.5, 250 mM NaCl, 25 mM EDTA pH 8, 0.5 % (w/v) SDS) using a homogenizer machine. The samples were centrifuged for 5 minutes at 13000 rpm. The supernatant was transferred to a new tube with the same volume isopropanol and thoroughly mixed. Genomic DNA was precipitated at room temperature for 5-10 minutes, and centrifuged at 4°C for 10 minutes at 14000 rpm. The pellet was washed with 200 µl

ethanol (70%, v/v) and was air-dried at room temperature. Finally, the DNA pellet was dissolved in ddH<sub>2</sub>O.

### **2.2.3.3 Total RNA isolation from *Arabidopsis* seedlings**

3-5 seedlings (7-10 day old) were harvested in a 1.5 ml Eppendorf tube and frozen in liquid N<sub>2</sub>. The tube was placed on a precooled plate and the seedlings were ground into fine powder with a precooled pestle. 300 µl Trizol (Chomczynski and Sacchi, 1987) was added immediately to the tube, followed by vortex mixing for 10 seconds and incubation for 10 minutes at room temperature. 60 µl chloroform was then added, and the mixture was vortexed again. The samples were incubated for 10 minutes at room temperature and then centrifuged at 14000 rpm for 10 minutes at room temperature. The upper aqueous phase was transferred into a new tube filled with 150 µl isopropanol and mixed by vortex. The samples were incubated for 1 hour at -80°C or overnight at -20°C. The precipitated RNA was collected by centrifugation at 14000 rpm for 10 minutes at 4°C. The RNA pellet was washed with 500 µl 70% (v/v) ethanol. Finally, the air-dried pellet was dissolved in 10 µl ddH<sub>2</sub>O.

### **2.2.3.4 Complementary DNA synthesis by Reverse Transcription (RT)**

2-5 µg total RNA in 1.5 µl was mixed with 0.5 µl 30 µM oligo-dT and denatured at 70°C for 10 minutes. Then 8 µl RT-mixture (2 µl 5x buffer, 1µl 2.5 mM each dNTPs, 0.5 µl RNAase inhibitor (Fermentas), 1 µl reverse transcriptase (Fermentas), 4.25 µl H<sub>2</sub>O) was added and incubated at 42°C for 90 min, followed by 70°C for 10 min.

### **2.2.3.5 Standard PCR**

In a 30µl reaction volume, 1 µl template was added into the mixture (3 µl 10x buffer, 0.5 µl 2.5 mM dNTPs, 0.5 µl 10 µM forward and reverse primer, 0.5 µl lab-made Taq polymerase). The reaction was performed in a PCR machine (PTC-200) with the following program: 94°C for 2 min, 30 cycles of 94°C 30 seconds, 55°C for 30 seconds, 72°C for 1 min/kb, 72°C 10 min.

### **2.2.3.6 DNA agarose gel electrophoresis**

DNA electrophoresis was performed on a 0.8-1.5 % agarose gel in 1x TAE buffer (40 mM Tris/acetate pH 8.0, 2 mM EDTA pH 8.0) at 60-120 V. A 1 kb ladder (Fermentas) was used as size marker. Ethidium bromide (0.5 µg /ml) or 6% (v/v) peqGREEN (Peqlab) present in the gel helped the visualization of DNA by a UV-Transilluminator (Infinity-3026 WL/26 MX, Peqlab).

### **2.2.3.7 Sequencing**

The constructs and PCR products were sequenced by GATC Biotech AG (Konstanz). 5µl DNA template with either 80-100 ng/µl plasmid or 20-80 ng/µl PCR product was added to 5 µl 5 µM sequencing primer. The results were analyzed using DNASTar or CLC main workbench software.

### **2.2.3.8 Quantitative fluorescent real time PCR**

2.5 µL seedling RNA or 1 µg leaf RNA was used for the cDNA synthesis (in 5µl total reaction volume). Leaf cDNA was diluted 3 to 5 fold for RT-qPCR experiments, whereas seedling cDNA was used undiluted. RT-qPCR amplifications and measurements were performed with the iQ5 Real Time PCR detection system from Bio-Rad. RT-qPCR amplifications were monitored using the SYBR Green Fluorescein Mix (Thermo Scientific). The gene expression data was quantified using the  $2^{-\Delta\Delta CT}$  method (Livak and Schmittgen, 2001). The normalization of the expression levels was done using the CT values obtained for the *EF-1 α* gene. The presence of a single PCR product was further verified by dissociation analysis in all amplifications. All quantifications were made in duplicate on RNA samples obtained from three independent experiments, each performed with a pool of two leaves or 3-5 seedlings.

### **2.2.3.9 Restriction endonuclease digestion**

DNA was digested in 20µl reaction volume with 1 U/µl DNA at 37°C (or the appropriate temperature for the given restriction endonuclease) for 1 hour according to the manufacturer's recommendations.

### **2.2.3.10 Isolation of DNA fragments from agarose gels**

PCR or DNA fragments were separated via agarose gel electrophoresis. DNA bands were excised from the gel with clean razor blades and extracted using the GeneJet Gel Extraction Kit (Fermentas) according to manufacturer's manual.

### **2.2.3.11 DNA ligation**

In 10 $\mu$ l reaction volume, 50 ng vector and insert DNA were incubated with ligation buffer and T4 DNA ligase (Fermentas) at 16°C overnight.

### **2.2.3.12 Gateway cloning**

In a BP reaction, 100 fmol of the insert and 100 fmol of donor vector were mixed with 2  $\mu$ l BP recombinase mix (Invitrogen). After brief vortexing, the mix was incubated overnight at 25°C. The reaction was stopped by adding 1  $\mu$ l of Proteinase K (Invitrogen) and the samples were incubated for 15 min at 37°C. 2 $\mu$ l of the reaction volume was used to transform *E. coli* DH5 $\alpha$  (2.2.3.13).

To add an A-overhang to PCR products, 40  $\mu$ M dATP was added to the reaction mixture after PCR and the PCR product was insert into the pCR8 vector using the pCR8/GW/TOPO Cloning Kit (Invitrogen) to generate an entry clone. Then, a LR reaction was performed to create a destination construct. 200 to 250 ng of the destination vector and TE buffer pH 8.0 up to a final volume of 4  $\mu$ l was added to a reaction mix containing 50 to 150 ng of the entry vector 1  $\mu$ l of the LR Clonase II mix (Invitrogen) was added and the mixture was incubated overnight at 25°C. The reaction was stopped by adding 1  $\mu$ l of Proteinase K (Invitrogen) and the samples were incubated for 15 min at 37°C. 2  $\mu$ l of the reaction volume was used to transform *E. coli* DH5 $\alpha$  (2.2.3.13).

### **2.2.3.13 Preparation and transformation of chemically competent *E.coli* cells**

A single colony of *E. coli* DH5 $\alpha$  was grown in 5ml LB overnight at 37°C and 250 rpm shaking. 400 ml of LB medium was inoculated with 4 ml overnight culture in sterile 2-liter flasks and grown at 37°C and 250 rpm to an OD<sub>590</sub> = 0.375. The culture was divided into 8 pre-chilled falcon tubes and incubated for 10 minutes on ice. After centrifugation at 1600g and 4°C for 7 minutes, pellets were suspended in 10 ml ice cold CaCl<sub>2</sub> solution

(60 mM CaCl<sub>2</sub>, 15% Glycerol, 10 mM PIPES pH 7,0) and incubated on ice for 30 minutes, followed by washing 2 times by centrifuging at 1100 x g and 4°C for 5 minutes and then incubation for 30 minutes on ice. The pellet was resuspended in 2ml of CaCl<sub>2</sub> and again put on ice, then aliquoted in 50µl into chilled Eppendorf tubes on ice and frozen in liquid nitrogen and stored at -80°C.

50µl chemically competent cells were taken from -80 °C and thawed on ice. Plasmid or ligation or recombination products were added to the aliquot and kept on ice for 20 minutes. The mixture was heat-shocked at 42°C for 45 seconds and immediately put on ice for 2-3 minutes. Then 800µl LB medium was added. The mixture was incubated at 37°C for 1 hour on a shaker. 200µl transformed cell culture was spread onto LB medium plates with appropriate antibiotics.

### **2.2.3.14 Preparation and transformation of electrical competent cells of *A. tumefaciens***

The agrobacterium strain was streaked out onto a LB plate with selective antibiotics and grown at 28°C for 2 days. A single colony was picked to inoculate 5 ml LB liquid medium with appropriate antibiotics. The culture was grown overnight at 28 °C and then enlarged with 500ml LB and grown to an OD600 of 0.5-1.0. Subsequently, the culture was chilled on ice for 15-30 minutes. From this time point onwards the cells were manipulated at 4°C. The cells were centrifuged at 4500 rpm for 15 minutes at 4°C and the pellet was suspended in 200 ml ice-cooled sterile water. The cells were again centrifuged at 4500 rpm for 15 minutes at 4°C and suspended in 100 ml of ice-cooled sterile water and centrifuged as described above. The cells was suspended in 4ml of ice-cold 10% glycerol and centrifuged as described above. The cells were resuspended in 1 ml of ice-cold 10% glycerol. 40 µl aliquots were frozen in liquid nitrogen and stored at -80°C.

40 µl electrically competent cells were thawed on ice for 20 minutes and 100 ng plasmid DNA was added, the mixture then was transferred to a precooled electroporation cuvette. The cells were pulsed once with 1500 voltage for 5 ms (Eppendorf, Hamburg), the cuvette was put back on ice and immediately 500 µl LB medium was added to the

cuvette. Cells were quickly resuspended by gentle pipetting up and down and then transferred to a 1.5 ml Eppendorf tube. The tube was incubated for 1 hour in a rotary shaker at 28°C. The mixture was plated onto selective LB plates and incubated for 2 days in a 28°C incubator.

### 2.2.4 Plant methods

#### 2.2.4.1 Isolation of mesophyll protoplasts from *Arabidopsis*

Isolation of mesophyll protoplasts from leaves of 4-5 week-old *Arabidopsis* plants was performed according to the protocol of (Yoo et al., 2007) with minor changes. Briefly, thin leaf strips were dipped into 1.5% cellulose 'Onozuka' R10 – 0.4% macerozyme R10 solution (Yakult Pharmaceutical Industry), vacuum-infiltrated for 30 min and digested for 3 h at 20°C in the dark. After two subsequent washing steps with W5 buffer *Arabidopsis* protoplasts were suspended in MMG buffer to a concentration of  $2 \times 10^5$  cells/ml prior to polyethylene glycol-mediated transfection. 100 µg plasmid DNA/ml protoplast suspension was used during transfection. Protoplasts samples were then incubated in W1 buffer at 20°C in the dark for 12 to 16 h allowing plasmid gene expression.

#### 2.2.4.2 Stable transformation of *Arabidopsis thaliana*

*A. thaliana* plants were stably transformed by the floral dip-method (Clough and Bent, 1998). 500 ml liquid LB medium containing appropriate antibiotics was inoculated with a pre-culture of selected agrobacteria and further cultivated for 18 – 24 hours. The cells were pelleted for 20 minutes at 4500 x g and resuspended in fresh 5 % (w/v) saccharose solution at a density of 0.8 (OD600 nm). After addition of 0.02 % (v/v) Silwet young *Arabidopsis* inflorescences were dipped for one minute into the bacterial suspension. Afterward the plants were incubated at 100 % humidity for 24 hours. Seeds from floral-dipped plants were then screened for resistance against Basta (glufosinate-ammonium) or kanamycin.

#### 2.2.4.3 Transient transformation of *Nicotiana benthamiana*

*Agrobacterium tumefaciens*-mediated transient transformation was used for the transient expression of proteins in *N. benthamiana*. The bacterial strain carrying the appropriate

expression vector was cultured as described in 2.2.2.3. After cells were harvested at 4°C for 10 minutes at 2000 x g, they were washed two times with 10mM MgCl<sub>2</sub>. The density of the culture was diluted to 0.1 of OD600 and 150 µM acetosyringone was added. The bacterial suspension was then incubated by shaking at RT for 3-6 hours. Afterwards the suspension was mixed 1:1 with a suspension of bacteria carrying an expression construct of p19 (Voinnet et al., 2003) and the mixture was then infiltrated into 3 week-old tobacco leaves. The leaf tissue was analyzed 2-4 days post infection for the presence of the protein.

#### 2.2.4.4 Generation of knock-down lines

Artificial microRNA-mediated gene silencing was used to specifically knock-down *cpk15* in the *Arabidopsis* Col-0 background. The Web microRNA Designer (WMD; <http://wmd.weigelworld.org>) was used to select the primers (see Appendix Table 8) for the generation of an artificial 21mer microRNA (Schwab et al., 2005). The insert was generated in four PCR-steps with pRS300 as PCR template and then cloned into the pCR8 vector. The amiRNA in pCR8 was then cloned into the pB2GW7 destination vector. The transformation of the resulting vector into agrobacteria was mediated using electrical transformation. The stable transformation of the construct into the *Arabidopsis* genome was performed using the floral dip method. Offspring were screened for phosphinothricin (Basta) resistance. Analysis of the *cpk15* transcript level in the *cpk15* knock-down line (*cpk15-kd*) was performed by quantitative RT-PCR using primers listed in Table 8.

#### 2.2.4.5 Genotyping analysis of T-DNA insertion lines

The T-DNA lines used in the frame of this work were analyzed for their genotype. Since diploid plants contain two copies of each gene and are thus able to segregate in offspring, it was necessary to confirm that the T-DNA insertion lines used for the experiments were homozygous. The discrimination between WT, heterozygous insertion and homozygous insertion lines was achieved by two sets of PCR reactions. In the WT-PCR, two primers bind two regions flanking the T-DNA insertion and thus amplify the

product only in the WT plants, because the large size of the T-DNA insertion inhibits the amplification in mutants.

In the second PCR a T-DNA specific left border amplifying primer (Lba primer) is used in a combination with a gene-specific primer allowing an amplification product only in plants carrying a T-DNA insertion. Thus, homozygous plants should show a product only in the Lba-PCR whereas heterozygous plants produce an amplicon in both WT-PCR and Lba-PCR.

### 2.2.5 Protein biochemistry

#### 2.2.5.1 Protein extraction from plant tissue

Total protein was extracted from plant tissue using either a protein extraction buffer specific for acidic chitinases (20mM sodium acetate, pH5.2/15mM  $\beta$ -mercaptoethanol supplemented with 1 proteinase inhibitor cocktail tablet/10ml from Roche) or an extraction buffer containing detergents for solubilization of membrane-bound proteins (50 mM Tris-HCl, pH 7.5, 150 mM NaCl, 1 % (v/v) Nonidet P40 and 1 protease inhibitor cocktail tablet/10 ml from Roche). The plant tissue was first homogenized in liquid N<sub>2</sub> and after addition of the extraction buffer the sample was incubated for 30 minutes on ice. Afterwards the soluble proteins were separated from cell debris using centrifugation at 4°C and the supernatant was used for further analysis.

#### 2.2.5.2 Immunoprecipitation

Leaf protein was extracted from the *LYS1* overexpression plants and approximately 200  $\mu$ g total proteins was used for the immunoprecipitation of LYS1-GFP. Next, protein extracts were incubated for 90 minutes at 4°C with gentle rotation either with 15  $\mu$ l  $\alpha$ -YFP (rabbit) or  $\alpha$ -GFP (goat) antibody (Acris). In control protein samples no antibody was added.

Meanwhile, 400  $\mu$ l agarose A bead solution (Roche) was washed three times with 800  $\mu$ l water (1 min 2000 rpm 4°C), and once with 800  $\mu$ l buffer A (50 mM Tris-HCl, pH 7.5, 5 mM EDTA, pH 8, 2 mM DTT, proteinase inhibitor cocktail). Finally, the agarose A beads were resuspended in buffer A (600  $\mu$ l) and 50  $\mu$ l bead solution was incubated with the

protein/antibody mixture for an additional 30 minutes in a rotator at 4°C. Afterwards, the beads were washed two times with 500 µl buffer A (1 min 1500 x g 4°C) and once with 500 µl buffer A containing 1 M NaCl. The immunoprecipitated proteins were then further analysed by immunoblot or activity assay.

### 2.2.5.3 LYS1 purification

500g 5-week-old leaves from *LYS1<sup>OE</sup>* leaves were frozen in liquid nitrogen and ground to a fine powder. Buffer A (20mM NaAc, pH5.2, 0.01% β-Mercaptoethanol) was added to the sample and incubated on ice for 4 hours. The sample was filtered through four layers of cheesecloth. The homogenate was centrifuged at 10000g for 30 minutes. The supernatant was loaded on a cation exchange column (SP Sepharose, GE Healthcare, Germany) equilibrated with buffer A. The proteins were eluted with a 0 to 1M NaCl gradient in buffer A. The elution fractions were monitored for LYS1 activity by the 4-MUCT assay and LYS1 presence was further confirmed by SDS-PAGE, coomassie blue staining and mass spectrometry. 4-MUCT active fractions were pooled and concentrated with vivaspin columns (GE Healthcare). Protein concentration was determined using the Bradford assay.

### 2.2.5.4 Transient expression and co-immunoprecipitation

Single colony *Agrobacterium tumefaciens* containing the indicated construct were inoculated in 3 ml liquid LB overnight at 37°C shaker. 100 µl culture was enlarged in 5ml fresh LB media in a 15 ml falcon tube overnight at 37°C shaker. The cells were collected by centrifugation for 10 min at 5000 rpm. The pellet was washed 2 times with 10 mM MgCl<sub>2</sub> and resuspended in 10mM MgCl<sub>2</sub> and 150µm acetosyringone to OD<sub>600</sub>1.0. The culture was kept at room temperature for 1-4 hours and mixed 1:1 with a p19 culture. The mixture was syringe-infiltrated into 4-week-old *N. benthamiana* leaves. After 2 days, the leaves were harvested by immediate freezing in liquid nitrogen. For total protein extraction, leaves were ground in liquid nitrogen and extraction buffer (50 mM Tris-Cl pH7.5, 150 mM NaCl, protease inhibitor cocktail (Roche) and phosphatase inhibitor, and 0.5% NP40) were added. The mixture was rotated at 4°C for 1 hour at 5-7 rpm and centrifuged at 13000rpm for 15 minutes at 4°C and repeated 2-3 times. Meanwhile, the

GFP-Trap beads (chromotek) were washed 3 times with extraction buffer. The supernatant was added to 40  $\mu$ l beads and rotated at 5 rpm for 2 hours at 4°C. The bead mixture was washed 1 time with extraction buffer, 1 time with washing buffer 1 (50 mM Tris-Cl pH7.5, 150 mM NaCl) and 1 time with washing buffer 2 (50 mM Tris-Cl pH7.5) by spinning down at 2000 rpm for 1 minute at 4°C. As much of the supernatant as possible was removed from the beads, which were then resuspended in 40  $\mu$ l SDS loading buffer. Then the samples were subjected to Laemmli SDS-PAGE for western blot detection.

### **2.2.5.5 Determination of protein concentration**

The protein concentration was measured using the Bradford method (Bradford, 1976) and the Roti-Quant solution (Carl Roth). A standard curve was calculated using bovine serum albumin (BSA).

### **2.2.5.6 SDS-PAGE**

SDS polyacrylamide gel electrophoresis was performed using the gel chamber system PROTEAN II from BioRad. 12 % SDS-PA gels were used as separating gels (with 5 % stacking gels) for the discontinuous SDS-PAGE using the Laemmli method (Laemmli, 1970) unless mentioned otherwise. The Pre-stained Protein Ladder Mix (Fermentas) was used as a protein marker.

### **2.2.5.7 Coomassie Brilliant Blue staining**

Proteins present in a gel or on a membrane after Western blotting were colored with staining solution (0.125 % (w/v) Coomassie blue R-250, 50 % (v/v) MeOH; 10 % (v/v) acetic acid). After incubation for 10 min at RT the unspecific stain was removed by destaining solution (50 % (v/v) MeOH, 10 % (v/v) acetic acid).

### **2.2.5.8 Western blot analysis**

For the western blot analysis the proteins were transferred after SDS-PAGE onto a Hybond nitrocellulose membrane (GE Healthcare) using a Mini Trans-Blot® Electrophoretic Transfer Cell (BioRad) for one hour at 100 V. The protein transfer was controlled by Ponceau S red stain (0.1 % (w/v) Ponceau S red and 5 % (v/v) acetic acid).

Unspecific binding sites were blocked by incubation of the membrane for 1 hour at RT with 5 % (w/v) milk in either 1 xTBST (150 mM NaCl, 20 mM Tris-HCl; pH 7.6 and 0.1 % (v/v) Tween 20) or 1 x PBST (140 mM NaCl, 2.7 mM KCl, 10 mM Na<sub>2</sub>HPO<sub>4</sub>, 1.8 mM KH<sub>2</sub>PO<sub>4</sub>, 0.1 % (v/v) Tween 20).

Afterwards the membrane was incubated with a primary antibody overnight at 4°C. Then the membrane was washed for 3 x 5 minutes with 1 x TBST or 1 x PBST and incubated for 1.5 hours with a secondary antibody. The signal of a horseradish peroxidase-coupled secondary antibody was detected using the Enhanced Chemiluminescence Kit (GE Healthcare) according to the manufacturer's instructions. For the detection of an alkaline phosphatase-coupled secondary antibody the membrane was washed with 1 x TBST for 3 x 5 minutes and then equilibrated for 2 minutes with a Tris 9.5-buffer (150 mM Tris-HCl; pH 9.5, 5 mM MgCl<sub>2</sub> and 100 mM NaCl). The staining reaction was performed with 1 x BCIP/NBT in Tris 9.5-buffer (5-bromo-4-chloro-3-indolylphosphate; 200 x stock solution 50mg/ml in 70 % (v/v) dimethylformamide; Nitro-blue tetrazolium chloride; 200 x stock solution 50mg/ml in 100 % (v/v) dimethylformamide). After staining the membrane was washed with water.

### **2.2.5.9 CTAB western blotting**

After CTAB-PAGE separation (zymography, 2.2.5.14), proteins were transferred to a nitrocellulose membrane with 1/20 lower buffer with 0.05% CTAB, 200 ml methanol 200 V 350 mA for 2 hours. The subsequent steps were the same as with western blotting above (2.2.5.8).

### **2.2.5.10 MAPK kinase assay**

Total plant crude protein extract was isolated and subjected to a 12 % SDS-PAGE with 20 µl per lane, transferred to a nitrocellulose membrane, and detected with a primary antibody against phospho-p44/42-MAPK and secondary antibody.

### **2.2.5.11 Turbidity assay (PGN-hydrolysis assay)**

The turbidity assay was performed as described in Park et al. (Park et al., 2002). In brief, lytic activity towards *Micrococcus luteus* cell wall or *Bacillus subtilis* peptidoglycan

(Sigma, Invivogen) was measured and compared to that of 1  $\mu\text{g}$  hen egg-white lysozyme (HEWL, Sigma). 1 ml 0.02 % (w/v) *M. luteus* cells or PGN in 20 mM sodium acetate, pH 5.2 were incubated at 37°C together with the enzyme, and the decrease in absorbance at 570 nm of the suspension was measured with a spectrophotometer over time. Approximately 60  $\mu\text{g}$  total protein of the leaf extract and 15  $\mu\text{g}$  total proteins of the protoplast samples were added to the reaction solutions.

### 2.2.5.12 4-MUC cellulose assay

The cellulose hydrolysis assay was performed using 4-methylumbelliferyl- $\beta$ -D-cellobioside (4-MUC, Sigma-Aldrich) as substrate. 1 mM 4-MUC was incubated in 20 mM sodium acetate (pH 5.2) at 37°C for 1 hour in a 96 well plate with either 40  $\mu\text{g}$  purified LYS1 or cellulose (Duchefa, Haarlem, The Netherlands) in a total volume of 100  $\mu\text{l}$ . The reaction was stopped with 0.2 M  $\text{Na}_2\text{CO}_3$ , and the intensity of the fluorescence was monitored with an MWG Sirius HT fluorescence microplate reader, using excitation and emission wavelengths of 365 nm and 455 nm, respectively.

### 2.2.5.13 4-MUCT assay (Chitin-hydrolysis assay)

The 4-MUCT assay was performed as described in Brunner et al. (Brunner et al., 1998). In brief, the hydrolytic activity towards the substrate 4-methylumbelliferyl- $\beta$ -D-N, N', N'' triacetylchitotriose (4-MUCT, Sigma) was measured and compared to that of 2  $\mu\text{g}$  *Streptomyces griseus* chitinase (Sigma). After enzyme incubation in 250  $\mu\text{l}$  final volume of 0.05 % (w/v) 4-MUCT in 20 mM sodium acetate, pH 5.2 at 37°C, 20  $\mu\text{l}$  of the reaction mixture were removed and added to 980  $\mu\text{l}$  0.2 M sodium carbonate solution. Free 4-MU (Sigma) was used for the generation of a standard curve. The intensity of the 4-MU fluorescence in the samples was monitored with an MWGt Sirius HT fluorescence microplate reader (absorbance at 360 nm and emission at 450 nm). The same protein amounts were used as for the turbidity assay (see above).

### 2.2.5.14 Zymography

A discontinuous CTAB polyacrylamid gel electrophoresis was performed using a 12% separating gel (43 mM KOH, 280 mM acetic acid, pH4.0, 12% acrylamide bisacrylamide

37.5:1, 8% glycerol, 1.3% ammonium persulphate and 0.16% TEMED), overlaid by a 4% stacking gel (64 mM KOH; 94 mM acetic acid, pH5.1, 4% acrylamide, 1.25% ammonium persulphate and 0.125 mM TEMED). Prior to loading, the gel was pre-run using anode buffer (40 mM beta-alanine, 70 mM acetic acid, 0.1% CTAB, pH4.0) and cathode buffer (50 mM KOH, 56 mM acetic acid, pH5.7, 0.1% CTAB) for 1 hour at 250 volt. Crude protein extracts were mixed with an equal volume of loading buffer (5 M urea, 25 mM KAc pH6.8, Methylene blue) and separated for 2 hours at 150 volt and 4°C. After electrophoresis, the CTAB gel was washed with 20 mM NaAc and then sprayed with 0.00625% 4-MUCT in 20 mM NaAc, pH5.2 and incubated at 37°C for 30 minutes. Fluorescent bands were documented under UV light using the infinit-3026 WL/26MX gel imaging system (PeqLab, Erlangen, Germany).

### 2.2.5.15 HPLC analysis of PGN fragments

500 µg/ml *B.subtilis* PGN was incubated with 140 µg LYS1 purified from *LYS1<sup>OE</sup>* plants or controls in 20 mM NaAc pH5.2 at 37°C with shaking for the indicated time. After stopping the reaction by heating at 100°C for 10 minutes, the reaction was centrifuged and the supernatant analysed by HPLC. The analyses were done by CeCo labs on an Agilent 1200 system with a ProntoSil C18-RP column (Bischoff Chromatography, Leonberg, Germany).

## 2.2.6 Bioassays

### 2.2.6.1 Infection with *Pseudomonas syringae*

For the bacterial infection assay, an overnight culture of *Pseudomonas syringae* pv. *tomato* DC3000 was harvested by centrifugation, washed once with 10 mM MgCl<sub>2</sub> and finally diluted with 10 mM MgCl<sub>2</sub> to a density of 1 x 10<sup>4</sup> cfu/ml (OD600 ~2 x 10<sup>-5</sup>) and was then infiltrated with a 1ml-needleless syringe into the leaf apoplast. Two leaves per plant and 8 plants were infected per plant genotype. The growth of bacteria was determined after 0 and 2 days post infection. For the quantification, infected leaves were harvested (2 leaves at 0 dpi and 3 leaves at 2 dpi) and washed for one minute in both 70 % (v/v) EtOH and water. Afterwards 2 leaf discs per leaf with a diameter of 5 mm were cut out and homogenized in 200 µl 10 mM MgCl<sub>2</sub>. 10 µl of each homogenate were

then plated undiluted and in different dilutions onto LB agar plates and incubated at 28°C for 24-48 hours. The growth of bacteria was determined by colony counting, and subsequently mean values and standard deviations were determined.

### **2.2.6.2 Elicitation assays in leaves or seedlings**

Leaves of 4-6 week old plants were infiltrated using a needle-less syringe with solutions of PAMPs and harvested after indicated time points. For the seedling elicitation, seedlings were first cultivated on sterile ½ MS plates for 5-6 days in long-day. Then they were transferred into liquid MS medium supplemented with 1 % (w/v) saccharose (4-6 seedlings in 200 µl medium/well, 48-er well plate) and equilibrated overnight. After addition of the PAMPs, the seedlings were incubated with gentle shaking and harvested at indicated time points.

The PAMPs were used in elicitation assays in the following concentrations: 1 µM flg22 and 100 µg/ml chitin or PGN.

### **2.2.6.3 Medium alkalization assay**

Medium alkalization in cell culture upon PAMP treatment was performed as described previously (Gust et al., 2007). In brief, 300µl cultured cells were transferred to 48-well plates and equilibrated at 150 rpm for 30 minutes. After addition of PAMPs, the pH in the cell culture was monitored with an in Lab Microelectrode (Mettler Toledo, Gießen, Germany). The changes in pH were monitored and recorded by the Observer II program (Brainchild Electronics Co., Ltd, Taipei, Taiwan).

### **2.2.6.4 Oxidative burst assay**

Leaf discs were excised from 6 week-old Arabidopsis plants and incubated in water overnight. The following day, the discs were transferred to a solution of 20 µM luminol L-012 (Wako Pure Chemical Industries) in a 96-well plate supplemented with PAMPs. The plates were analyzed for a period of at least 30 min using a multiplate reader Centro LB 900 (Berthold Technologies). For each data point, at least 6 replicates were measured.

### 2.2.7 Microscopy

The visualization of fluorescence in samples was done using confocal laser scanning microscopy (TCS SP2, Leica). The images were taken using the 63x/1, 2 Plan Apo H<sub>2</sub>O objectives. The Software LCS Lite Version 2.61 was used for the processing of the images.

### Statistical analysis

Statistical analysis was performed using Microsoft Office Excel. The data represent the average of replicates with standard deviation (SD) or standard error (SE). Statistical significance between two groups has been checked by using a two-tailed unpaired Student's t test. For multiple comparisons, the one-way ANOVA method was performed combined with the Tukey's honest significant difference (HSD) test. Significant differences are indicated with different letters ( $p < 0.01$ ). Asterisks represent significant differences (\* $p < 0.05$ ; \*\* $p < 0.01$ ; \*\*\* $p < 0.001$ ).

### 3. Results

#### 3.1 Identification of an *Arabidopsis* PGN hydrolase

##### 3.1.1 An induced PGN-degrading activity in *Arabidopsis* is not due to PGN receptors LYM1 and LYM3

Both, complex insoluble PGN fractions prepared from bacterial cell walls as well as mixtures of soluble oligomeric PGN fragments have previously been shown to stimulate plant immune responses in *Arabidopsis* (Gust et al., 2007; Erbs et al., 2008; Willmann et al., 2011), suggesting that partially hydrolyzed ligands could potentially serve PRR-mediated immune activation. Therefore we aimed to identify such PGN-hydrolase activity in *Arabidopsis*. Plant genomes do not encode lysozyme-like proteins, but many plant species engage in lysozyme-like activities under induced conditions (Brunner et al., 1998; van Loon et al., 2006). In *Arabidopsis*, we tested if lysozyme-like activities can also be induced by bacteria-derived PAMPs. To do this, a standard lysozyme assay (Park et al., 2002) was employed to determine PGN-degrading activity based on turbidity reduction in suspensions of Gram-positive *Micrococcus luteus* cell wall preparations. As shown in Figure 1, significant cell wall-degrading activities were detected in the extracts from leaves infiltrated with both Flg22 and PGN, compared with the water infiltration, indicating that these PAMPs induce *Arabidopsis* leaves to generate lysozyme-like lytic activities.

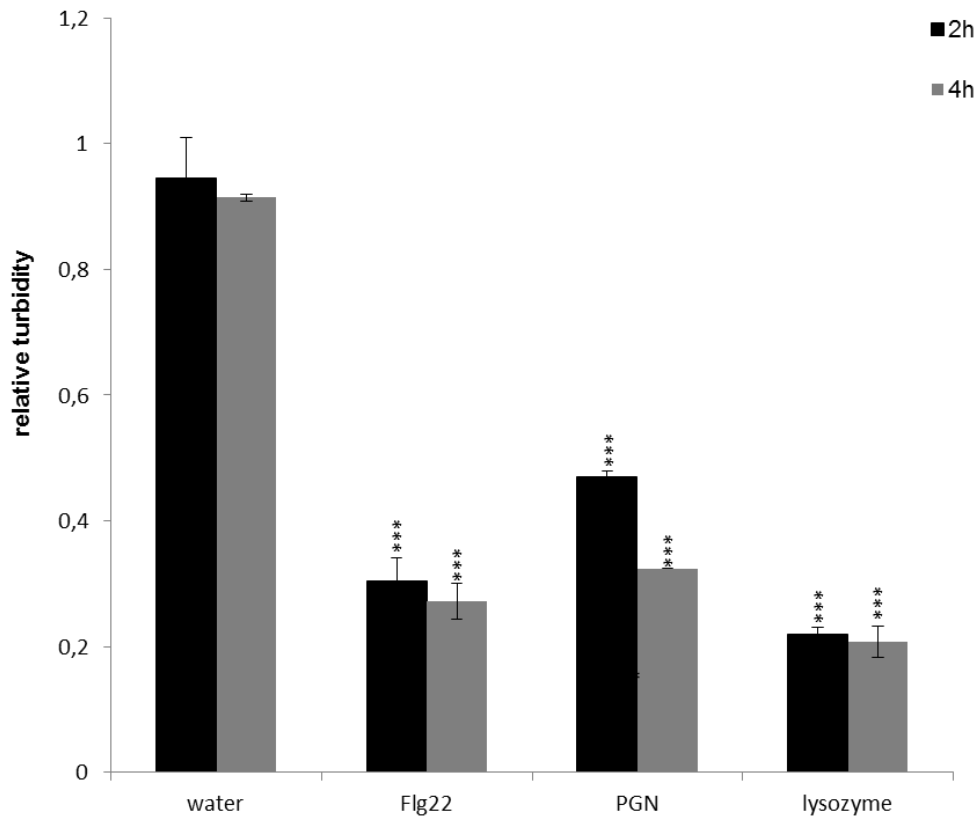


**Figure 1. Bacterial PAMPs induce lysozyme-like activities in *Arabidopsis*.**

*Micrococcus luteus* cell wall preparations were incubated with 40  $\mu\text{g}$  protein crude extracts from *Arabidopsis* leaves 6 hours post infiltration with water, 1  $\mu\text{M}$  Flg22 or 100  $\mu\text{g}/\text{ml}$  PGN. PGN hydrolytic activity was assayed in a turbidity assay at the indicated time points. *M.luteus* cells were incubated together with the crude extracts and the turbidity in absorbance at 570 nm of the suspension was measured with a spectrophotometer over time. As positive control, *Micrococcus luteus* cell wall preparations were incubated with 0.5  $\mu\text{g}/\text{ml}$  hen egg white lysozyme. Means  $\pm$  SD of three replicates per sample are given. Statistical significance compared with the water infiltration (\*\*\* $p < 0.0001$ , Student's t test) is indicated by asterisks.

In metazoan, some PGN recognition proteins (PGRPs) harbor PGN lytic activities (Gelius et al., 2003; Wang et al., 2003). Here, we investigated whether LYM1 and LYM3, the two *Arabidopsis* PGN receptors (Willmann et al., 2011), were also able to catalyze PGN degradation in a standard lysozyme assay. As shown in Figure 2, neither recombinantly expressed and purified LYM1 nor LYM3 displayed cell wall-degrading

activity. Thus we propose that the induced lysozyme activities in *Arabidopsis* result from some other, yet unknown PAMP-induced enzyme(s).

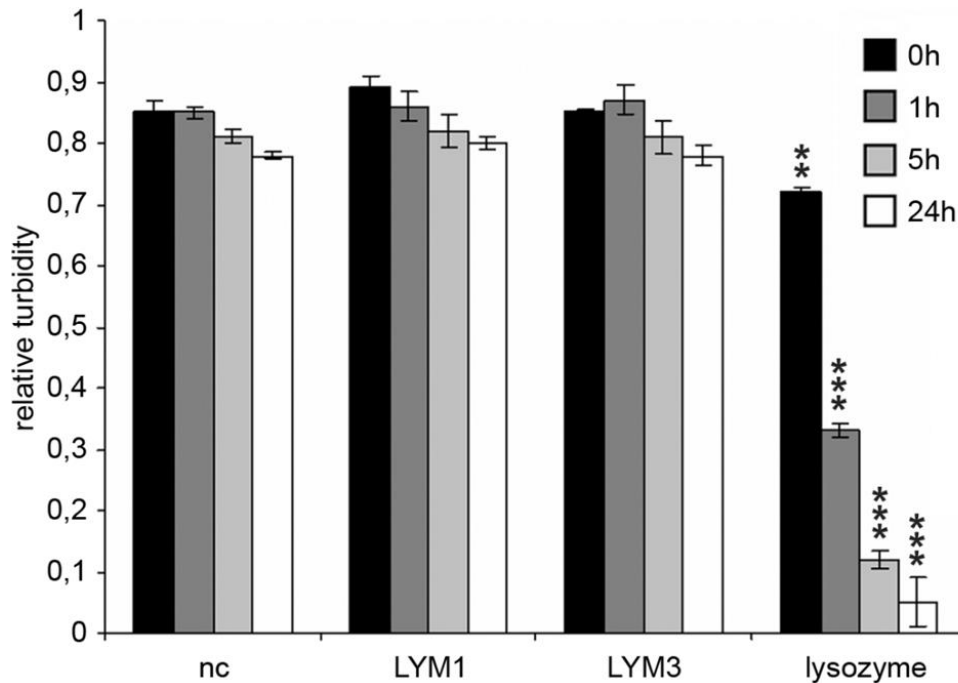


**Figure 2. LYM1 and LYM3 do not possess PGN hydrolytic activity.**

*Micrococcus luteus* cell wall preparations were incubated with 20  $\mu$ g affinity-purified His6-tagged LYM1 or LYM3 or 0.5  $\mu$ g hen egg-white lysozyme and PGN hydrolytic activity was assayed in a turbidity assay at the indicated time points. As negative control (nc), non-induced His6-tagged LYM3 bacterial lysates were used for affinity purification and elutes were subjected to turbidity assays. Means  $\pm$  SD of three replicates per sample are given. Statistical significance compared with the negative control (\*\* $p < 0.001$ , \*\*\* $p < 0.0001$ , Student's t test) is indicated by asterisks. The data for this figure were kindly provided by Roland Willmann.

### 3.1.2 Identification of LYS1 as a potential PGN hydrolase

Lysozymes (EC 3.2.1.17) hydrolyze  $\beta$  (1, 4) linkages between GlcNAc and MurNAc residues in PGNs and between GlcNAc residues in chitodextrins (enzyme.expasy.org). Although lysozyme-like sequences were not found in plant genomes, some plant chitinases were reported to display lysozyme-like activities (Audy et al., 1988; Sakthivel et al., 2010). For example, hevamine, one class III chitinase from the rubber tree has been shown to harbor PGN hydrolysis activity (Bokma et al., 1997). Similarly, two

tobacco class III chitinases, lysb1 and lysb2 were also found to harbor lysozyme activity (Brunner et al., 1998).

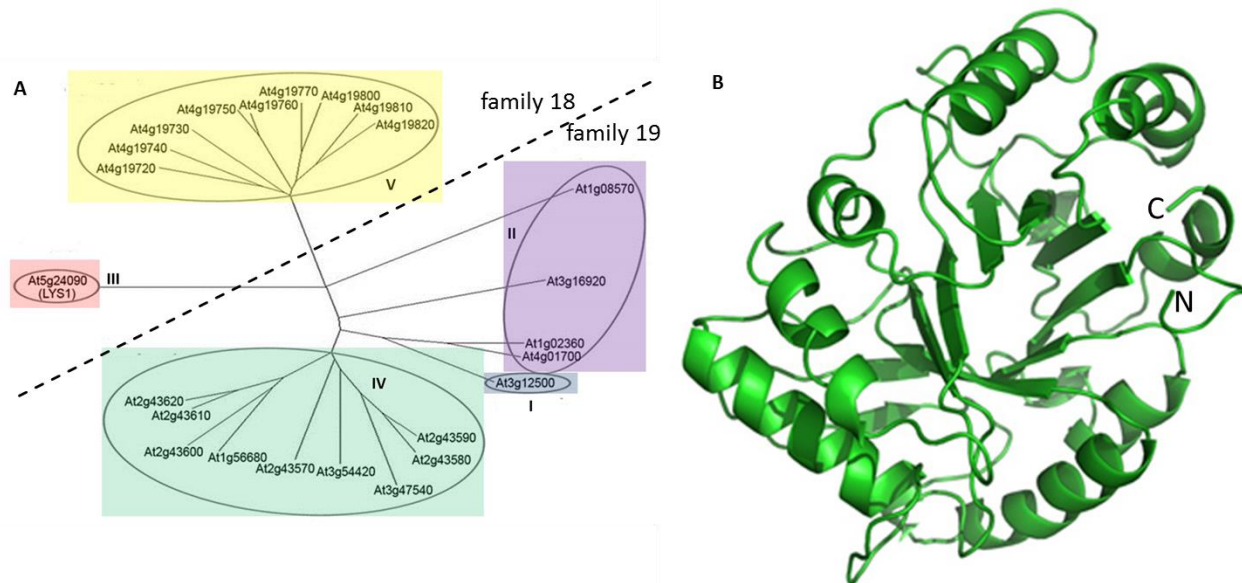


**Figure 3. Protein sequence alignment of the 24 *Arabidopsis* chitinases and cartoon diagram of the 3D structure of LYS1.** (A) Full length amino acid sequences were aligned with the ClustalW2 algorithm and subgroups were classified according to their sequences and structures (Passarinho and de Vries, 2002). *Arabidopsis* lysozyme 1 (LYS1, At5g24090, formerly also named CHIA) represents the only member of class III. (B) Full length amino acid sequences of LYS1 (At5g24090) was predicted using Phyre server (Kelley and Sternberg, 2009) and a ribbon diagram was created with the Pymol program. A typical (βα)<sub>8</sub> barrel fold is shown in the image. N and C indicate N-terminus and C-terminus of LYS1, respectively.

Chitinases (EC 3.2.1.14) hydrolyze β (1, 4) linkages between GlcNAc in chitin and chitodextrins (enzyme.expasy.org). *Arabidopsis* chitinases fall into five groups (Figure 3A) (Passarinho and de Vries, 2002), and are grouped into structurally unrelated families 18 and 19 of glycosyl hydrolases (Henrissat, 1991), respectively. As mentioned above, the class III chitinases (glycosyl hydrolase family 18) from rubber tree and tobacco displayed bifunctional activities: chitinase and lysozyme activity. Of the 24 annotated members of *Arabidopsis* chitinases, LYS1 (At5g24090, formerly also named CHIA) is the only member of class III (Figure 3A). Alignment of LYS1 with rubber tree hevamine resulted in approximately 70% identity (Grabherr, 2011). LYS1 was predicted to have a

typical ( $\beta\alpha$ )<sub>8</sub> barrel fold (Figure 3B). All these information make LYS a perfect PGN hydrolase candidate. Thus, we chose LYS1 as a putative lysozyme candidate for further studies.

### 3.1.3 Expression of epitope-tagged LYS1 and identification of active LYS1

In order to analyze the enzymatic properties of LYS1 *in vitro*, heterologous expression of LYS1 was attempted. Overexpression in *E.coli* failed to produce active enzyme and LYS1 production in eukaryotic *Pichia pastoris* entirely failed to produce recombinant protein (Grabherr, 2011). Thus, *LYS1* overexpression (*LYS1*<sup>OE</sup>) lines carrying a *p35S::LYS1-GFP* cassette were created in the Col-0 background using the floral dipping method (Grabherr, 2011). We first examined LYS1 protein levels in *LYS1*<sup>OE</sup> lines using two different antibodies for Western blotting analysis. The first antibody was anti-GFP which could be used to detect the fused LYS1-GFP in the *LYS1*<sup>OE</sup> plants. The second antibody, which was raised in rabbit against the tobacco class III chitinases (kindly provided by Dr.Frédéric Brunner), could be tested for recognition of the native LYS1 and the LYS1-GFP fusion. The  $\alpha$ -GFP antibody detected specific bands in leaf extracts of *LYS1*<sup>OE</sup> lines with sizes of approximately 60 kDa and 30 kDa (Figure 4, right panel), which correlated with the expected sizes of the LYS1-GFP fusion (60.1 kDa) and free GFP (27 kDa).

The detection of LYS1 using the  $\alpha$ -class III chitinase antibody revealed a more complex pattern of protein bands. In the *LYS1*<sup>OE</sup> lane a clear band appeared below the 35 kDa marker band (Figure 4, left panel). This protein band possibly represents the free LYS1 protein, which has the calculated size of 33.1 kDa without the GFP tag. A weak band in the size of the LYS1-GFP fusion protein at about 60 kDa was also present in the *LYS1*<sup>OE</sup> lane. It is possible that the large GFP tag interferes with the recognition of the LYS1 protein by the  $\alpha$ -class III chitinase antibody, leading to weaker detection of the GFP-tagged LYS1. Alternatively, a major amount of LYS1 in the *LYS1*<sup>OE</sup> line is not present as GFP-fusion but as free LYS1 (Figure 4, left panel). In the same immunoblot analysis we also included an amiRNA knockdown line, which will be introduced in chapter 2.4.1. Here, the two antibodies detected no band either in the WT samples or in the *LYS1*<sup>KD</sup>

lanes, indicating undetectable levels of native LYS1 in the WT and absence of any GFP in both plant types (Figure 4).

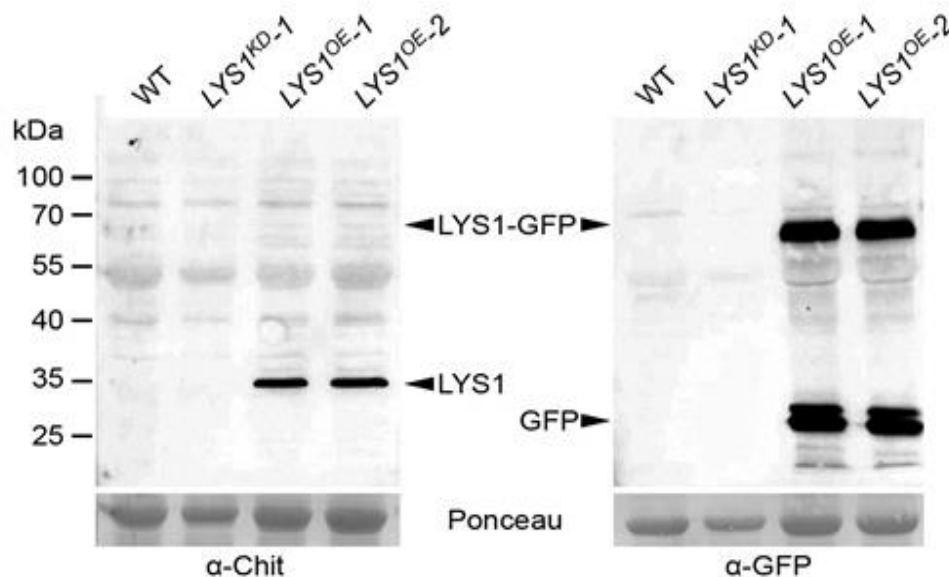


**Figure 4. Analysis of LYS1 protein levels in  $LYS1^{OE}$  lines.** Immunoblot analysis of protein extracts from leaves of two independent  $LYS1^{OE}$  lines, a  $LYS1$  knock-down line ( $LYS1^{KD-1}$ , see chapter 3.4.1) and wild-type plants (WT). Total leaf protein was separated by SDS-PAGE and blotted onto a nitrocellulose membrane. Immunodetection was carried out using antibodies raised against  $\alpha$ -tobacco class III chitinase ( $\alpha$ -Chit) or green fluorescent protein ( $\alpha$ -GFP). Ponceau S red staining of the large subunit of RuBisCO served as loading control.

To analyze LYS1 enzymatic properties, we resorted to isolating active LYS1 from plant hosts including the stable LYS1 expressor-*Arabidopsis* lines  $LYS1^{OE}$  and transient LYS1 expression in *N. benthamiana*. At first an immunoprecipitation (IP) approach was exploited to enrich and purify LYS1 from  $LYS1^{OE}$  plants. Protein-G agarose beads were coupled with the anti-GFP antibody and then used to pull down LYS1-GFP from protein extracts of  $LYS1^{OE}$  plants (Figure 5A). Protein G-isolated LYS1 was subjected to a PGN hydrolysis assay (Figure 5B) and immunoblotting (Figure 5C). As shown in Figure 5C, western blot analysis showed a clear band of LYS1-GFP in the lane with the Protein-G-bound sample from  $LYS1^{OE}$  plants, indicating successful isolation and enrichment of LYS1-GFP by this IP. However, the PGN activity assay revealed that the immunopurified LYS1-GFP protein did not display any PGN hydrolytic activity in comparison to respective samples derived from the wild type control (Figure 5B). If we compare PGN

hydrolytic activities of fractions shown in Figure 5B with their corresponding Western blot band intensities shown in Figure 5C, obviously LYS1-GFP amounts did not correlate with PGN hydrolytic activity.

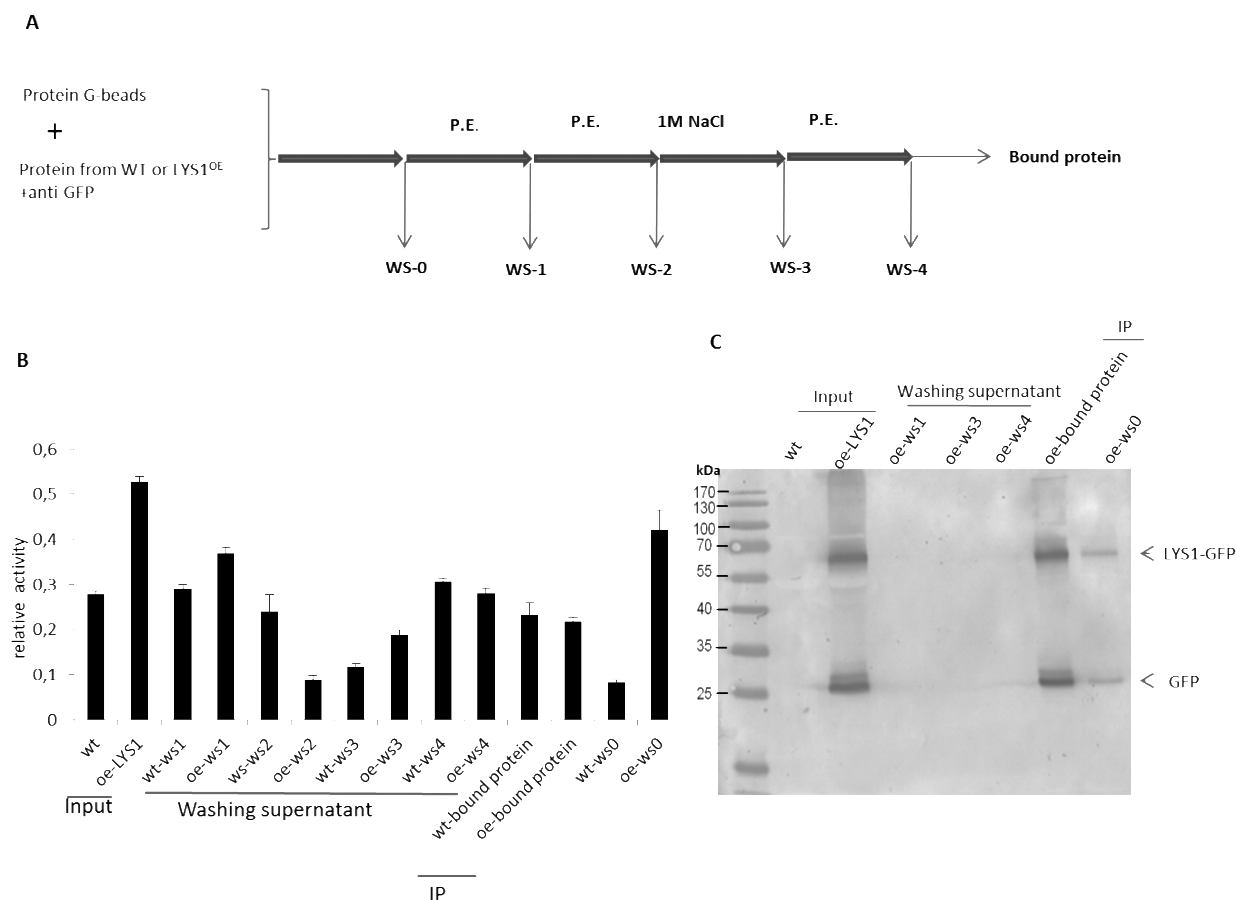


**Figure 5. Isolation and analysis of LYS1-GFP via immunoprecipitation (IP).** (A) Schematic drawing of purification steps. Protein-G beads were incubated with crude protein extracts of LYS1<sup>OE</sup> (oe) or wild type (wt) plants, and washed afterwards four times with the indicated buffers (P.E., protein extraction buffer), collecting the washing supernatant (ws) after each step (0-4). Bound proteins were collected and used for a PGN hydrolysis assay (B) and Western blotting analysis (C). (B) *Bacillus subtilis* PGN suspension was incubated with the fractions indicated in (A). Relative PGN hydrolytic activities were calculated after 2 hours incubation using hen egg-white lysozyme as standard (set to 1). Shown are the means  $\pm$  SD of 3 replicates. (C) Fractions indicated in (A) were separated by SDS-PAGE and blotted onto a nitrocellulose membrane. Immunodetection was carried out using an anti-GFP antibody. Arrowheads indicate positions of LYS1-GFP and GFP.

We thus assume that the IP-isolated LYS1-GFP does not have any lysozyme-like activity, irrespective of higher PGN hydrolytic activities measured in the *LYS1<sup>OE</sup>* input samples expressing *p35S::LYS1-GFP* than in wild type samples (Figure 5B).

To further confirm our assumption that LYS1-GFP does not harbor lysozyme-like activity, a CTAB-PAGE zymography assay was performed to analyze the protein extracts derived from *LYS1<sup>OE</sup>* plants. In a conventional Laemmli SDS-PAGE (Laemmli, 1970) in which proteins are separated based on their sizes, SDS often destroys the protein activities. In contrast, in a CTAB-PAGE protein activities can be retained while proteins are also separated based on their sizes (Akins et al., 1992). The CTAB-PAGE system was therefore employed here to identify the responsible protein for lysozyme-like activity in *LYS1<sup>OE</sup>* lines. Following some initial experiments with various buffer systems based on *in silico* design (Jovin, 1973), an acidic buffer system was finally chosen as the only one that yielded LYS1 activity in a following zymography (see details in the method section).

As shown in Figure 6A, the zymography results revealed that in the LYS1-GFP sample fluorescent bands appeared at the expected position of LYS1 (33.1 kDa) but not at the expected size of LYS1-GFP (60.1 kDa) (Figure 6A, left panel), although a parallel immunoblot detection showed visible bands for LYS1-GFP in the LYS1-GFP sample (Figure 6A, right panel), suggesting that free LYS1 but not the LYS1-GFP fusion protein harbors enzyme activity. As a negative control, protein extracts from plants stably expressing secreted GFP (secGFP) (Teh and Moore, 2007) were included. The result is in agreement with the one shown in Figure 5, where IP-isolated LYS1-GFP was also not responsible for PGN hydrolytic activity (Figure 5B). Likewise, CTAB-PAGE-zymography analysis of transiently expressed LYS1-GFP from *N. benthamiana* revealed that LYS1-GFP did not display hydrolytic activity (Figure 6B).

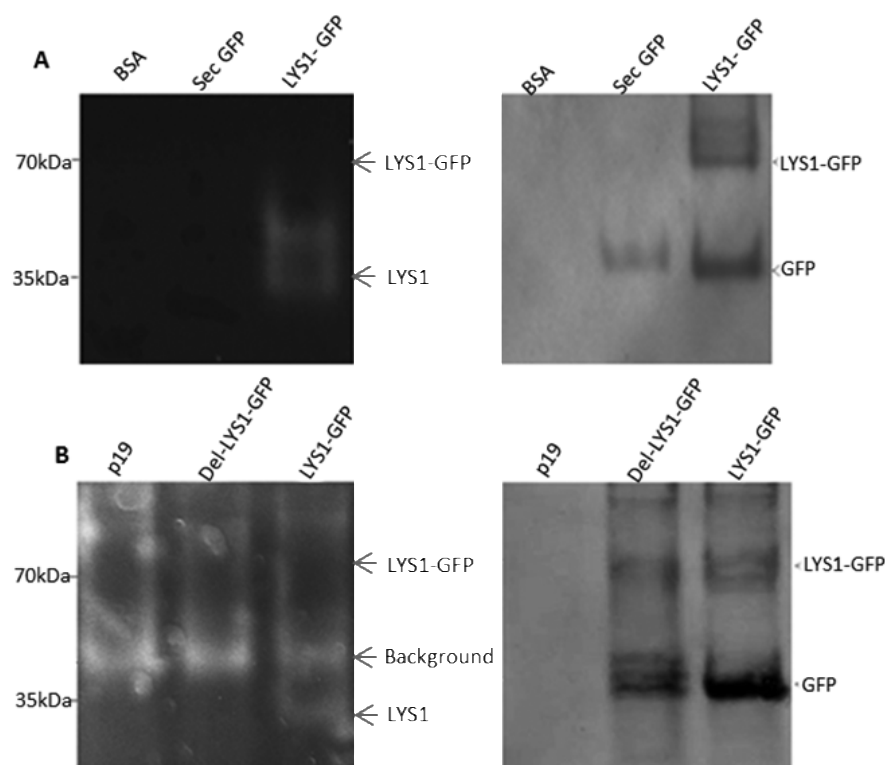


**Figure 6. CTAB-PAGE zymography and immunoblot analysis of extracts of *LYS1<sup>OE</sup>* plants and *N. benthamiana* transiently expressing LYS1-GFP.** (A) Protein extracts from *LYS1<sup>OE</sup>-1* or *secGFP* plants were separated on a cetyltrimethylammonium bromide (CTAB) –polyacrylamide (PA) gel and hydrolytic activity was assayed in a zymogram by overlaying the gel with the substrate 4-MUCT. BSA served as negative control. Fluorescent bands are indicative of substrate cleavage (left panel). The proteins were blotted from the CTAB gel onto a nitrocellulose membrane and detected using an anti-GFP antibody (right panel). Arrowheads indicate the positions of LYS1-GFP, LYS1 and GFP. (B) Protein extracts from *N. benthamiana* leaves transiently expressing *p35S::LYS1-GFP*, *p35S::del-LYS1-GFP* (deletion of signal peptide) or p19 were separated on a CTAB-PA gel, and hydrolytic activity (left panel) or protein expression using an anti-GFP Western blot (right panel) were analysed as described in (A). Indicated by arrowheads are the positions of the LYS1-GFP fusion and free LYS1 or GFP and of an unspecific background band appearing due to *Agrobacterium* infiltration, thus also present in the p19 negative control.

Here a construct expressing LYS1-GFP without the LYS1 secretion peptide (del-LYS1-GFP) (Grabherr, 2011) was included. Notably, no activity was detected at the expected position of LYS1 (33.1 kDa) in the del-LYS1-GFP sample (Figure 6B, left panel), although del-LYS1-GFP was detected in immunoblotting analysis (Figure 6B, right panel), indicating that proper secretion is required for LYS1 activity. We thus assume

that LYS1 undergoes some posttranslational processing to generate an active form in a secretion pathway

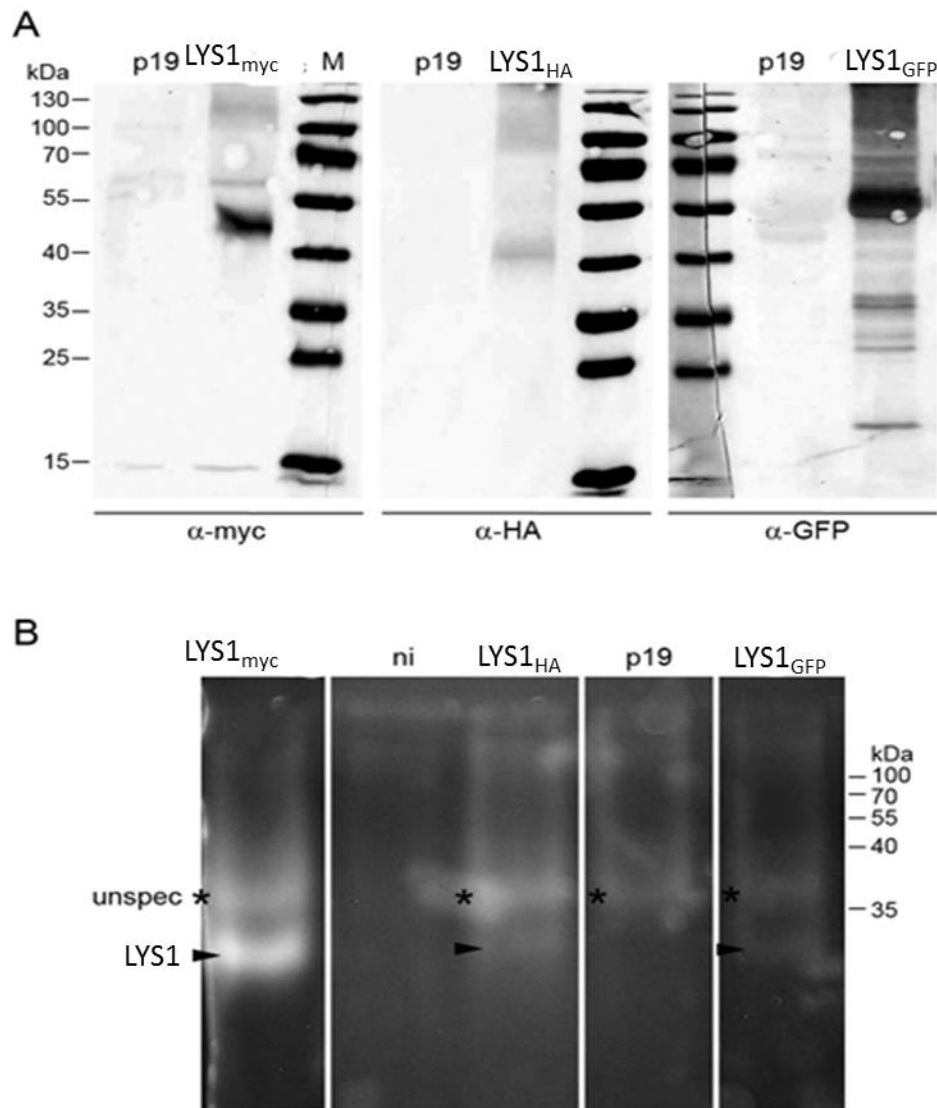


**Figure 7. Transiently expressed LYS1 is a glucan hydrolase.** (A) Protein extracts from *N. benthamiana* leaves expressing *p35S::LYS1* constructs containing different epitope tags ( $LYS1_{myc}$ ,  $LYS1_{HA}$  or  $LYS1_{GFP}$ ) were separated on a SDS-polyacrylamid gel and analysed by western blot using antibodies raised against the myc-, HA- or GFP-epitope tags. As control, plants were infiltrated with agrobacteria harboring the p19 suppressor of silencing construct (p19). Protein sizes (kDa) are indicated on the left. (B) *N. benthamiana* protein extracts expressing LYS1 ( $LYS1_{myc}$ ,  $LYS1_{HA}$  or  $LYS1_{GFP}$ ) or as control extracts from non-infiltrated (ni) or p19-infiltrated leaves were separated on a CTAB-polyacrylamid gel and hydrolytic activity was assayed by overlaying the gel with the substrate 4-MUCT. Fluorescent bands are indicative of substrate

cleavage. Arrowheads indicate the positions of epitope-tagged LYS1, an unspecific band in all samples infiltrated with agrobacteria is labelled with an asterisk.

We assumed that the large GFP tag in the LYS1-GFP fusion protein disturbed LYS1 activity while small tags might not. To address this question, *p35S::LYS1* with small and large epitope tags (myc, HA, GFP) were transiently expressed in *N. benthamiana*. Western blotting analysis showed that the three proteins were successfully expressed (Figure 7A), and a following CTAB-PAGE zymography revealed that all three extracts contain the active LYS1 at the expected position (Figure 7B). However, as myc and HA are very small epitope-tags and as the CTAB-PAGE has a poor resolution, it cannot be distinguished whether 4-MUCT-hydrolytic activity is derived from epitope-tagged LYS1 or the cleaved, native LYS1. Nevertheless, it was also observed that all three extracts displayed lysozyme-like activity towards 4-MUCT, *M. luteus* cells and *B. subtilis* PGN as shown in Figure 8A-C. Notably, the PGN hydrolytic activity of extracts expressing *LYS1<sub>myc</sub>* was the highest at about pH 5-6 (Figure 8D), which is approximately the same pH optimum observed for extracts from *LYS1<sup>OE</sup>* plants (Grabherr, 2011; Liu et al., 2014).

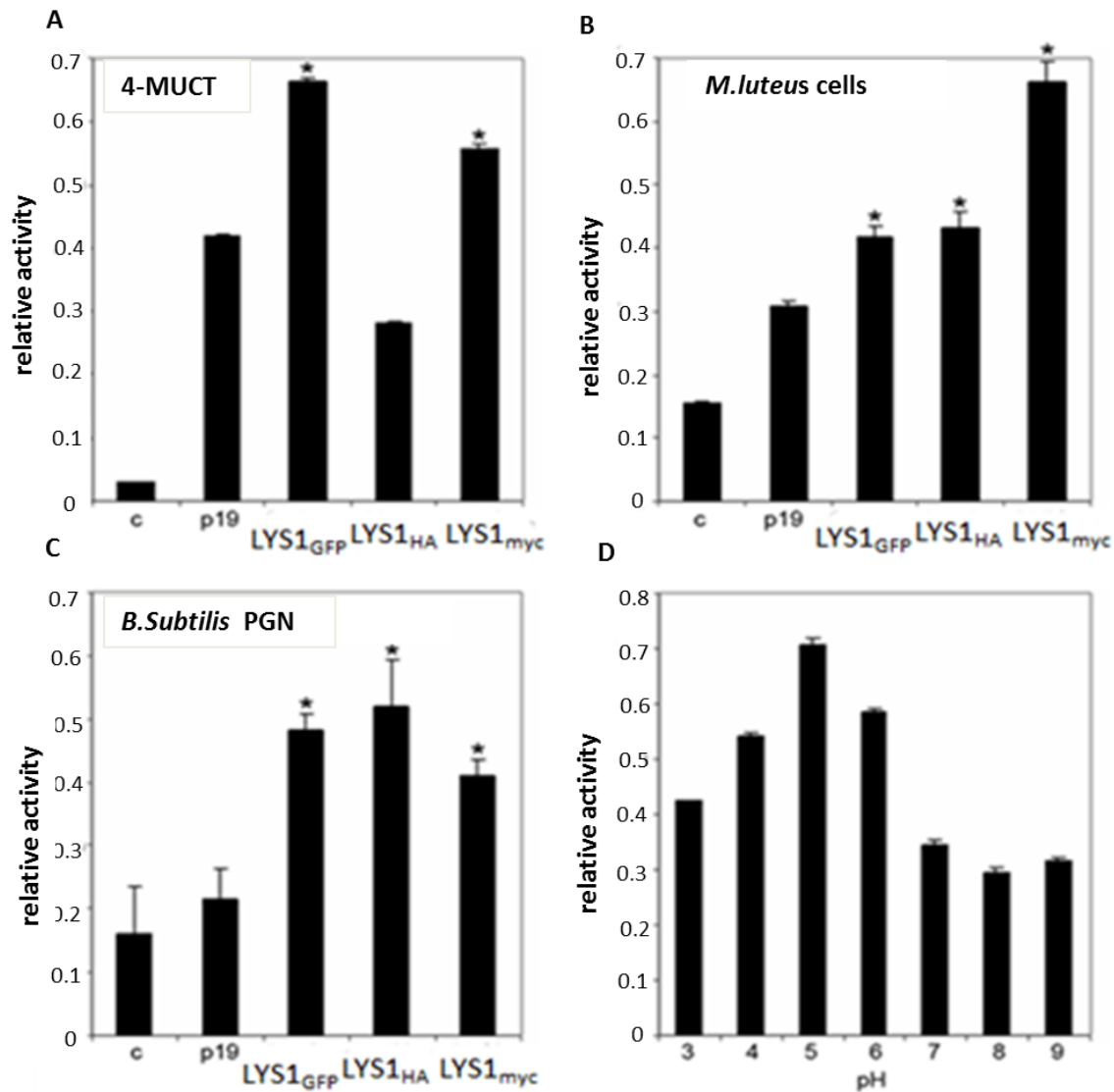


**Figure 8. Analysis of the activity of transiently expressed LYS1.** Protein extracts from *N. benthamiana* leaves expressing *p35S::LYS1* constructs containing different epitope tags (*LYS1<sub>GFP</sub>*, *LYS1<sub>HA</sub>* or *LYS1<sub>myc</sub>*) were assayed for chitinolytic activity with 4-MUCT substrate (A) or for PGN hydrolytic activity in a turbidity assay using *M. luteus* cells (B) or *Bacillus subtilis* PGN (C). Relative activities (2 hours incubation) were calculated using *Streptomyces griseus* chitinase (A) or hen egg-white lysozyme (B-D) as standards (set to 1). As control, plants were left untreated (c) or infiltrated with agrobacteria harboring the p19 suppressor of silencing construct (p19). (D) Lysis of *M. luteus* cells was determined in a turbidity assay with *LYS1<sub>myc</sub>* leaf protein extracts as described in (B) at the indicated pH. Means  $\pm$  SD of two replicates per sample are given. Significant differences in enzyme activities relative to those in the p19 control are indicated (\*,  $p \leq 0.05$ ; Student's t-test).

Next, the active LYS1 in the extracts expressing *LYS1<sub>myc</sub>* was separated by CTAB-PAGE, followed by pull-down and subsequent SDS-PAGE, and then analyzed by nano-LC MS/MS, which confirmed the identity of LYS1 (Figure 9). However, in the following PGN hydrolytic activity assay, IP-isolated LYS1-HA and LYS1-myc fusion proteins did not display enriched PGN-degrading activities either (Figure 10).

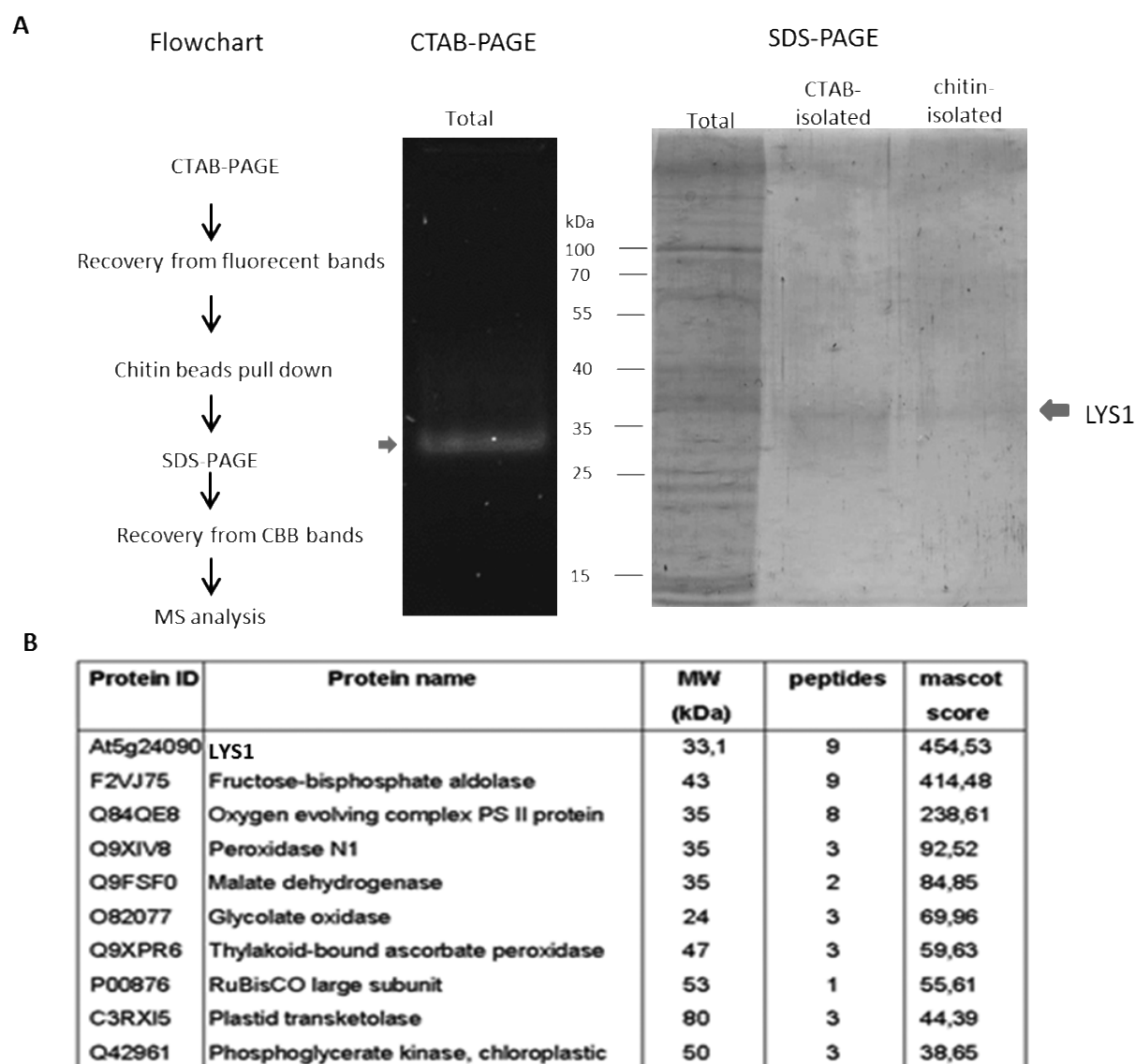


**Figure 9. Isolation and identification of active LYS1 transiently expressed in *N. benthamiana*.** (A) Total *N. benthamiana* protein extracts expressing *LYS1<sub>myc</sub>* were prepared (Total), separated on a CTAB-gel and hydrolytic activity was assayed by overlaying the gel with the substrate 4-MUCT (middle panel). Fluorescent bands were excised, and the eluted proteins were precipitated with insoluble chitin and separated by SDS-PA gel electrophoresis followed by Coomassie Brilliant Blue staining (right panel). A

flow chart illustrates the purification steps (left panel). (B) The band visible at approximately 35 kDa in (A) (arrow) was excised and the eluted proteins were subjected to nano-LC MS/MS analysis. Shown is a summary of protein hits obtained by MS/MS analysis. Only hits with a peptide number  $\geq 2$  and a Mascot score sum  $\geq 37$  were retained. Identification number (ID) from the tobacco proteome database and molecular weight (MW) of the identified proteins are indicated.

From these results we reasoned that all tested tags (GFP, HA or myc) were interfering with LYS1 enzymatic activity and the only active form is the untagged LYS1 derived from overexpression of epitope-tagged LYS1 in both *Arabidopsis* and *N. benthamiana*. As the LC-MS/MS analysis of the enzymatically active band shown in Figure 9 did not yield any chitinase-like enzymes in the cut-out band (Figure 9B), we could, however, rule out that a *N. benthamiana* protein is responsible for the observed 4-MUCT-cleavage.

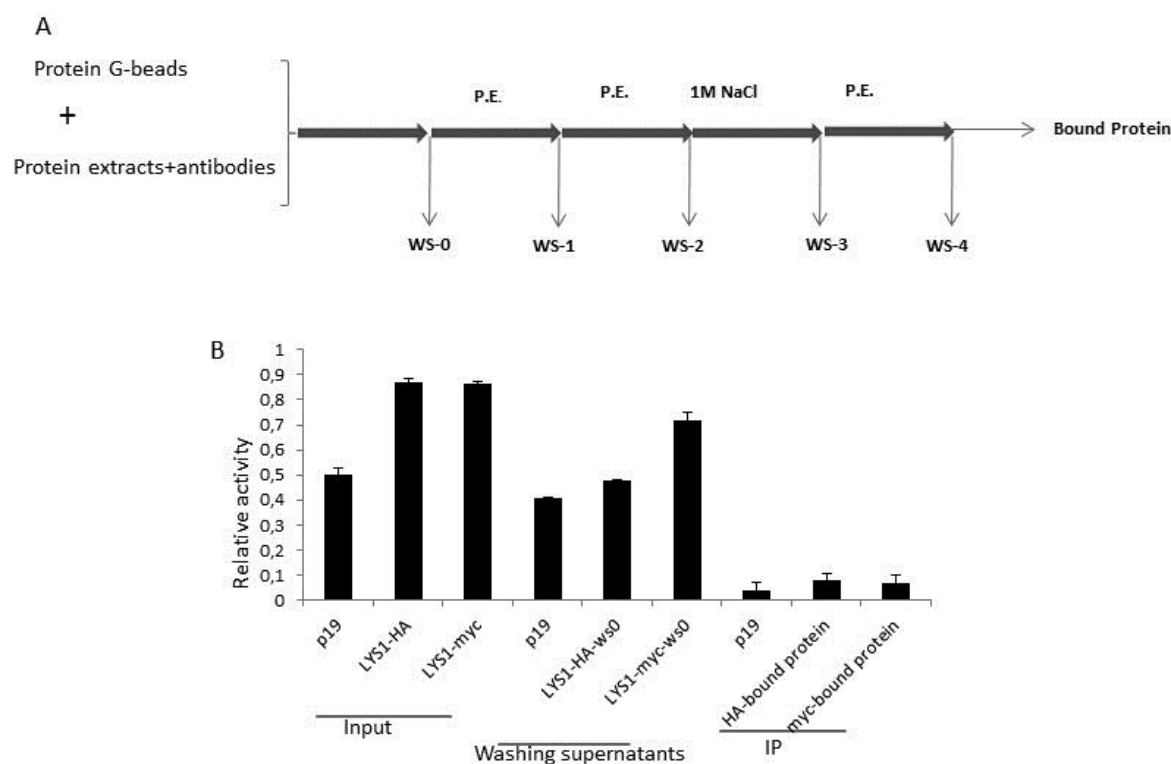


**Figure 10. Isolation and analysis of LYS1-myc and LYS1-HA via immunoprecipitation (IP).** (A) Schematic drawing of purification steps. Protein-G beads were incubated with crude protein extracts from *N. benthamiana* leaves expressing *p35S::LYS1-HA*, *p35S::LYS1-myc* or control leaves which were infiltrated with agrobacteria harboring the p19 suppressor of silencing construct (p19), and afterwards washed four times with the indicated buffers (P.E., protein extraction buffer), collecting the washing

supernatant (ws) after each step (0-4). (B) Proteins bound to Protein-G beads were collected and used for a PGN hydrolysis assay. *B.subtilis* PGN suspension was incubated with the fractions indicated in (A). Relative PGN hydrolytic activities were calculated after 2 hours incubation using hen egg-white lysozyme as standard (set to 1). Means  $\pm$  SD of 3 replicates per sample are given.

### 3.1.4 Purification of active LYS1 using FPLC

Since only the active LYS1 form seems to be the free LYS1 in *Arabidopsis* and *N. benthamiana*, and additional unspecific hydrolytically active proteins were induced upon *Agrobacterium*-infiltration in *N. benthamiana* (Figure 7B and 8), we next aimed at isolating the free LYS1 directly from *LYS1<sup>OE</sup>* leaf extracts. Based on some properties of the tested LYS1, we developed a method based on fast protein liquid chromatography (FPLC) to isolate and purify the active, untagged LYS1. Firstly, the isoelectric point of LYS1 was predicted to be 9.3 (arabidopsis.org), hence a cation-exchange chromatography was selected to separate LYS1 as a basic protein. Secondly, the optimum pH for LYS1 enzyme activity is between pH 5 and 6 (Figure 8D), and thus an acidic NaAc pH 5.2 buffer was used as FPLC buffer (Figure 11A). As shown in Figure 11, the collected fractions from the FPLC were validated for their activities by a 4-MUCT assay. The results revealed that fractions 41-45 displayed strong fluorescent signals, indicative of cleavage of the 4-MUCT substrate (Figure 11B, left panel). Further SDS-PAGE analysis with subsequent Coomassie Brilliant Blue staining of these fractions confirmed a band at around 35 kDa, the expected size of native LYS1 (Figure 11B, right panel). This 35 kDa-band was excised from the gel for subsequent nano-LC MS/MS analysis. The peptide mass fingerprint not only confirmed the identity of LYS1 in this band, but also yielded peptides spanning the whole protein sequence, except for the first 53 amino acids which are predicted to present a signal peptide (Figure 11C).

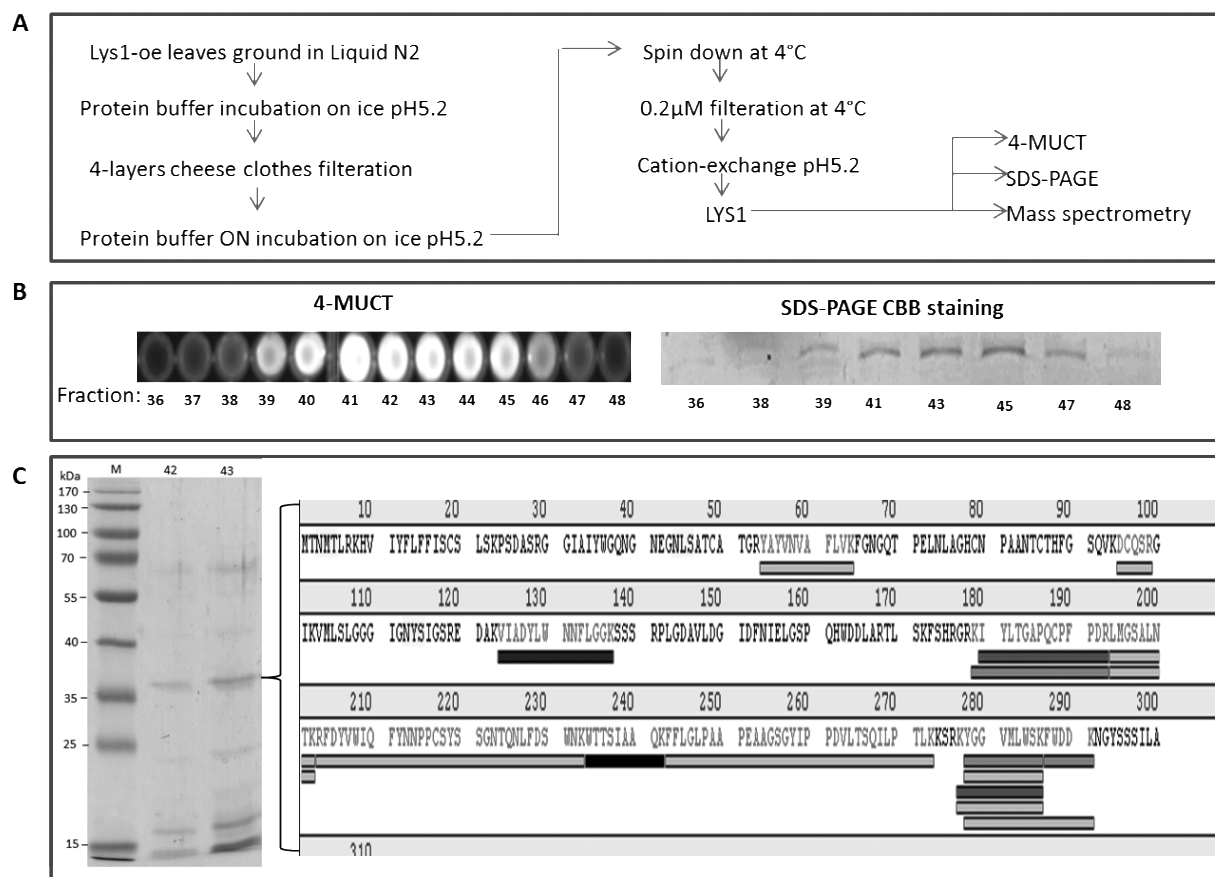


**Figure 11. FPLC purification of active LYS1 from  $LYS1^{OE}$ .** Cleaved untagged LYS1 was isolated via FPLC-purification (see materials and methods) from leaf tissue of transgenic  $LYS1$ -overexpressing ( $LYS1^{OE}$ ) *Arabidopsis* lines. (A) Flowchart of purification of LYS1. (B) FPLC elution fractions 36 - 48 were assayed for enzymatic activity using the 4-MUCT assay (left panel) and the presence of LYS1 protein was confirmed by SDS-PAGE and Coomassie Brilliant Blue staining (CBB, right panel). (C) Fraction 42 and 43 of the FPLC elution were separated on a SDS-PAGE and stained with Coomassie Brilliant Blue (left panel). The protein band at the expected size of LYS1 was excised and subjected to nano-LC MS/MS analysis. The MS identified peptides (highlighted in light grey letters in the sequence and indicated by grey bars below the sequence) were matched to the LYS1 amino acid sequence (right panel).

### 3.2 Characterization of LYS1

#### 3.2.1 LYS1 is a bifunctional enzyme with lysozyme- and chitinase-activity

FPLC-purified LYS1 was tested for its chitinolytic activity in a 4-MUCT assay. As shown in Figure 12A, compared with the control (respective purification with WT protein extract), purified samples from  $LYS1^{OE}$  extracts exhibited significant cleavage activities towards

4-MUCT. Thus, LYS1 indeed has the expected chitinase activity. Next, LYS1 was tested for its ability to solubilize complex PGN presented by intact Gram-positive *M. luteus* cells and to cleave preparations of complex, insoluble *B. subtilis* PGN. Again, purified samples from *LYS1<sup>OE</sup>* extracts exhibited significant cell-decomposing (Figure 12B) and PGN-degrading activities (Figure 12C) in comparison to the WT control.

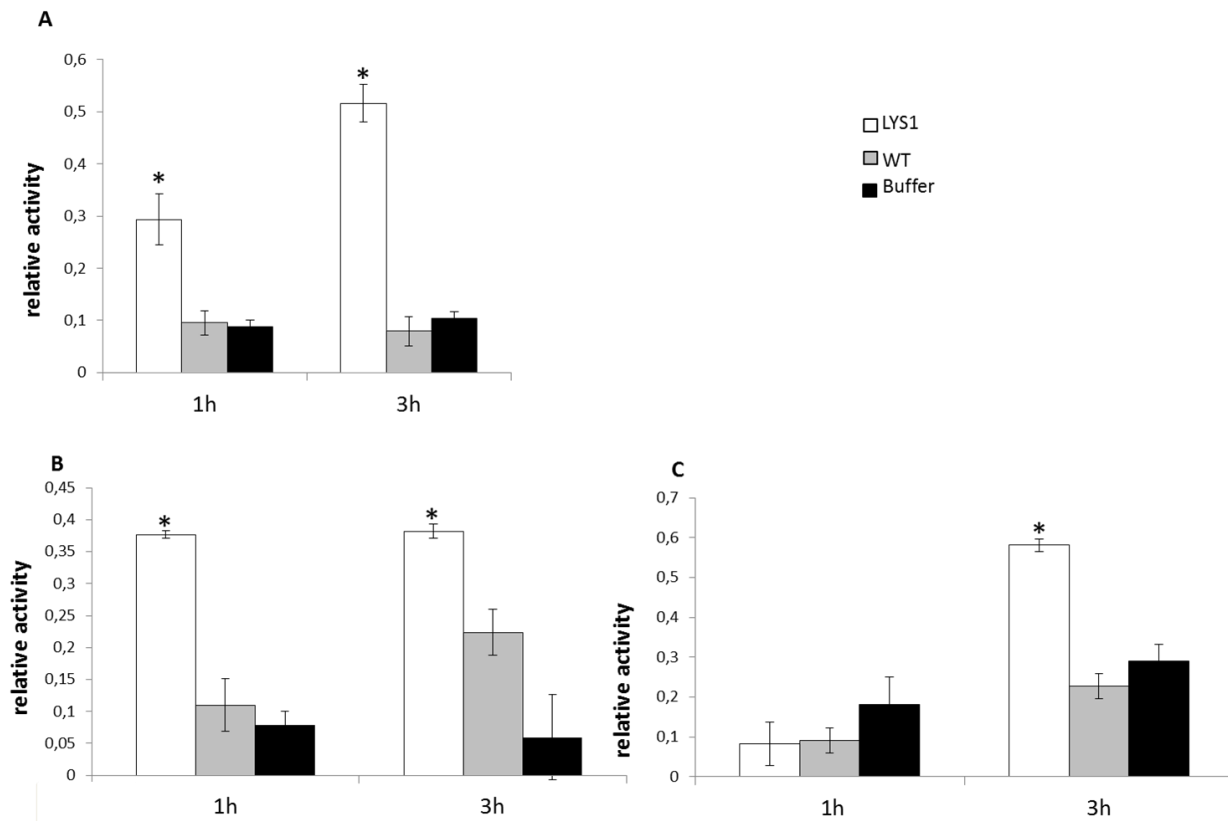


**Figure 12. Purified LYS1 from *LYS1<sup>OE</sup>* has glucan-hydrolase activity.** FPLC purified LYS1 protein (LYS1) from *LYS1<sup>OE</sup>* protein extracts and, as a control, a comparable FPLC-purified fraction from wild type leaf material (WT) were assayed for hydrolytic activity towards glycan substrates. (A) Assay for chitinolytic activity using the 4-MUCT substrate. Relative activities at 1 and 3 hours post treatment were calculated using *Streptomyces griseus* chitinase as standard. *S. griseus* chitinase activity was set to 1. (B, C) *Micrococcus luteus* cells (B) or *Bacillus subtilis* PGN (C) were subjected to hydrolysis by FPLC-purified LYS1 and hydrolytic activity was calculated at 1 and 3 hours after treatment using hen egg-white lysozyme as standard (set to 1). Significant differences compared with the buffer control (buffer) are indicated by asterisks (\* $p < 0.05$ ; Student's t test).

In addition, we also tested if LYS1 might have a potential cellulase activity. As shown in Figure 13, LYS1 did not display any cellulase activity compared to a commercial

cellulase. Hence, we conclude that LYS1, formerly identified as a chitinase, harbors a bifunctional lysozyme/chitinase activity.

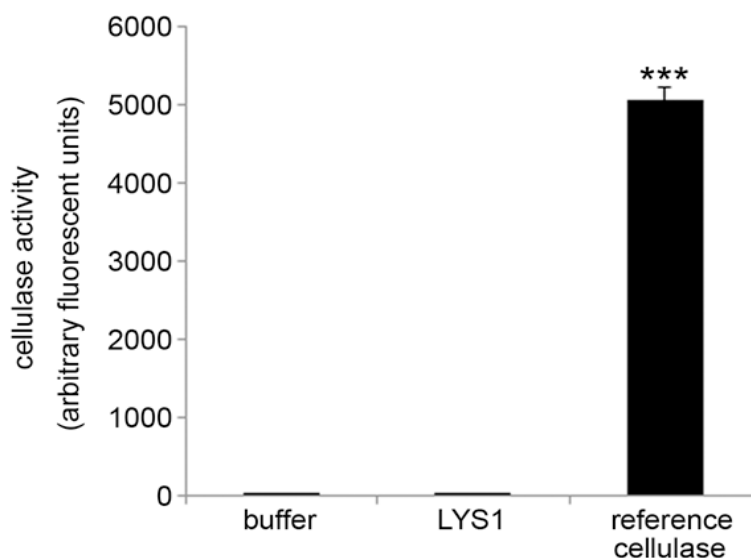


**Figure 13. LYS1 is devoid of cellulose hydrolytic activity.** LYS1 was purified from 5-week-old *LYS1<sup>OE</sup>* plants and used for cellulase activity assays. The substrate 4-methylumbelliferyl- $\beta$ -D-cellobioside was incubated for 1 hr with purified LYS1, commercial reference cellulase, or buffer as control. Fluorescence was determined (ex/em = 365 nm/455 nm) after stopping the reaction with 0.2 M sodium carbonate. Means  $\pm$  SD of three replicates per sample are given. Statistical significance compared with the buffer control (\*\*\*) $p < 0.001$ , Student's t test) is indicated by asterisks.

### 3.2.2 Enzyme Kinetics of LYS1

To determine specific enzyme activities, untagged LYS1 was purified from *LYS1<sup>OE</sup>* *Arabidopsis* lines by FPLC and used for enzyme assays. In a 4-MUCT assay LYS1 yielded a  $K_m$  of  $70 \pm 14 \mu\text{M}$  and a  $V_{max}$  of  $378 \pm 42 \mu\text{M min}^{-1} \text{mg}^{-1}$  for LYS1, and a  $K_m$  of  $53 \pm 27 \mu\text{M}$  and a  $V_{max}$  of  $397 \pm 145 \mu\text{M min}^{-1} \text{mg}^{-1}$  for commercial *S. griseus* chitinase. In a turbidity assay with *M. luteus* cell wall preparations, a  $K_m$  of  $18,2 \pm 2,5 \text{ mg/ml}$  and  $V_{max}$  of  $4,4 \pm 0,6 \text{ mg mg}^{-1} \text{ min}^{-1}$  were obtained for LYS1, and a  $K_m$  of  $8,4 \pm 0,8 \text{ mg/ml}$  and  $V_{max}$  of  $192 \pm 120 \text{ mg mg}^{-1} \text{ min}^{-1}$  for commercial hen egg white lysozyme. Thus, the  $K_m$  values for LYS1 are comparable to the commercial enzymes.

### 3.2.3 LYS1 localizes to the apoplast

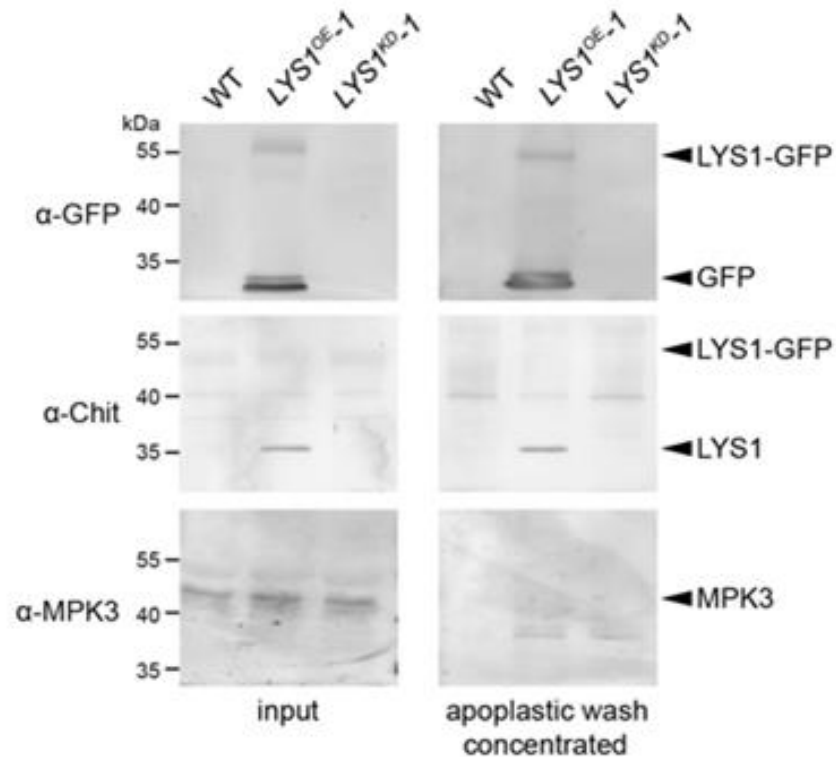


**Figure 14. LYS1 is localized to the apoplast.** Apoplastic washes were prepared from leaves of wild-type *Arabidopsis* plants or the *LYS1*<sup>OE-1</sup> and *LYS1*<sup>KD-1</sup> lines. Apoplastic fluids (concentrated tenfold) or total leaf protein extracts were subjected to western blot analysis using antibodies raised against green fluorescent protein ( $\alpha$ -GFP), tobacco class III chitinase ( $\alpha$ -chit), or the cytoplasmic mitogen-activated protein kinase 3 (MPK3).

LYS1 is predicted to contain a signal peptide and to be secreted into the plant apoplast. To confirm this localization of LYS1, we prepared apoplastic washes from *LYS1*<sup>OE</sup> *Arabidopsis* lines. Both the LYS1-GFP fusion protein as well as free LYS1 were detectable in concentrated apoplastic fluids whereas the cytoplasmic mitogen-activated protein kinase MPK3 was only present in the total leaf protein samples (Figure 14). Moreover, previous identification within the *Arabidopsis* cell wall proteome (Kwon et al., 2005) suggests that LYS1 acts in the plant apoplast. Furthermore, Heini Grabherr could demonstrate in her thesis that, in preparations of protoplasts from the *LYS1*<sup>OE</sup> line, increased hydrolytic activity as compared to the wild-type was mostly found in the

protoplast medium, again indicating that LYS1 has been secreted by the protoplasts (Grabherr, 2011; Liu et al., 2014).

### **3.3 Role of LYS1 in the generation of immunogenic PGN fragments**

#### **3.3.1 LYS1 generates plant immunogenic PGN fragments**

As LYS1 was shown to harbor PGN hydrolytic activity, we subsequently wanted to analyze immunogenic activities of PGN cleavage products generated by LYS1. Untagged LYS1 was purified from *LYS1<sup>OE</sup> Arabidopsis* lines by FPLC and used for degradation of *B. subtilis* PGN. Solubilized PGN fragments found in the supernatant of LYS1-digested PGN were subsequently analyzed by high performance liquid chromatography (Figure 15A). Few peaks could be detected in the supernatant of PGN incubated with a buffer control or with heat-inactivated LYS1. In contrast, PGN-digests produced by native FPLC-purified LYS1 (see 3.1.4) yielded several characteristic peaks that were also detectable in the supernatants of PGN preparations treated with mutanolysin, which has been shown to cleave O-glycosidic bonds between GlcNAc and MurNAc residues in complex PGN (Yokogawa et al., 1975)

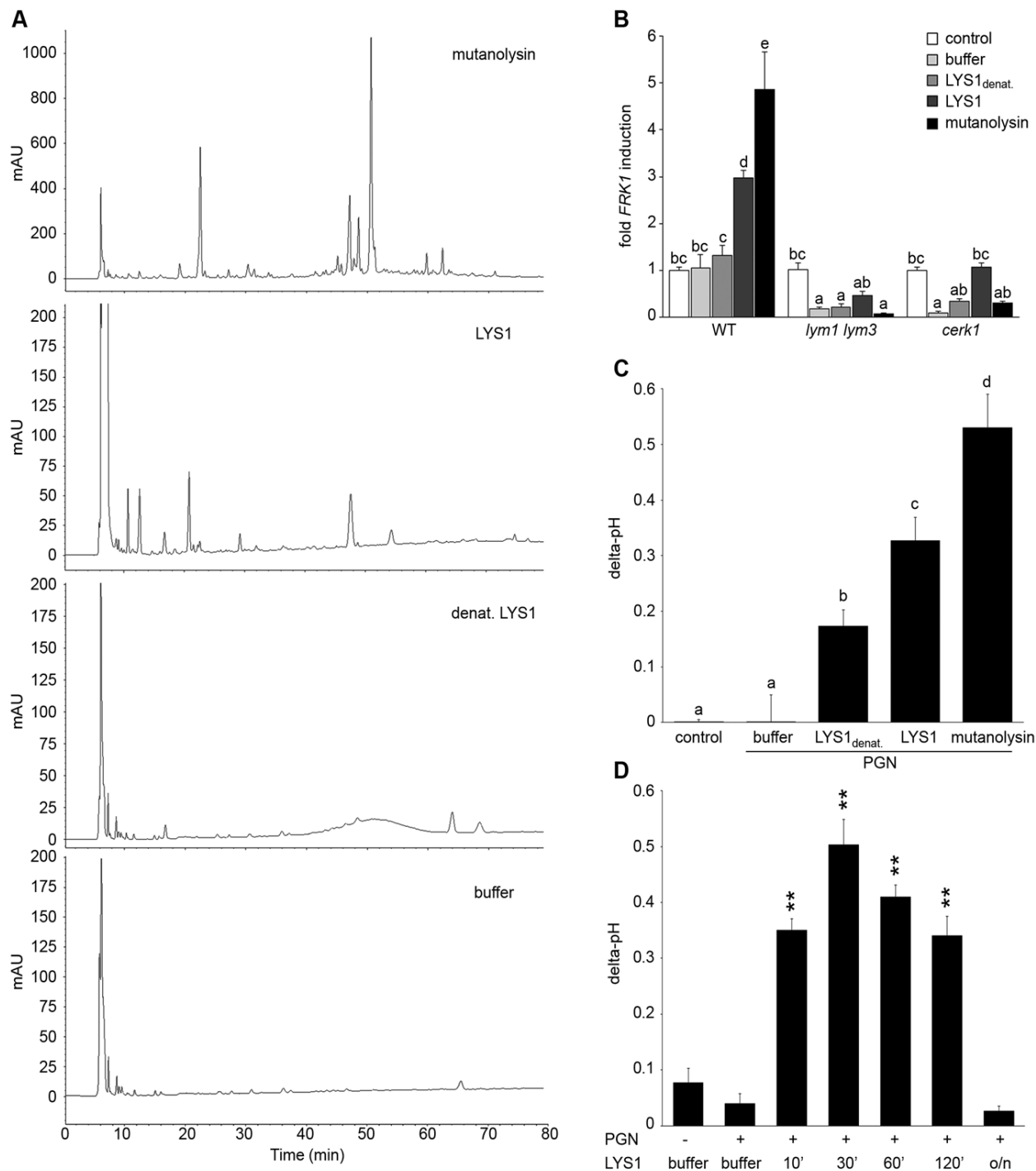


**Figure 15. Purified LYS1 generates immunogenic PGN fragments.** LYS1 was purified from 5 weeks old *LYS1<sup>OE</sup>* plants and used for PGN digestion. (A) 500  $\mu$ g of *Bacillus subtilis* PGN were digested for 7 hours with either mutanolysin (50  $\mu$ g/ml), native purified LYS1 (140  $\mu$ g/ml), heat-denatured purified LYS1 (140  $\mu$ g/ml) or the reaction buffer alone and subjected to HPLC fractionation. Shown are the peak profiles of representative runs. The signal intensity is given in milli absorbance units (mAU). (B) *B. subtilis* PGN

was digested for 4 h as described in (A) and *Arabidopsis* wild type seedlings or the indicated mutant lines were treated for 6 h with 25  $\mu$ l/ml digest supernatant containing solubilized PGN fragments. Total seedling RNA was subjected to RT-qPCR using *Flagellin responsive kinase (FRK1)* specific primers. *EF1 $\alpha$*  transcript was used for normalization; water treatment served as control and was set to 1. (C) Supernatants of digested PGN (25  $\mu$ l/ml) were added to cultured rice cells and medium alkalization was determined at 20 min post addition. Treatment with water or MES buffer served as control. All data represent triplicate samples  $\pm$  SD, and bars with different letters are significantly different based on one-way ANOVA ( $p < 0.05$ ; B, C). (D) *B. subtilis* PGN was digested with native purified LYS1 for the indicated times or overnight (o/n), and digest supernatant was used to trigger medium alkalization in rice cells as described in (C). All data represent triplicate samples  $\pm$  SD; asterisks indicate significant differences compared to the buffer control (\*  $p < 0.05$ ; \*\*  $p < 0.01$ ; \*\*\*  $p < 0.001$ ; Student's t test).

LYS1-generated PGN-fragments were subsequently tested for their abilities to trigger plant immunity-associated responses (Figures 15B-C). Firstly, supernatants of PGN preparations treated with either native or heat-denatured LYS1 were used to trigger immune marker gene *FRK1* expression in *Arabidopsis* seedlings. Importantly, only supernatants from PGN-digests produced by native LYS1 or mutanolysin induced *FRK1* expression whereas buffer controls or digests produced by heat-inactivated LYS1 did not release immunogenic soluble fragments from complex PGN (Figure 15B). Notably, activation of immune responses by LYS1-generated PGN-fragments was dependent on *Arabidopsis* PGN receptor complex components LYM1, LYM3 and CERK1 (Willmann et al., 2011) as the respective mutant genotypes failed to respond to immunogenic PGN fragments (Figure 15B). Secondly, we tested whether LYS1-generated PGN fragments were able to trigger an immunity-associated response, medium alkalization, in rice cell suspensions. This plant was chosen for testing as a PGN receptor system, because it has recently been reported to be very similar to that in *Arabidopsis* (Liu et al., 2012a) and because rice cells have been observed to be much more sensitive to PGN than *Arabidopsis* cells (Roland Willmann, personal communication). As shown in Figure 15C, LYS1-released PGN-fragments triggered medium alkalization in cultured rice cells, suggesting that immune defence stimulation by soluble PGN fragments is not restricted to *Arabidopsis* only.

### 3.3.2 LYS1-overdigested PGN induces weaker immunity responses

We further investigated the kinetics of PGN fragment release from complex PGN. As shown in Figure 15D, release of immunogenic PGN-fragments into solution occurred rapidly within 10 min of incubation with native LYS1. Incubation of complex PGN with LYS1 yielded the highest immunogenic activity of the digested supernatant after 30 min, suggesting that at that time point the maximum amount of immunogenic PGN fragments was generated. However, prolonged incubation with LYS1 again resulted in a loss of activity with overnight digestion completely abolishing stimulatory activity of the PGN digest. We assume that LYS1 is capable of releasing immunogenic fragments from complex PGN, but extensive or complete digest into PGN-monomers or small PGN fragments appears to abolish the immunogenic activity of PGN fragments. This result is in accordance with previous observations that prolonged digestion of PGN with mutanolysin diminishes its defence-inducing activity (Gust et al., 2007).

### **3.4 LYS1 is required for immune responses to PGN**

#### **3.4.1 Characterization of *LYS1*<sup>KD</sup> lines**

To examine a role of LYS1 in plant immunity, attempts were undertaken to genetically inactivate *LYS1* expression. Three independent *LYS1* T-DNA insert lines were obtained from the Nottingham Arabidopsis Stock Center (NASC) and the Cold Spring Harbor Laboratory (CHSL), but transcription analysis of the three lines revealed similar *LYS1* transcript levels in these mutants to those in the corresponding wild types (Grabherr, 2011). Alternatively, transgenic *LYS1* knockdown (*LYS1*<sup>KD</sup>) lines were successfully generated using artificial microRNA technology (Schwab et al., 2006; Grabherr, 2011). To ensure silencing of *LYS1* in every generation of plants used for experiments, we analyzed the transcript levels of *LYS1* in *LYS1*<sup>KD</sup> lines (generated by Heini Grabherr) (Grabherr, 2011). As shown in Figure 16, *LYS1*<sup>KD</sup> lines contained only approximately 5-20% of WT *LYS1* transcript amounts.

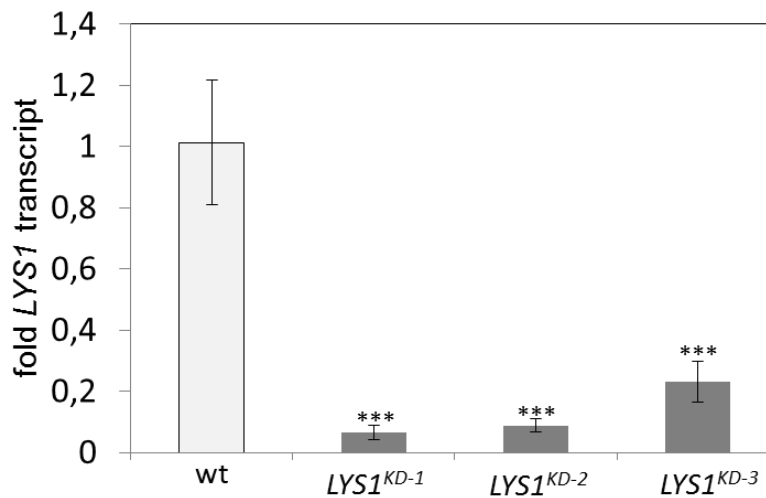


**Figure 16. Analysis of *LYS1* knockdown lines.** RT-qPCR analyses of transcript levels in mature leaves of three independent amiRNA knockdown lines (*LYS1*<sup>KD</sup>) relative to expression levels in wild-type leaves, which was set to 1. *EF1 $\alpha$*  transcript was used for normalization. Error bars, SD (n = 3). Statistical significance compared with wild-type (\*\*p<0.001, Student's t test) is indicated by asterisks.

To exclude the possibility that transcripts of potential amiRNA off-target genes were degraded in *LYS1*<sup>KD</sup> lines, we identified potential off-target genes using the Web microRNA Designer and investigated transcripts of the top four hits of the identified off-target genes by RT-qPCR. As shown in Figure 17, the results revealed that transcript levels of these potential off-target genes are not affected.

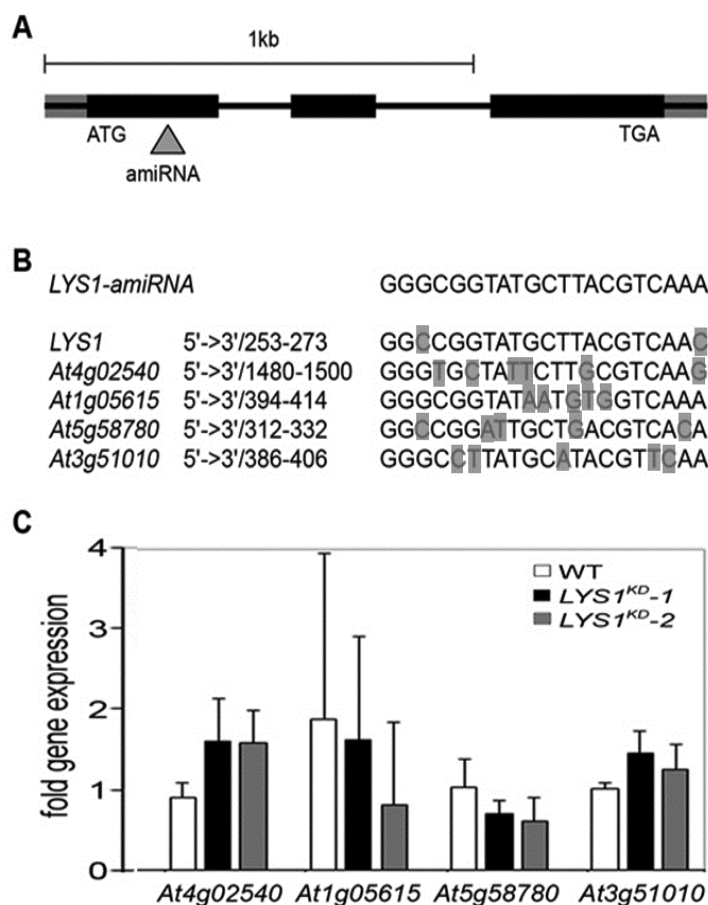


**Figure 17. Determination of putative *LYS1* amiRNA off-targets.** (A) Predicted *LYS1* gene structure (exons, black bars; introns, black lines; untranslated regions, grey). The region targeted by the amiRNA construct is indicated by an arrowhead. (B) Off-target genes for the *LYS1-amiRNA* construct were identified using the Web microRNA Designer (WMD; <http://wmd.weigelworld.org>). The region targeted by the amiRNA is given for each gene, mismatches are indicated with grey boxes. Potential off targets either possess more than one mismatch at positions 2–12 or have mismatches at position 10 and/or 11 which will limit amiRNA function. (C) Transcript levels of the four top hits shown in (B) were determined by RT-qPCR in untreated seedlings of two independent transgenic *LYS1*-amiRNA knock-down lines (*LYS1<sup>KD-1</sup>*, *LYS1<sup>KD-2</sup>*) using gene-specific primers for *At4g02540*, *At1g05615*, *At5g58780*, and *At3g51010*. *EF1 $\alpha$*  transcript was used for normalization. Error bars, SD (n = 3). No statistically significant differences to the wild-type control (which was set to 1 for each primer set) could be observed (Student's t test).

### 3.4.2 Lack of *LYS1* PGN-degrading activity dampens plant immunity.

To examine a role of LYS1 in immunity to bacterial infection, we infected wild type plants or *LYS1<sup>KD</sup>* and *LYS1<sup>OE</sup>* lines with virulent *PtoDC3000*. Two independent *LYS1<sup>KD</sup>* lines exhibited hypersusceptibility to bacterial infection (Grabherr, 2011; Liu et al., 2014), suggesting that lack of PGN-degrading activity results in reduced plant immunity. Likewise, immunity to hypovirulent *PtoDC3000 ΔAvrPto/PtoB* was compromised in these lines (Grabherr, 2011; Liu et al., 2014). Transcriptional up-regulation of defence-related genes is one of the PTI responses (Felix et al., 1999). Thus, we further examined whether LYS1 protein levels in the transgenics might affect the up-regulation of resistance-related genes. The results showed that expression of the immune marker gene *FRK1* upon administration of complex PGN was greatly impaired in the *LYS1<sup>KD</sup>* mutants (Figure 18). These findings suggest that the enzymatic activity of LYS1 on PGN contributes substantially to plant immunity against bacterial infection.

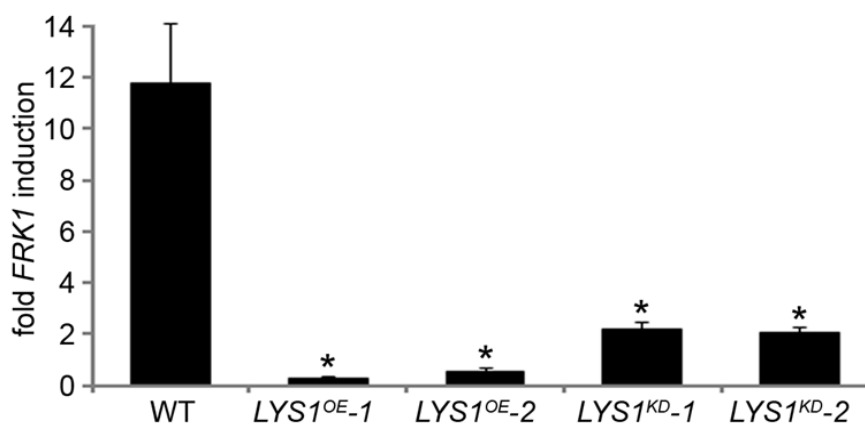


**Figure 18. Manipulation of *LYS1* levels causes a loss of PGN-triggered immune responses.** Leaves of wild type plants or transgenic *LYS1* plants were treated for 6 hours with 100  $\mu$ g *B. subtilis* PGN and total RNA was subjected to RT-qPCR using *FRK1* specific primers. *EF1 $\alpha$*  transcript was used for normalization. Data represent means  $\pm$  SD of triplicate samples, and shown is the result of one out of three independent experiments. Statistical significance compared to wild-type (\*  $p < 0.05$ , Student's t-test) is indicated by asterisks.

Unexpectedly, bacterial growth on *LYS1<sup>OE</sup>* lines was also significantly enhanced as compared to those observed on wild type plants (Grabherr, 2011; Liu et al., 2014). Likewise, *FRK1* transcript accumulation upon administration of complex PGN was also strongly reduced in *LYS1*-overexpressors (Figure 18), indicating that a manipulation of

LYS1 protein levels, irrespective of increasing or decreasing them, results in an impaired immune response towards PGN treatment.

To exclude a direct effect of LYS1-overexpression on PGN receptor abundance, we examined transcript levels of *LYM1*, *LYM3* and *CERK1* but found no effect on the transcription of these receptor genes in the *LYS1<sup>OE</sup>* lines (Figure 19A). Also, CERK1 protein levels were unaltered in the *LYS1<sup>OE</sup>* lines, whereas there was no CERK1 protein detectable in the *cerk1-2* mutant (Figure 19B).

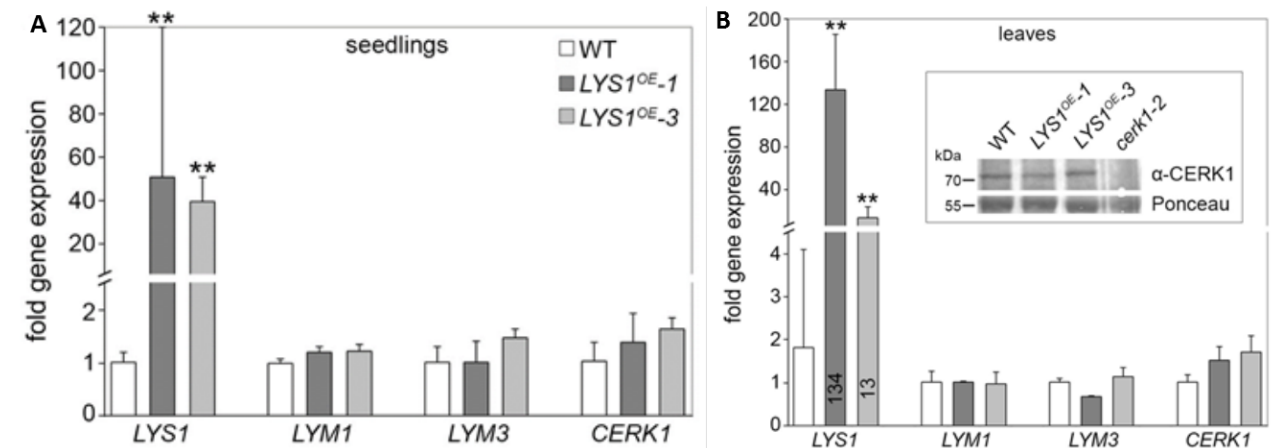


**Figure 19. *LYS1* overexpression does not affect PGN receptor expression.** Transcript levels of *LYS1* and the PGN receptors *LYM1*, *LYM3* and *CERK1* in the strong *LYS1<sup>OE-1</sup>*, compared to the weak overexpressor line *LYS1<sup>OE-3</sup>*. Total RNA from untreated seedlings (A) or mature leaves (B) was subjected to RT-qPCR using specific primers for *LYS1*, *LYM1*, *LYM3* or *CERK1*. *EF1α* transcript was used for normalization. Data represent means  $\pm$  SD of triplicate samples. For mature leaves, also CERK1 protein levels were determined using an anti-CERK1 antibody (B, inset). Ponceau S red staining of the large subunit of RuBisCO served as loading control.

Moreover, we included the *LYS1<sup>OE-3</sup>* line with only moderately increased *LYS1* transcript and protein levels in mature leaves (Figure 19B and 20A). Susceptibility to *Pseudomonas* infection in the *LYS1<sup>OE-3</sup>* line was only slightly but not significantly increased ( $p = 0,064$ , Student's t-test) (Figure 20B). These results indicate that lowering *LYS1* expression levels, accompanied by lower *LYS1* hydrolytic activity on PGN brings down these lines close to wild-type. Thus, massive *LYS1* overexpression and loss-of-

function mutations are phenocopies of each other, irrespective of the fact that *LYS1<sup>KD</sup>* and *LYS1<sup>OE</sup>* lines show dramatic differences in LYS1 enzymatic activities (Grabherr, 2011; Liu et al., 2014).

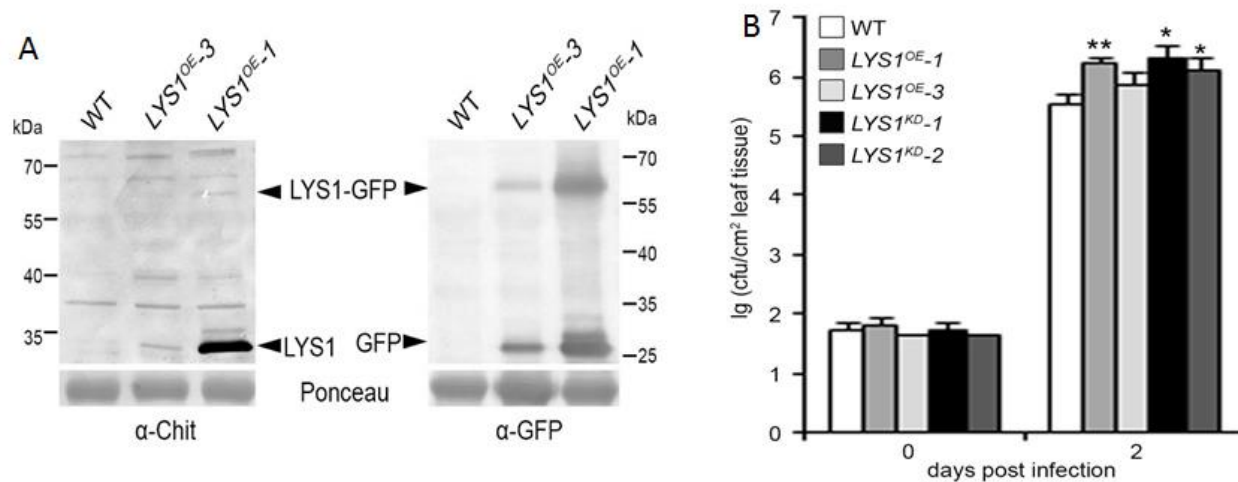


**Figure 20. Impact of weak *LYS1* overexpression.** (A) Immunoblot analysis of protein extracts from leaves of two independent *LYS1<sup>OE</sup>* lines (*LYS1<sup>OE-1</sup>*, *LYS1<sup>OE-3</sup>*) and wild type plants. Total leaf protein was subjected to Western blot analysis using  $\alpha$ -tobacco class III chitinase ( $\alpha$ -Chit) or  $\alpha$ -GFP (both from rabbit) and an anti-rabbit HRP-coupled secondary antibody. Ponceau S red staining of the large subunit of RuBisCO served as loading control. (B) Growth of *PtoDC3000* was determined 2 days post infiltration of  $10^4$  colony forming units  $\text{ml}^{-1}$  (cfu/ml). Data represent means  $\pm$  SD of six replicate measurements/genotype/data point. Statistical significance compared to wild-type (\*  $p < 0.05$ ; \*\*  $p < 0.01$ , Student's t-test) is indicated by asterisks.

### 3.4.3 *LYS1* is able to decompose *PtoDC3000* cell but does not inhibit their growth

To further elucidate the role of *LYS1* in the interaction between host and pathogen, we compared the effect of *LYS1* on *PtoDC3000* and *E.coli* cells in a digestion assay and a growth inhibition assay. Firstly, we tested the ability of *LYS1* to degrade bacterial cell walls in a turbidity assay. As shown in Figure 21, *LYS1* displayed direct hydrolytic activities towards *E.coli* (Figure 21A) but not against *PtoDC3000* cells (Figure 21B). In a following growth inhibition assay, *LYS1* displayed its inhibitory activity on bacterial growth only towards *E.coli* cells (Figure 21C) but not *PtoDC3000* (Figure 21D), suggesting that *PtoDC3000* has probably evolved some mechanism to counteract *LYS1*

activity. However, these are preliminary data are still awaiting confirmation. If this holds true, it will be interesting in the future to investigate how *Pto*DC3000 interferes with the ability of LYS1 to inhibit bacterial growth.

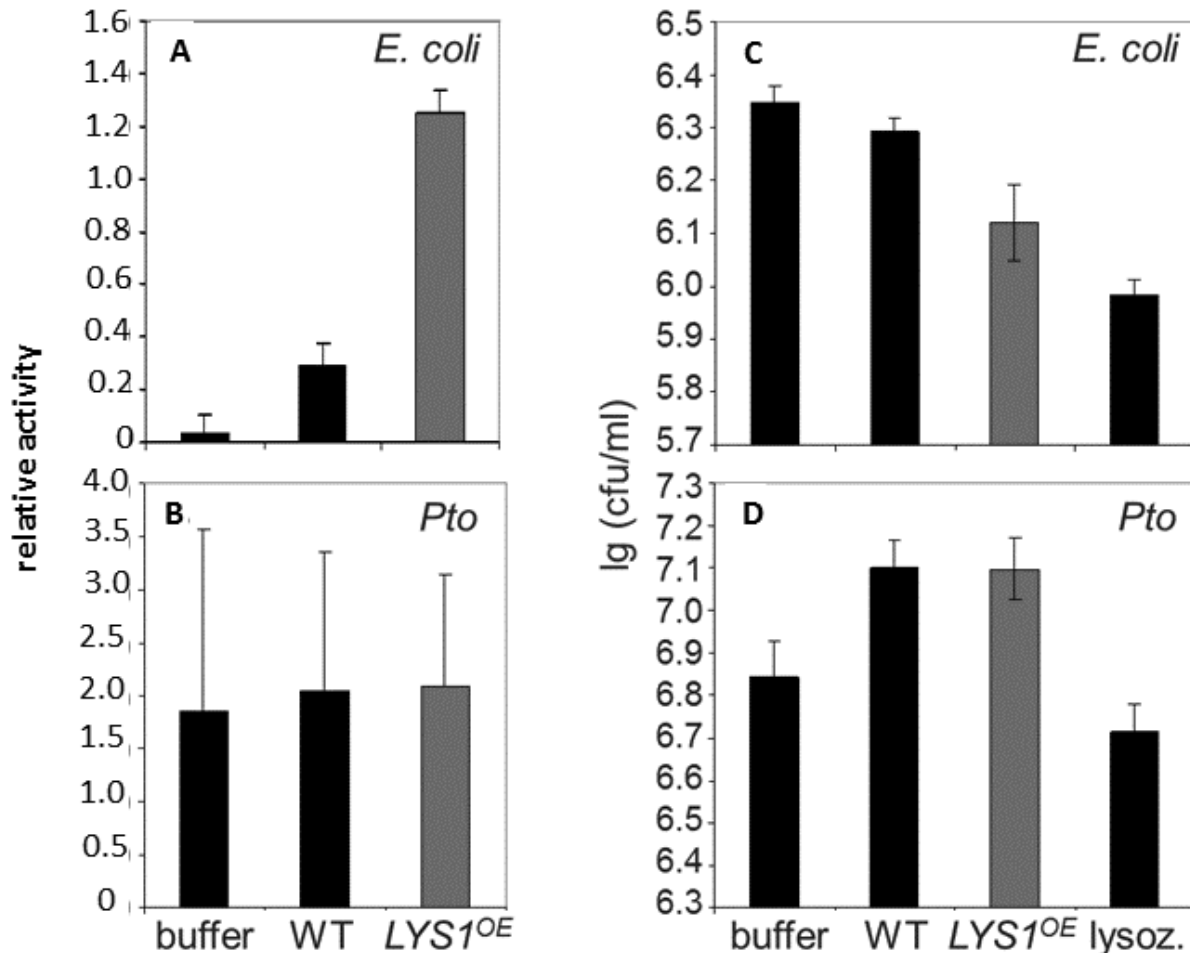


**Figure 21. LYS1 can digest bacteria cells and inhibit bacterial growth.** (A, B) Overnight cultured *Pto*DC3000 and *E.coli* were incubated with LYS1 purified from 5-week-old LYS1 overexpressing (*LYS1*<sup>OE</sup>) *Arabidopsis* plants or a protein preparation from wild type *Arabidopsis* plants as a control. After 3 hours the turbidity reduction of the respective culture was determined (A, *E.coli*; B, *Pto*DC3000) and set in relation to lysozyme activity, which was set to 1. (C, D) An aliquot of each remaining culture (C, *E. coli*; D, *Pto*) was re-cultured overnight and plated on LB medium. Bacterial growth given in colony forming units (cfu per ml) was determined after 24 hours.

Altogether, we propose that LYS1 contributes to plant immunity against bacterial infection by decomposition of bacterial PGN and generation of soluble PGN-derived

patterns that trigger immune activation in a LYM1-LYM3-CERK1 receptor-complex-dependent manner.

### **3.5 Identification of a CERK1-interacting calcium-dependent protein kinase**

#### **3.5.1 Identification of putative CERK1 interactors from a Y2H database**

To better understand the signaling pathways induced by PGN and chitin, respectively, we next aimed at identifying novel interacting proteins for CERK1. The yeast two-hybrid system is a useful and powerful genetic technique for the *in vivo* analysis of protein-protein interactions (Bartel and Fields, 1995). However, its application is limited in that hybrid proteins generated in the two-hybrid assay are targeted to the nucleus. Therefore, integral membrane proteins, which exist in the lipid bilayer, are excluded because they are unlikely to be able to enter the nucleus, or will be misfolded if they do. To overcome limits of the conventional yeast two-hybrid system, an alternative split-ubiquitin system was developed in 1994 (Johnsson and Varshavsky, 1994) and then modified for the *in vivo* analysis of membrane proteins on a small-scale basis (Stagljar et al., 1998). Later on, a mating-based split ubiquitin system (mbSUS) was developed for systematic identification of interactions between membrane proteins as well as between membrane and soluble proteins on a large-scale basis (Obrdlik et al., 2004). In the mbSUS, two integral membrane proteins are fused to the two halves of ubiquitin and expressed in yeast cells of opposite mating types. Upon mating, the diploid yeast cell co-expresses the proteins. An interaction of membrane proteins brings the two halves of ubiquitin into close proximity, forming a reconstituted molecule that is cleaved by ubiquitin-specific proteases, releasing the transcription factor to enter the nucleus and activate reporter gene transcription.

With this mbSUS system, Frommer and his colleagues used a library of more than 3000 Arabidopsis membrane proteins and soluble signaling proteins to screen over 3 million binary interactions. The results lead to a membrane-based interactome network database (M.I.N.D.) containing 12102 high confidence protein-protein interactions that were identified in repeated rounds of interaction screening ([associomics.org](http://associomics.org)).

**Table 7. Putative CERK1 interacting proteins identified from the Membrane-based Interactome Network Database (M.I.N.D. 0.5).**

AGI ID	Annotation (Lookup from 2009-07-29) - for multiple identifier mappings only the annotation for the first identifier is shown, except in the case of the multi-line output option
AT1G04310	ERS2__ethylene response sensor 2
AT1G35720	ANNAT1_ATOXY5_OXY5__annexin 1
AT1G69910	Protein kinase superfamily protein
AT2G01490	phytanoyl-CoA dioxygenase (PhyH) family protein
AT2G25600	AKT6_SPIK__Shaker pollen inward K <sup>+</sup> channel
AT2G26180	IQD6__IQ-domain 6
AT2G30490	ATC4H_C4H_CYP73A5_REF3__cinnamate-4-hydroxylase
AT2G40540	ATKT2_ATKUP2_KT2_KUP2_SHY3_TRK2__potassium transporter 2
AT2G40890	CYP98A3__cytochrome P450, family 98, subfamily A, polypeptide 3
AT3G08040	ATFRD3_FRD3_MAN1__MATE efflux family protein
AT3G12180	Cornichon family protein
AT3G23000	ATSR2_ATSRPK1_CIPK7_PKS7_SnRK3.10__CBL-interacting protein kinase 7
AT3G26830	CYP71B15_PAD3__Cytochrome P450 superfamily protein
AT4G11840	PLDGAMMA3__phospholipase D gamma 3
AT4G21940	CPK15__calcium-dependent protein kinase 15
AT5G09400	KUP7__K <sup>+</sup> uptake permease 7
AT5G49630	AAP6__amino acid permease 6
AT5G52860	ABCG8__ABC-2 type transporter family protein
AT1G58520	RXW8__lipases;hydrolases, acting on ester bonds
AT1G79820	SGB1__Major facilitator superfamily protein

In order to identify novel components interacting directly with CERK1, we searched CERK1-interacting proteins in the database of the M.I.N.D and obtained 20 putative interacting proteins (Table 1).

Of these 20 putative CERK1-interacting proteins, three protein kinases were selected for further study: a protein kinase without known function (*PK*, At1g69910), CBL-interacting protein kinase 7 (*CIPK7*, At3g23000) and calcium-dependent protein kinase 15 (*CPK15*, At4g21940).

## 3.5.2 Analysis of M.I.N.D.-interactors for CERK1

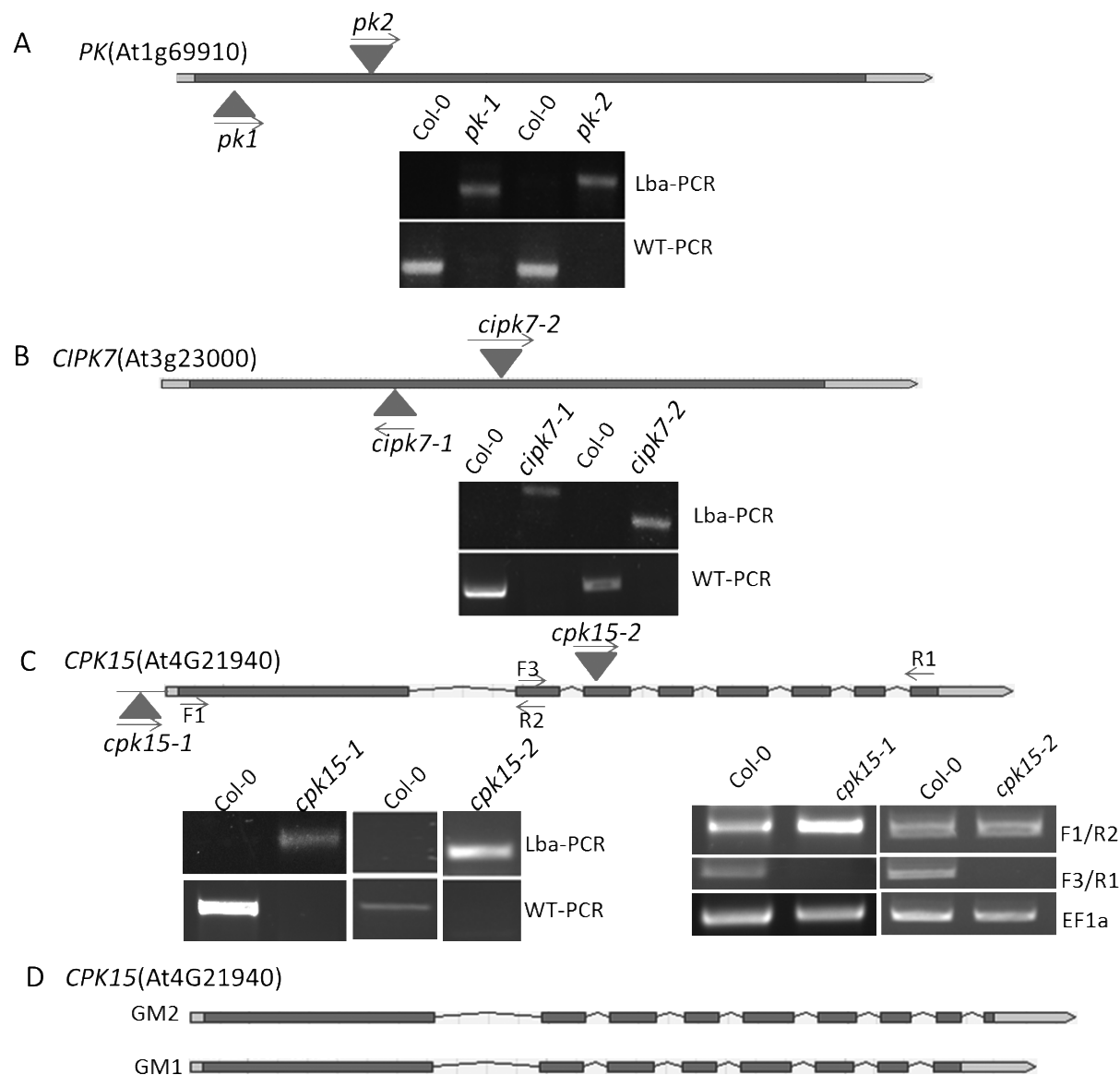


**Figure 22. Gene models and genotyping of T-DNA insertion mutants of three putative CERK1 interactors.** Gene models of *CIPK7* (A), *PK* (B) and *CPK15* (C, D) including the positions of the T-DNA insertions. Exons and introns are indicated by grey bars and grey lines, respectively. 5'- and 3'-UTR regions are represented by light grey bars and the T-DNA insertions by grey triangles. Promoter regions are indicated by thin lines. For genotyping the mutants, leaf genomic DNA was isolated and genotyping PCRs were performed. (A) Genotyping of *pk-1* and *pk-2* was done with primer pairs Salk-Lba/*pk1*-rp and GK-Lba/*pk2*-rp for the Lba-PCR, and *pk1*-lp/*pk1*-rp and *pk2*-lp/*pk2*-rp for the WT-PCR. (B) Genotyping of *cipk7-1* and *cipk7-2* was done with primer pairs Salk-Lba/*cipk1*-rp and GK-Lba/*cipk2*-rp for the Lba-PCR, and *cipk1*-lp/*cipk1*-rp and *cipk2*-lp/*cipk2*-rp for the WT-PCR. (C) Genotyping of *cpk15-1* and *cpk15-2* was

done with primer pairs Sail-Lba/cpk15-rp and F3/JL-270 for the Lba-PCR, and cpk15-lp/cpk15-rp and F3/R3 for the WT-PCR. For transcript analysis using semi-quantitative RT-PCR total RNA was isolated from leaves and transcribed into cDNA. EF1a-s and EF1a-as primers were used to amplify the transcript of the house-keeping gene *EF1α*. F3/R2 and F3/R1 primer pairs were used to amplify the transcripts of *CPK15*. (D) Two gene models of *CPK15* are indicated by GM1 and GM2.

Two independent T-DNA mutant lines of each selected gene (*PK*, *CIPK7*, and *CPK15*, Table 1) were obtained from the Nottingham Arabidopsis Stock Center (NASC). Genotyping analyses of these mutants were performed by Lba-PCR and WT-PCR, revealing that these mutants were homozygous T-DNA insertion mutants (Figure 22, A-C).

The accumulation of ROS in an oxidative burst is an early response triggered by PAMPs and is also observed in *Arabidopsis* upon treatment with chitin (Miya et al., 2007). We thus investigated if the oxidative burst was impaired in these potential CERK1 interacting protein mutants in response to chitooctamers in a leaf ROS assay. As shown in Figure 23, no significant changes were detected in the two *PK* mutants and the two *CIPK7* mutants in comparison to the Col-0 wild type. However, *cpk15-1* plants displayed a significant reduction in ROS production whereas *cpk15-2* mutants did not (Figure 23, right panel). We thus chose *CPK15* for a more detailed investigation as a putative CERK1 interactor.

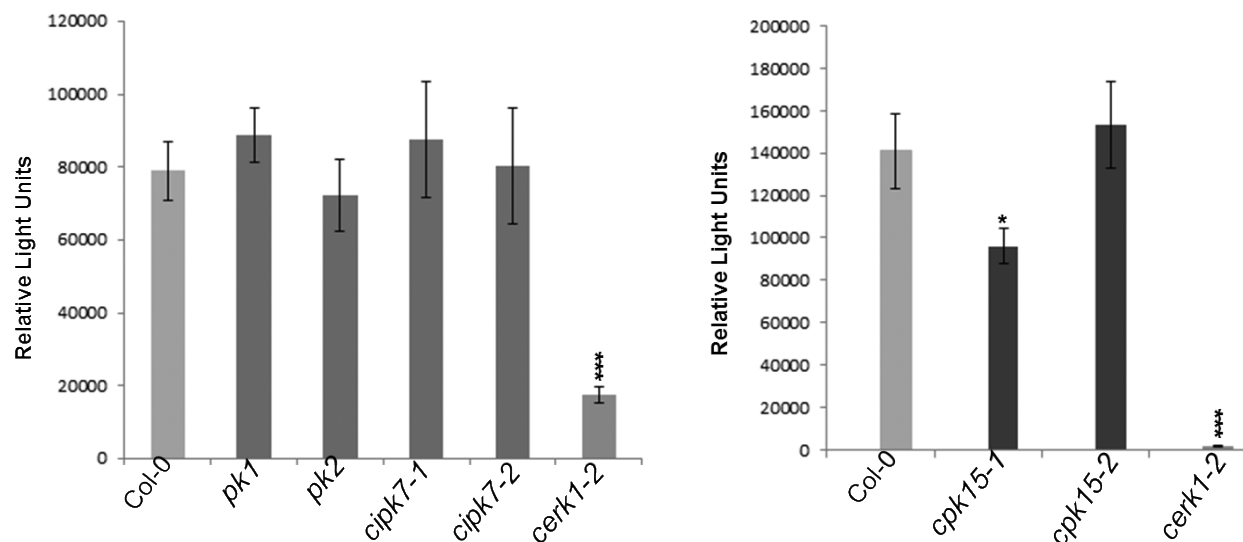


**Figure 23. Screening analysis of T-DNA mutants of *PK*, *CIPK7* and *CPK15* in a ROS oxidative burst assay.** Leaf pieces from 5-week old Col-0, *pk*, *cipk7*, *cpk15* and *cerk1-2* mutants were elicited with 1  $\mu$ M chitooctamer (C8) and the oxidative burst was measured in a 96-well plate using a plate reader (for more details see method section). The *cerk1-2* mutant served as a negative control. Mean and standard error of 6 replicates are presented. Asterisks indicate significant differences of C8 treatment in comparison to Col-0 (\* $p < 0.05$ , \*\*\* $p < 0.001$ , Student's t test).

### 3.6 CPK15 is involved in the CERK1-mediated PTI pathway

#### 3.6.1 Characterization of *cpk15* T-DNA insertion lines

It was predicted that there are two possible gene models of CPK15 as shown in Figure 22D, with gene model 1 (GM1) comprised of 8 exons while gene model 2 (GM2) contains 9. In order to examine which of two gene models is correct, the constructs *p35S::GM1-YFP* and *p35S::GM2-YFP* were expressed in *N. benthamiana*. YFP fluorescence signals could only be observed in leaves expressing *GM1-YFP* (Tina Romeis, personal communication), suggesting GM1 is the correct model.

Next we analyzed *cpk15* T-DNA mutant lines more thoroughly. Sequence comparison of two T-DNA flanking regions with CPK15 genomic DNA revealed that the T-DNA was inserted in the promoter region in *cpk15-1* and in the third exon in *cpk15-2* as shown in Figure 22C. To examine the transcript levels of *CPK15* in the two T-DNA insertion

mutants, total RNA was isolated from leaves of the two mutants and used for semiquantitative RT-qPCR analysis with gene-specific primer pairs (Figure 22C). The agarose gel electrophoresis analysis of the amplified products revealed that no 3'-end but the 5'-end transcript of the *CPK15* could be detected in the two *cpk15* mutants (Figure 22C). Since *cpk15-2* did not display significant differences in the ROS-based screening, we next focused on the *cpk15-1* line. Morphology observation of *cpk15-1* mutant plants revealed no differences between Col-0 and *cpk15-1* mutants except that *cpk15-1* leaves displayed curved edges (Figure 24). However, a southern blot to exclude multiple T-DNA insertion events in the *cpk15-1* line is still outstanding. Thus, so far we cannot rule out that this leaf phenotype is caused by a secondary T-DNA insertion and not by genetic inactivation of the *CPK15* gene itself.

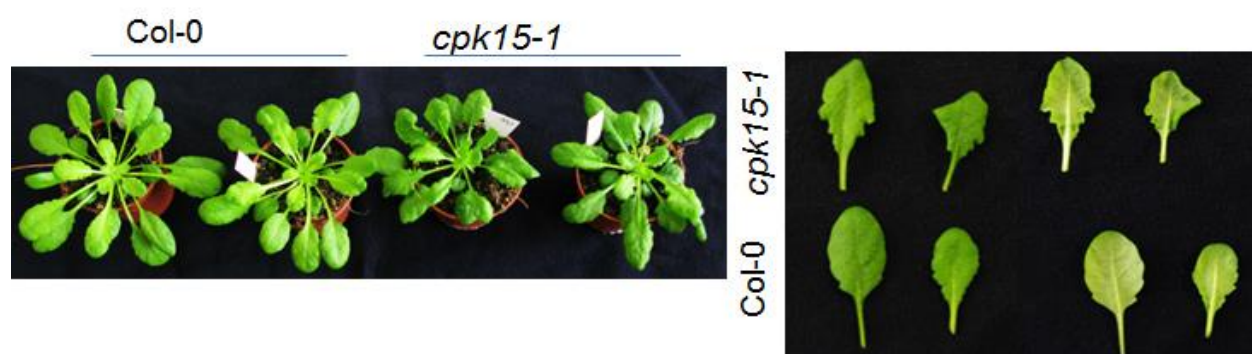


**Figure 24. Morphological phenotypes of *cpk15-1* T-DNA insertion lines.** 5-week old plants of the *cpk15-1* line and the Col-0 wild type were photographed to show whole plants from the top (left) and leaves from the adaxial and abaxial sides (right).

### 3.6.2 *cpk15-1* produces less ROS in response to complex or soluble chitin

In order to investigate if *cpk15-1* mutants were compromised in ROS accumulation in response to complex chitin as well, five-week old leaves of *cpk15-1* and Col-0 plants were treated with Flg22, complex crab chitin and soluble chitooctamer and subsequent ROS production was determined in a 96-well plate reader. The results showed that upon treatment with both crab chitin and C8, *cpk15-1* mutants exhibited a significant reduction of ROS accumulation compared to Col-0 plants (Figure 25). Notably, *cpk15-1* displayed a tendency of higher ROS levels in response to Flg22 treatment (Figure 25). The *cerk1-*

2 mutation almost abolished ROS accumulation in response to chitin, although in other experiments this mutant showed a normal Flg22-induced response level (data not shown)

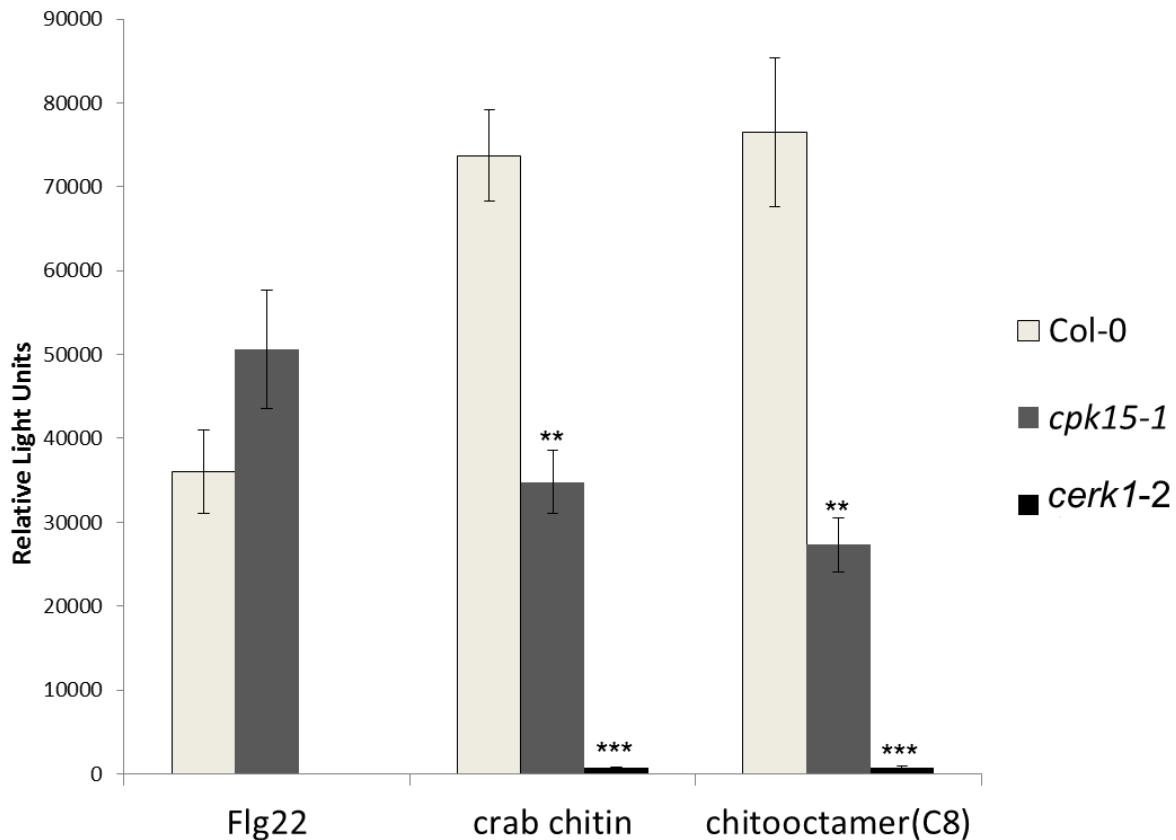


**Figure 25. Determination of ROS accumulation in *cpk15-1* mutant plants.** Leaf pieces from 5-week old Col-0, *cpk15-1*, and *cerk1-2* plants were treated with 100  $\mu$ g/ml crab chitin or 1  $\mu$ M chitooctamer (C8). The oxidative burst was measured at 20 min after treatment in a 96-well plate reader (for more details see method section). The oxidative burst triggered by 100 nM Flg22 served as a positive control. The *cerk1-2* mutant served as a negative control only for chitin treatment. Mean values with standard errors of 6 replicates are represented. Asterisks indicate significant differences of each treatment in comparison to the Col-0 control (\*\* $p < 0.01$ , \*\*\* $p < 0.001$ , Student's t test).

### 3.6.3 Chitin-induced activation of MAPK is not affected in *cpk15-1*

In addition to the production of reactive oxygen species, early cellular events upon perception of PAMPs also involve the post-translational activation of mitogen-activated protein kinase (MAPK) cascades (Boller and Felix, 2009). To investigate if the activation

of MAPKs is affected in the *cpk15-1* mutant line, comparative studies with Col-0 upon treatment with chitin were performed. MAPK activities were analyzed by immunoblot assays using the p44/12 antibody raised against phosphorylated MAPKs (Boller and Felix, 2009). As shown in Figure 26, chitohexamers (C6) strongly activated the defence-associated MPK3, MPK4/11 and MPK6 in *cpk15-1*, which was indistinguishable from the induction pattern obtained in Col-0 plants. In *cerk1-2* plants used as negative control, C6-induced activation of MAPKs was completely abolished, and water treatment did not induce the activation of MAPKs in all tested plants. In contrast, as positive controls, Flg22 induced a high level of activation of MAPKs in all plant types (Figure 26). Hence, we conclude that CPK15 is involved in a signaling pathway independent from chitin-induced MAPK activation.

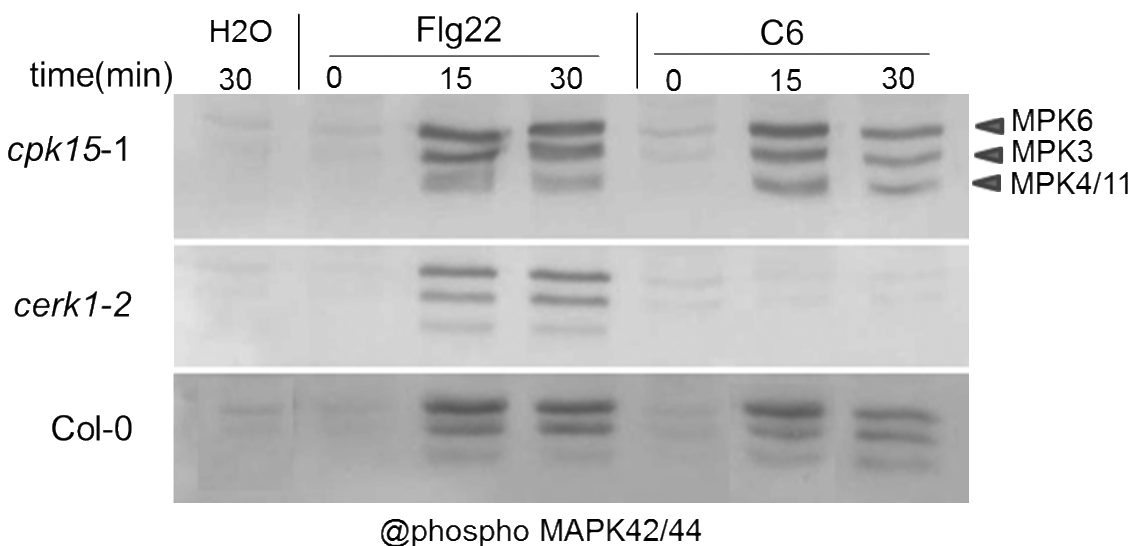


**Figure 26. Chitin induced MAPK activation is not impaired in the *cpk15-1* mutant.** 7-day old seedlings of the *cpk15-1* or *cerk1-2* mutant, or Col-0 as a control, were collected at indicated time points after treatment with 10  $\mu$ M chitohexamer (C6). Treatment with water and 100 nM Flg22 served as negative and positive controls, respectively. The crude protein extracts from these seedlings were separated on a SDS-PA gel and blotted onto a nitrocellulose membrane. Immunodetection was carried out using the anti-phospho p44/42 antibody. Arrowheads indicate the positions of MAP kinases 6, 3 and 4/11.

### 3.6.4 CPK15 localizes to the plasma membrane

Most CDPKs have a predicted N-myristoylation site involved in membrane targeting (TermiNator, [http:// www.isv.cnrs-gif.fr/terminator2/index.html](http://www.isv.cnrs-gif.fr/terminator2/index.html)). This irreversible co-translational acylation requires a second post-translational signal to maintain the membrane association, such as reversible palmitoylation (Martin and Busconi, 2000), leading to most CDPKs anchored in the membrane.

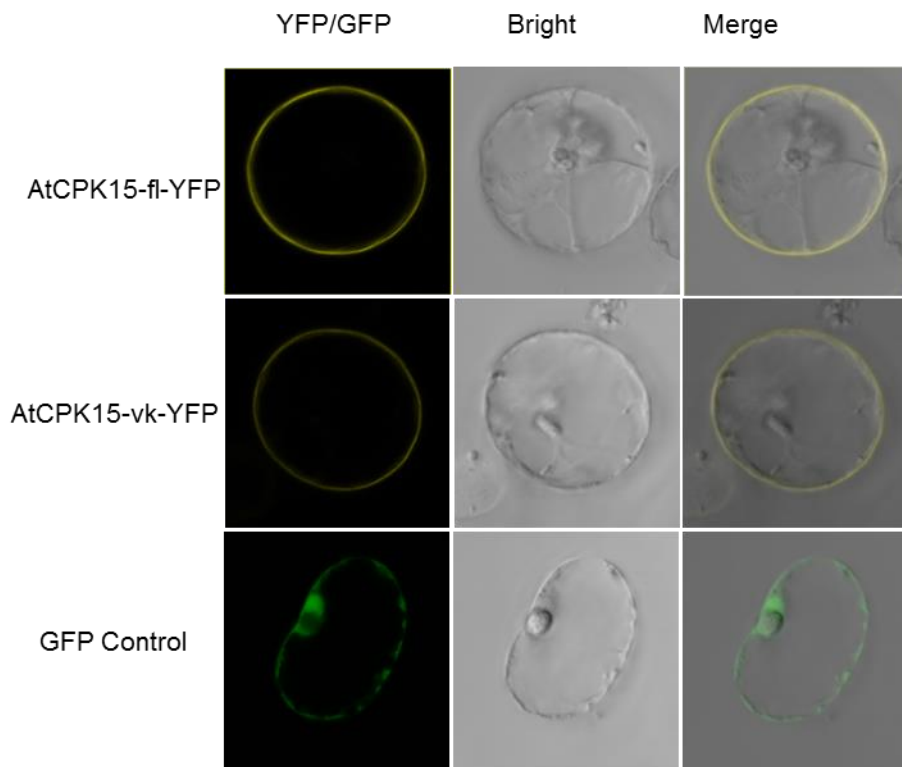


**Figure 27. Subcellular localization of the CPK15-YFP fusion protein.** Constructs *p35S::CPK15-fl-YFP* (upper panel) and *p35S::CPK15-vk-YFP* (middle panel) were expressed in *Arabidopsis* mesophyll protoplasts. VK represent a truncated CPK15 version (variable domain and kinase domain). The localization was visualized by laser scanning confocal microscopy. *p35S::GFP* was used as a control (lower panel).

CPK15 has a predicted N-myristoylation site and could be localized at the plasma membrane. To examine the localization of CPK15, we expressed a *p35S::CPK15-fl-YFP* construct and a construct for a truncated version *p35S::CPK15-vk-YFP* (containing only the variable and kinase domain of CPK15, see also Figure 29, constructs kindly

provided by Prof. Tina Romeis) in *Arabidopsis* mesophyll protoplast. As shown in Figure 27, confocal images revealed that YFP-fluorescence signals appear on the plasma membranes of protoplasts expressing the full length and the truncated version of CPK15, confirming a localization of CPK15 at the plasma membrane as predicted, whereas the control-GFP signal could only be found in the cytoplasm. Moreover, these results indicate that the variable and kinase domain of CPK15 are sufficient to target the protein to the plasma membrane.

### 3.6.5 CERK1 physically interacts with CPK15

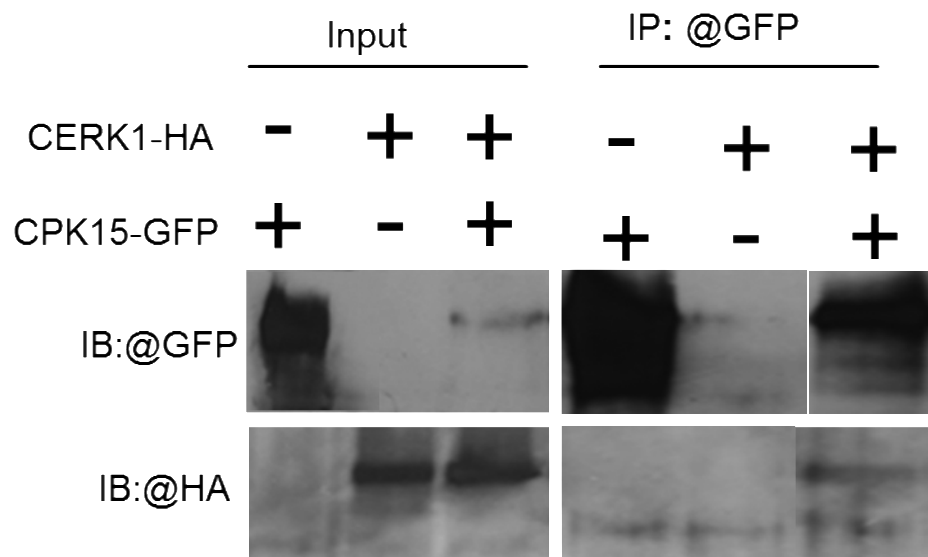


**Figure 28. CERK1 physically interacts with CPK15.** Constructs *p35S::CERK1-HA* and *p35S::CPK15-GFP* were transiently (co-)expressed in *N. benthamiana* leaves by agrobacteria-mediated transformation. After 36 hours, CPK15-GFP was immunoprecipitated from total protein extracts using GFP-Trap and detected with an anti-GFP antibody. Co-immunoprecipitated CERK1-HA was detected with anti-HA antibody. Western blot analysis with anti-HA and anti-GFP of corresponding total proteins served as input controls.

Identification via the M.I.N.D. already suggested that CERK1 has the ability to interact with CPK15 in a yeast-based system. Thus, we next investigated if CERK1 directly physically interacts with CPK15 *in planta*. To do this, CERK1-HA and CPK15-GFP were transiently co-expressed in *N. benthamiana* and protein extracts were used for a co-immunoprecipitation analysis. An immunoprecipitation of CPK15-GFP with GFP-Trap (a GFP-binding protein coupled to agarose beads) was performed and co-immunopurified

proteins were subjected to immunoblotting analysis with HA antibodies. The results revealed that CERK1-HA could be co-immunoprecipitated by CPK15-GFP (Figure 28), indicating a direct physical interaction between CPK15 and CERK1. Thus, CERK1 and CPK15 can interact both in yeast cells and in plant tissue.

### 3.7 Characterization of knockdown lines of *CPK15* and *CPK15 /CPK21/CPK23*

#### 3.7.1 Structure and classification of *Arabidopsis* CDPKs

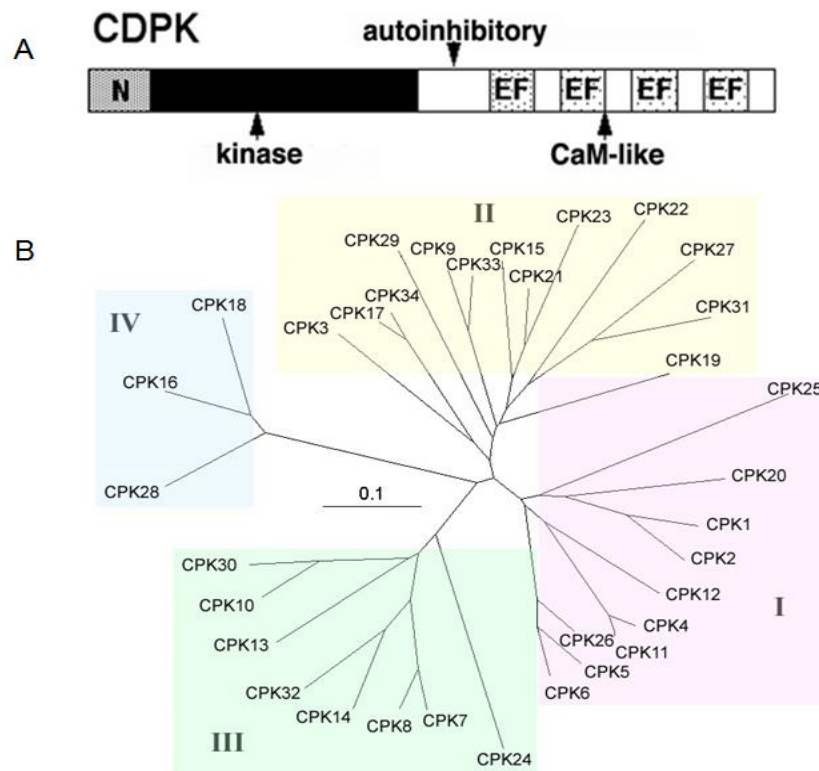


**Figure 29. Structure and subfamilies of *Arabidopsis* CDPKs.** (A) Schematic general structure of CDPKs. N, N-terminal variable domain; CaM, calmodulin-like domain. The four bars within the CaM-like domain represent the EF hand Ca<sup>2+</sup>-binding sites. (B) Subfamilies of *Arabidopsis* CDPKs. The complete protein sequences of the *Arabidopsis* CDPKs were aligned and analyzed by the Treeview 1.6.5 program (<http://taxonomy.zoology.gla.ac.uk/rod/rod.html>). The unrooted distance tree reveals the presence of four distinct, branched subgroups (I–IV). The branch lengths are proportional to divergence, with the scale of “0.1” representing 10% change. *CPK15* and its closest homologs *CPK21/23* belong to group II. This figure was modified from Cheng *et al.* (Cheng *et al.*, 2002).

There are 34 *Arabidopsis* CDPKs in *Arabidopsis* which are highly homologous to each other (Boudsocq and Sheen, 2013) (Figure 29B). Pair-wise analyses with the full protein sequences indicated that the overall identities and similarities are 39% to 95% and 56% to 96%, respectively. High homologies may indicate redundant functions. Based upon sequence homology, the CDPKs of *Arabidopsis* cluster into four subgroups (I–IV). Subgroup IV is the least complex, with three members, and subgroup II is the most complex, with 13 members. Subgroups I through III are closer in sequence identity to each other than to subgroup IV. CPK15 belongs to subgroup II and its closest homologs are CPK21 and CPK23.

### 3.7.2 Generation of artificial microRNA lines of *CPK15*, *CPK21* and *CPK23*.

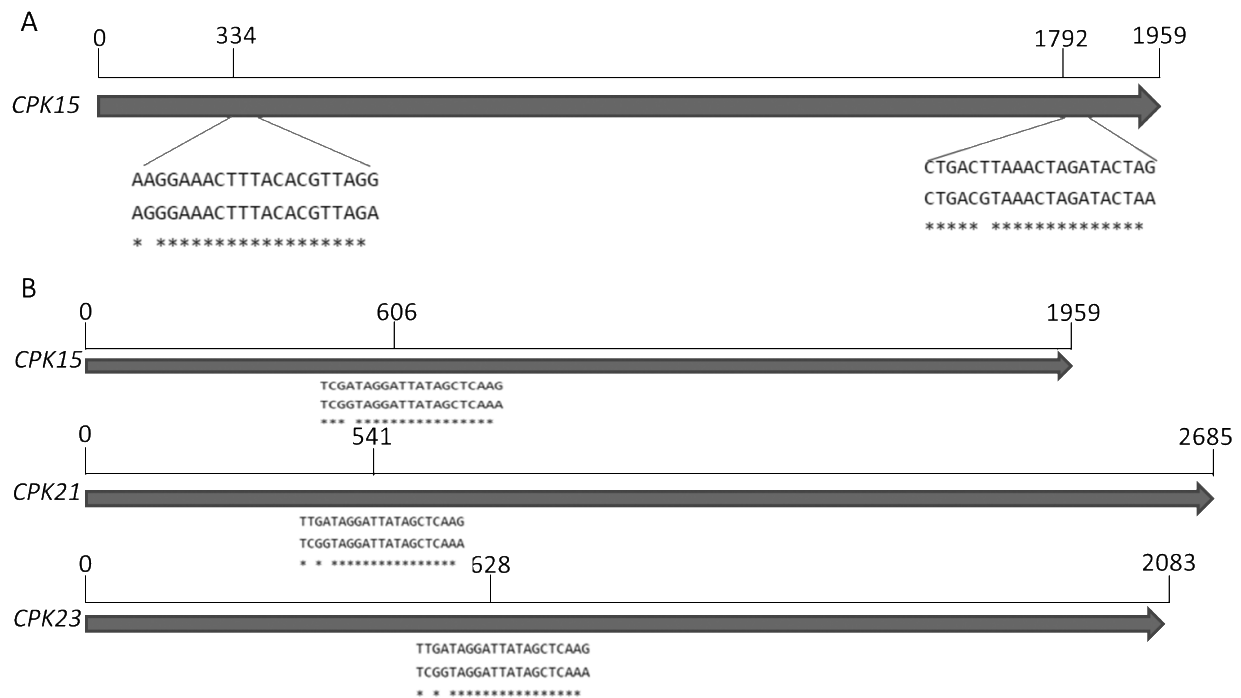


**Figure 30. Generation of *CPK15* single and *CPK15/21/23* triple knockdown lines.** (A) *CPK15* gene with regions targeted by the artificial microRNA. Two sets of amiRNA constructs were generated with one targeting the region from 334-354 nucleotides (nt) and another targeting the region from 1792-1802 nt of the *CPK15* gene. (B) For the multiple gene knockdowns one construct was generated with an amiRNA targeting the three genes *CPK15*, *CPK21* and *CPK23*.

To generate a second *CPK15* knockdown (*CPK15<sup>KD</sup>*) allele and to genetically inactivate *CPK15* together with its homologs, we made use of an artificial microRNA system

(Schwab et al., 2006) to create single *CPK15* knockdown plant (Figure 30A), in which only *CPK15* is targeted, and triple knockdown plants, in which *CPK15*, *CPK21* and *CPK23* are targeted (Figure 30B). T1 seeds of *CPK15<sup>KD</sup>* have been harvested and need to be further confirmed by qPCR and the constructs for *cpk15/21/23* amiRNA triple knockout mutants are under construction.

### **4. Discussion**

Although plant-microbe interactions have occurred for several millions years, a close look at the underlying molecular mechanism was initiated only some fifty years ago. It is understood that plants activate their immune responses by perceiving microbe-derived molecular patterns via cell surface-localized immune receptors. However pre- and post-perception events remain largely a mystery. It is unclear if and how microbial pattern supermolecules are processed prior to perception by cell surface receptors. The mechanism linking perception with diverse downstream immune responses is also largely unknown. Therefore, this thesis focused on these topics and aimed at answering these important questions.

It is generally little understood whether, and if so, how microbial patterns derived from complex extracellular assemblies, such as bacterial cell walls, are accessible to host PRRs for host immune activation in eukaryotes. This is true not only for bacterial PGNs, but also for other microbial patterns such as bacterial LPS, flagellin, fungal chitin or glucan structures, all of which have been identified as inducers of innate immunity in metazoans and plants (Boller and Felix, 2009; Kumar et al., 2013; Newman et al., 2013; Pel and Pieterse, 2013). Recent research into the 3D structure of ligand-PRR complexes, as well as studies on ligand structural requirements for plant immune activation, suggest that small ligand epitopes are crucial for binding to host PRRs (Liu et al., 2012b; Sun et al., 2013). It is thus generally assumed that soluble fragments derived from complex microbial matrices serve as ligands for host PRRs and subsequent immune activation in both metazoans and plants.

#### **4.1 LYS1 is involved in the apoplastic battle between plants and pathogens**

In general, upon invasion foliar plant pathogens encounter plant defence in three battlegrounds: the plant surface, plant cell apoplast, and the plant cell symplast (Senthil-Kumar and Mysore, 2013). Plant defences in the three battlegrounds are generally classified into two types: preformed defence and inducible defence. Pathogens that attempt to invade plants are initially exposed to a wide range of preformed plant defence including both physical barriers (Gottwald and Graham, 1992; Xiao et al., 2004) and

chemical inhibitors (Dixon et al., 2002; Aires et al., 2009; Che et al., 2011). Subsequently, pathogens that overcome these preformed defence encounter the plant inducible defence (Li et al., 2005; Nicaise et al., 2009; Sohn et al., 2012). Both preformed and inducible defence are integrated by plants across the three battlegrounds and deployed during infection to combat pathogens.

Preformed defence, although important, are passive and constitutive responses. Inducible defence, in contrast, are active and stimuli-oriented responses (Senthil-Kumar and Mysore, 2013). Thus, the inducible defence allows plants to induce immune responses at appropriate levels in response to a given pathogen infection and thus is rather cost-saving (Heil and Baldwin, 2002), compared to the constitutive defence which use the same plant energy resources. As a result, plants can divert the saved cost from defence to growth and reproduction, which is a benefit for plant fitness (Heil and Baldwin, 2002).

Of the three battlegrounds, the apoplast is the first place where the pathogens establish their physical contact with plant cells. On the one hand, pathogens attempt to adapt to and colonize the apoplast. On the other hand, plants impede these colonization attempts via preformed and induced barriers. This opposition makes the apoplast a key battleground where the fate of both the pathogens and the plants will be determined during infection.

Plant apoplastic defence involves physical barriers, antimicrobial chemical compounds and antimicrobial enzymatic activities of pathogenesis-related (PR) proteins. For instance, cell wall reinforcement by callose, lignin, and suberin deposition is induced by pathogens as part of the plant defence against pathogens (Senthil-Kumar and Mysore, 2013). In addition, some chemical compounds, such as phytoanticipins and phytoalexins, are also present constitutively or inducibly in the apoplast and act as antimicrobial agents (Senthil-Kumar and Mysore, 2013). Moreover, important components of the plant defence response against microbial pathogens in the apoplast involve proteins such as PR proteins that are produced upon pathogen perception in order to restrict pathogen growth. The apoplastic PRs, which actually comprise all PR families except the ribonuclease-like PR-10, can be found in cell wall appositions in response to pathogen attack. PRs have various antimicrobial activities, some of which harbor carbohydrate-

degrading hydrolytic enzyme activities. In the case of the  $\beta$ -1,3-glucanase PR-2 or the chitinases PR-3/4/8/11, these hydrolytic enzymes have been implicated in plant immunity via their enzymatic attacks on major components of fungal cell walls (van Loon et al., 2006).

In this study, we showed that the immunity-associated lysozyme-like protein LYS1 functions in the apoplast. LYS1, a PR-8 protein, is predicted to have a 22-amino acid secretion signal at its N-terminus (Grabherr, 2011). This signal peptide directs LYS1 to be secreted into the apoplast and is then removed by a peptidase to produce a mature LYS1. This is in accordance with the results of our LYS1 MS analysis, which showed that none of the identified peptides of the purified mature LYS1 were mapped to this N-terminal signal peptide region (Figure 11C). Moreover, immunoblotting analysis of the apoplastic fluid of *LYS1<sup>OE</sup>* plants further confirmed the presence of LYS1 in the *Arabidopsis* apoplast (Figure 14). Finally, a previous apoplast proteome analysis supported our finding that LYS1 was an apoplastic protein (Kwon et al., 2005).

Many secretory proteins undergo some posttranslational modifications, (e.g. glycosylation), which are often required for enzyme activities (Tekoah, 2004). The glycosylation of LYS1 was investigated and confirmed by deglycosylation experiments (Grabherr, 2011). In contrast, LYS1 lacking the signal peptide cannot properly be secreted into the apoplast (Grabherr, 2011) and displayed no enzymatic activity (Figure 6B).

In addition to posttranslational modification, the correct folding of a mature protein is also critical for its activity. The prediction of the LYS1 three dimensional structure using the Phyre server (Kelley and Sternberg, 2009) revealed that LYS1 has a  $(\beta\alpha)_8$  barrel fold and that the substrate-binding cleft is formed by the C-terminal residues of barrel  $\beta$ -strand and subsequent loops (Figure 3B). Therefore, C-terminally fused tags might interfere with the correct folding of LYS1 and the tight binding of substrates, resulting in a loss of the enzymatic activity. Indeed, in this study all three LYS1 fusions with C-terminal tags (HA, myc and GFP) displayed no detectable enzymatic activities (Figure 7 and 10).

Taken together, LYS1 is an apoplastic protein whose activity depends on the required posttranslational modifications and correct folding. Since LYS1 lysozyme-like activity is

considered to be related to plant immunity, we conclude that LYS1 functions as an immunity-associated protein in the apoplast battleground.

### **4.2 LYS1 is involved in plant inducible defence**

The inducible defence responses can occur through PAMP-triggered immunity (PTI) or through effector-triggered immunity (ETI) (Jones and Dangl, 2006). In PTI, some highly-conserved, microbe-derived molecular patterns can be recognized by plant surface-localized pathogen recognition receptors (PRRs) to induce immune responses.

Structural analyses have demonstrated that ligand-induced oligomerization of PRR is a common theme for the activation of plant PRRs (Chinchilla et al., 2007; Liu et al., 2012b; Sun et al., 2013), suggesting that small ligand epitopes are crucial for binding to the host PRRs. It is generally assumed that PAMPs are present as soluble fragments in the plant apoplast to gain better access to the plasma membrane-localized PRRs and thus activate the immune responses. In fact, it was reported that soluble chitin oligomers are bound by the LysM domains of two receptor monomers, resulting in the receptor dimerization and the activation of subsequent signaling (Liu et al., 2012b; Hayafune et al., 2014). It has also been shown that soluble oligomeric PGN fragments stimulate plant immune responses in *Arabidopsis* (Gust et al., 2007; Erbs et al., 2008; Willmann et al., 2011).

Soluble PAMPs are proposed to be generated from macromolecular assemblies in two possible ways. First, imperfect recycling of bacterial wall components might serve passively as sources of soluble ligands for host PRRs sensing (Nigro et al., 2008). Second, host hydrolytic enzymes might release actively soluble ligands from bacterial envelope structures (Wang et al., 2006). The second option prompted us to investigate whether this way also is important in *Arabidopsis* immunity, and if so, which protein is responsible for the generation of soluble PGN from the insoluble PGN complex. The results in this study showed that LYS1 harbored PGN hydrolytic activity (Figure 12) and was able to release soluble fragments from insoluble PGN (Figure 15). More importantly, these LYS1-generated soluble PGN fragments harbored immunogenic activity and triggered immunity-associated responses in a PGN receptor-dependent manner (Figure 15B).

Therefore, we conclude that lysozyme-like LYS1 contributes to the inducible defence in *Arabidopsis* by generating the soluble PGN fragments to activate PTI.

It was demonstrated that soluble chitin oligomers induced the formation of a receptor complex at the plasma membrane to activate subsequent signaling in *Arabidopsis* and rice (Cao et al., 2014; Hayafune et al., 2014). Likewise, it was postulated that soluble PGN oligomer binding to LYM1 and LYM3 results in the formation of a tripartite complex of LYM1, LYM3 and CERK1 to activate subsequent immune responses (Willmann et al., 2011), but the direct evidence of physical LYM1/LYM3/CERK1 interaction *in planta* is still lacking. It remains to be elucidated if LYM1, LYM3 and CERK1 form a protein complex, and if so, how the receptor complex formation is associated with the PGN ligand.

Recent advances in the study of chitin receptor structures revealed that a sandwich-type dimerization of receptor monomers is induced by chitin oligomers and is required for activation of immune signaling in *Arabidopsis* and rice (Liu et al., 2012b; Cao et al., 2014; Hayafune et al., 2014). In both *Arabidopsis* and rice, the fragment sizes of eight GlcNAc were defined as the minimum length for inducing dimerization of the receptor complex. The similarity of receptors and substrates between the chitin-perception system and the PGN-perception system raises the question if the minimum immunogenic unit model in the chitin-perception system can be generalized to the PGN-perception system. Previous data showed that a PGN glycan chain that is longer than the disaccharide can display immunogenic activity, but the exact minimum immunogenic unit of PGN is still unknown (Gust et al., 2007). Attempts to identify the minimum immunogenic motif of PGN have failed so far due to technical limits. The synthesized PGN oligomers up to heptamers (kindly provided by Koichi Fukase and Yukari Fujimoto, Osaka University) showed no immunogenic activity, and higher oligomers could not be obtained (data not shown). Although LYS1-digested PGN can be efficiently separated by HPLC (Figure 15A), the amount of PGN in each collected peak is so far not enough to perform subsequent immune assays. These limitations could be overcome in the future by advancements in HPLC purification and PGN synthesis.

In summary, based on the activation mechanism of the chitin receptors, it is most likely that plants can only perceive PGN ligands within a defined range, possibly generated by

LYS1, whereas insoluble complex PGN and smaller units do not have immunogenic activity.

### **4.3 LYS1 is a bifunctional lysozyme/chitinase**

Plants do not contain chitin in their cell walls, whereas major agricultural pests such as most fungi and insects do, which leads to the hypothesis that plant chitinases act as a defence mechanism against pathogens. Indeed, plant chitinases are often considered as PR-proteins, since their activities can be induced by abiotic and biotic stress (Graham and Sticklen, 1994).

Plant chitinases play diverse physiological roles in plants (Grover, 2012) and are classified into two classes, GH18 and GH19, which do not share amino acid sequence similarity (Henrissat, 1991). These two chitinase families have completely different 3-dimensional structures and molecular mechanisms despite shared chitinolytic activity (Hamid et al., 2013), possibly indicating convergent evolution of the two families from different ancestors. Chitinases of the GH18 class are ubiquitously found in all organisms, whereas those of the GH19 class are found almost exclusively in plants.

A comparative study of class I (GH19) and class III (GH18) chitinases revealed that an excess of amino acid replacements can be found at the active site and substrate binding cleft of class I chitinases (Bishop et al., 2000). This highly unusual pattern of replacements in the plant class I chitinases was proposed as a rapid adaptation to the fungal pathogens that had evolved to overcome plant chitinolytic activity through enzymatic inhibition or modification of their cell wall. Such an anomaly suggests that class I chitinases face a highly positive selective pressure from the fungal pathogens. Therefore, similar to R genes, plant defence proteins such as chitinases might also undergo a rapid adaptive evolution driven by an arms race between plants and fungal pathogens. This raises the question why the class III chitinases did not display such frequent amino acid substitutions within the active site cleft. One possibility is that the similarity of the protein fold and function between plant class III and microbial class III chitinases could protect the plant class III chitinases from evolutionary pressure. In other words, if a given pathogen evolves to produce an inhibitor for plant class III chitinases, this inhibitor likely also inhibits its own class III chitinase, thereby interfering with



2011)(Grabherr, 2011)(Grabherr, 2011) (Grabherr, 2011). For example, plants with LYS1/CHIA levels less than 10% of that of the wild-type showed no sign of increased susceptibility to *Botrytis cinerea* (Samac and Shah, 1994). These results are in agreement with our lab's finding that *LYS1<sup>KD</sup>* plants did not display higher susceptibility to *B. cinerea* and *A. brassicicola* (Grabherr, 2011). This may suggest that LYS1 has lost its role in defence against these fungi possibly due to an unknown counteractive mechanism co-evolved by the fungal pathogens. However, LYS1 still plays an important role in plant defence against bacterial pathogens like *PtoDC3000* (Figure 20), and this anti-bacterial function is associated with its lysozyme activity (Figure 15).

Taken together, the bifunctional LYS1 has likely lost its anti-fungal activities towards *B. cinerea* and *A. brassicicola* but retained anti-bacterial activities towards *PtoDC3000* possibly due to co-evolutionary interaction of plants and pathogens, and thus it plays a unique role in plant immunity in *Arabidopsis*.

#### **4.4 How does LYS1 contribute to defence: direct killing or generating PAMPs?**

When microbes invade the apoplast of plant cells, the host cells secrete hydrolytic enzymes, such as chitinases and glucanases, to target the constituents of the microbial cell wall and thus disrupt cell wall integrity (Schlumbaum et al., 1986). Thus, hydrolytic enzyme activities can have a dual function for the host plant: Firstly, releasing PAMP molecules that further stimulate immune responses and secondly, causing cell collapse in the invader to inhibit its growth (Kombrink et al., 2011).

In mammals, PGN hydrolytic enzyme activities such as lysozymes have been ascribed functions in direct bacterial killing (Cho et al., 2005) and in generating soluble PGN fragments as ligands for PRRs (Cho et al., 2005; Dziarski and Gupta, 2010; Davis et al., 2011). For example, human PGRP-S, one PGN recognition protein, is co-located with lysozyme in the granules of human neutrophils. The two proteins act together to kill bacteria trapped in the neutrophil extracellular traps (Cho et al., 2005). In addition, lysozymes in mice can release PGNs as PAMPs for recognition by NOD2 to activate immune responses (Davis et al., 2011).

A role for plant glycosyl hydrolases in immunogenic PAMP generation and immune activation has also been proposed previously (Mithöfer et al., 2000; Fliegmann et al.,

2004). An extracellular soluble bipartite soybean glucan binding protein (GBP) was shown to harbor 1,3- $\beta$ -glucanase activity and binding activity for glucan fragments of DP > 6 derived of intact glucans. Complex glucans constitute major constituents of various *Phytophthora* species, many of which are plant pathogens (Kroon et al., 2011). It was hence suggested that during infection GBP endoglucanase activity produces soluble *Phytophthora*-derived oligoglucoside fragments as ligands for the high-affinity binding site within this protein (Fliegmann et al., 2004). While this study supported the concept of plant hydrolases tailor-making ligands for plant PRRs, causal evidence for the involvement of the endoglucanase activity in plant immunity was not provided.

In this study, LYS1 was identified as a plant lysozyme-like enzyme which harbors PGN hydrolytic activity (Figure 12). We assume two possible scenarios as to how LYS1 is involved in plant defence. First, LYS1 might directly kill bacterial cells via hydrolyzing bacterial cell walls. In an *in vitro* digestion and inhibition assay, LYS1 could indeed digest *E. coli* cells directly, subsequently leading to a reduced growth of *E. coli* on agar plate (Figure.21C). The bactericidal activity of LYS1 could contribute to plant basal immunity against non-adapted bacteria and even some adapted bacterial pathogens. In response, adapted bacterial plant pathogens may have evolved a counteractive mechanism to avoid digestion of their cell wall. As we observed in Figure 21, LYS1 could not digest *PtoDC3000* cells and could not inhibit its growth, indicating that phytopathogenic *PtoDC3000* might have evolved inhibitory mechanisms against *Arabidopsis* LYS1. This could also explain our observation that *LYS1<sup>OE</sup>* transgenics are more susceptible and not more resistant to *PtoDC3000* in spite of high LYS1 levels in the *LYS1<sup>OE</sup>* lines (Figure 20B), which argues against an important role for LYS1 in killing *PtoDC3000*. Second, LYS1 most likely provides the PGN receptors with soluble immunogenic ligands that stimulate the plant immune system to fend off invading bacterial pathogens. Our analysis showed that LYS1 can generate soluble fragments from PGN complex, and these fragments displayed immunogenic activities in rice and *Arabidopsis* (Figure 15). These immune responses were PGN receptor-dependent, thereby confirming that LYS1-generated PGN fragments are subsequently recognized by the receptors to trigger downstream responses.

The two LYS1 functions involved in defence may co-exist in plants to promote synergetic plant immunity. However, the second LYS1 function of generating soluble PAMPs to induce the immune system seems to be more efficient. In order to directly and completely kill bacteria via bactericidal activity, LYS1 protein is most likely required in relatively high amounts in the plant apoplast. In comparison, relatively little amounts of LYS1 are able to release PGN ligands, which initiate signaling and later even amplify the immune responses. Moreover, in the co-evolution of pathogens and plants, plant-secreted LYS1 could be targeted by inhibitors of pathogens and lead to reduced enzymatic activity. Such compromised enzymatic activity of LYS1 could not kill bacteria directly, but could still release PGN ligands from bacterial cells to induce immune responses.

Indeed, although we did not find LYS1 hydrolytic activity towards *PtoDC3000* cells (Figure 21), *LYS1<sup>KD</sup>* lines are more susceptible to *PtoDC3000* than WT (Figure 20B). We assume that LYS1 in WT could still retain weak hydrolytic activity at levels sufficient to produce enough PAMPs for induction of immune responses in plants (Figure 20B).

Taken together, LYS1 contributes to plant resistance to *PtoDC3000* by generating immunogenic ligands rather than directly killing bacteria.

### **4.5 Dynamics of LYS1 protein levels are related to immunity performance**

In plants, there is generally a trade-off between growth and immunity. In order to reduce the fitness cost, plants fine-tune appropriate immune responses to invading pathogens. LYS1-mediated immunity is no exception.

In wild type plants, LYS1 was constitutively expressed at low level (Figure 4). When pathogenic bacteria enter the apoplast, positively-charged LYS1 at low levels could efficiently bind to the invading negatively-charged bacterial cell walls and hydrolyze them, at least partially. Then LYS1-released PGN ligands get better access to plasma membrane-localized receptors and bind to them to activate subsequent immune responses, including increased LYS1 levels at the infected site. The induced, high-level LYS1 could contribute to immunity via direct bacterial killing (in case of non-adapted pathogens) and by generating more soluble ligands (in case of adapted and non-

adapted pathogens), serving to enhance immune activation, not only locally, but also systemically. Not surprisingly, in *LYS1<sup>KD</sup>* plants, a lack of LYS1 led to compromised plant immunity and resulted in a higher susceptibility to pathogens (Figure 20B).

In wild type plants, once the invading pathogens are successfully warded off, pathogen numbers will decrease accordingly, thus reducing the amount of newly released immunogenic PGN fragments. The high LYS1 levels in the apoplast might continually degrade the soluble PGN fragments into smaller units that do not induce immunity, but only bind to receptors. As a result, receptor stimulation will gradually be attenuated, followed also by a decrease in LYS1 levels back to the un-induced basal levels. Therefore, in *LYS1<sup>OE</sup>* plants where LYS1 is constitutively expressed at high levels, this LYS1 will most likely always over-digest PGN into small fragments, which have no immunogenic activities (Figure 15D). These over-digested short fragments might compete with long immunogenic fragments for binding to their receptors and consequently block the receptor-mediated immune signaling, resulting in a reduced activation of the immune system. Direct killing of bacteria in *LYS1<sup>OE</sup>* lines, however, was not observed and is likely inhibited by adapted pathogens, resulting in a total reduced resistance to adapted pathogens. This model could explain our observation that *LYS1<sup>OE</sup>* plants with high constitutive LYS1 levels displayed an elevated susceptibility to *PtoDC3000* in comparison to wild type plants (Figure 20).

In conclusion, LYS1 levels are fine-tuned in response to external flexible stimuli to defend against pathogens. Inappropriate LYS1 levels will compromise plant immunity as shown in *LYS1<sup>KD</sup>* and *LYS1<sup>OE</sup>* mutant lines. There is another prominent example where overexpression of a protein mimics the effect of genetic inactivation. Strong overexpression of BAK1, a co-receptor of leucine-rich-repeat receptor kinases, triggers inappropriate plant cell death (Belkhadir et al., 2012) as is also observed in *bak1* mutants (Kemmerling et al., 2007). Hence, it can be assumed that wild-type levels of proteins are optimized during evolution and it is therefore not surprising that either too little or too much activity might have a deleterious effect on plant.

These results should also remind us to be aware of possible complications arising from manipulation of protein levels in transgenic plants used in agriculture.

#### 4.6 Known signaling components in CERK1-mediated immunity

Plant LysM-type PRRs recognize GlcNAc-containing ligands, such as fungal chitin, bacterial PGN (PGN), and thus have functions in innate immunity (Böhm et al., 2014). However, downstream signaling events are so far poorly understood.

In rice, upon perceiving chitin, the chitin elicitor binding protein (CEBiP) dimer likely recruits *Oryza sativa* chitin elicitor receptor kinase 1 (OsCERK1), which is subsequently (auto)-phosphorylated and thus activates the downstream immune response (Hayafune et al., 2014). In the process, OsCERK1 phosphorylates OsRacGEF1 (*Oryza sativa* RAC guanine nucleotide exchange factor 1), which activates the small GTPase OsRAC1 (Akamatsu et al., 2013). In turn OsRAC1 was proposed to interact with downstream signaling components and regulate the final steps of the signaling pathways, including the generation of reactive oxygen species, phytoalexins, lignins, the activation of MAPK cascades, and the expression of PR proteins (Akamatsu et al., 2013). In addition, two RLKs, *Oryza sativa* receptor-like cytoplasmic kinase 185 (OsRLCK185) and *Oryza sativa* receptor-like cytoplasmic kinase 176 (OsRLCK176), were shown to mediate chitin-induced signaling, potentially constituting additional links between PRRs and the MAPK cascades (Yamaguchi et al., 2013; Ao et al., 2014). Finally, two LysM-receptor-like proteins, OsLYP4 and OsLYP6, were reported to heterodimerize with OsCERK1 upon chitin binding and thereby induce immune responses (Liu et al., 2012a; Ao et al., 2014). Interestingly, OsRLCK176, OsCERK1, OsLYP4 and OsLYP6 do not only respond to chitin, but also have been implicated in PGN responses. Thus, OsCERK1 most likely acts as an adaptor for signal transduction of multiple LysM-type PRRs and is not solely involved in chitin-induced but also PGN-induced immunity (Ao et al., 2014; Kouzai et al., 2014).

In *Arabidopsis*, it was suggested that chitin oligomers (DP>6) are bound by the LysM domains of two CERK1 monomers, resulting in receptor dimerization and trans-phosphorylation of their cytoplasmic kinase domains (Liu et al., 2012b). This dimerization model is based on relatively long (DP=8), not short (DP=5 or 6), chitin oligomers, despite the findings that short chitin oligomers can also induce chitin-triggered responses via a currently unknown mechanism (Felix et al., 1993; Liu et al.,

2012b). Upon perception of chitin, CERK1 immediately phosphorylates two receptor-like cytoplasmic kinases (RLCKs), BOTRYTIS-INDUCED KINASE1 (BIK1) and PBS1-like protein 27 (PBL27), and then regulates partially overlapping but also different downstream signaling pathways. Both RLCKs were involved in the regulation of MAMP-induced callose deposition, but only BIK1 was involved in MAMP-induced accumulation of ROS. Likewise, only PBL27 was involved in the activation of MAPK cascades (Shinya et al., 2014).

Interestingly, LYM2, which has high affinity binding with chitin, mediates immunity via a CERK1-independent pathway (Faulkner et al., 2013). Recently, LYK5, a kinase-inactive LYK, was proposed to form a chitin-inducible complex with CERK1, which leads to CERK1 phosphorylation and the induction of chitin-activated immunity (Cao et al., 2014). Such a sandwich-like complex model, as similarly proposed for OsCERK1 in rice, would argue that chitin perception systems of rice and *Arabidopsis* are somehow similar to each other.

### 4.7 CDPKs in plant immunity

In order to identify further novel components of the chitin- and PGN-induced CERK1-mediated signaling pathways, we searched the M.I.N.D. yeast-two-hybrid database for putative CERK1 interacting proteins. One candidate protein chosen for further analysis was the calcium-dependent protein kinase CPK15.

Upon perception of PAMPs, plant PRRs immediately activate opening of  $\text{Ca}^{2+}$  channel in the plasma membrane and induce rapid  $\text{Ca}^{2+}$  influx, thus resulting in a rapid increase of cytosolic  $\text{Ca}^{2+}$  concentration (Lecourieux et al., 2006).  $\text{Ca}^{2+}$  has long been recognized as a conserved second messenger and principal mediator in plant immune and stress signaling through  $\text{Ca}^{2+}$  sensors (Boudsocq and Sheen, 2013). Plants possess three main families of calcium sensors: calmodulins (CaM), calcineurin B-like proteins (CBL) and CDPKs. Unlike CaM and CBL that relay the  $\text{Ca}^{2+}$ -induced conformational change to protein partners, CDPKs have the unique feature that both  $\text{Ca}^{2+}$  sensing and receiver domains are combined within a single protein to directly translate  $\text{Ca}^{2+}$  signals into phosphorylation (Boudsocq and Sheen, 2013).

CDPKs are encoded by 34 members in *Arabidopsis* and divided into four subgroups (Cheng et al., 2002). Typically, a CDPK harbors an N-terminal variable domain, a Ser/Thr kinase domain, an auto-inhibitory junction region and a regulatory calmodulin-like domain (CaM-LD) (Harper et al., 2004). The CaM-LD is composed of the four EF-hand  $\text{Ca}^{2+}$ -binding motifs which have high  $\text{Ca}^{2+}$  affinities resulting in  $\text{Ca}^{2+}$ -mediated CDPK regulation. In the basal state, the interaction between the auto-inhibitory region and the kinase domain keeps the kinase in an inactive state by a pseudosubstrate mechanism (Harper et al., 2004). The C-terminal lobe of the CaM-LD exhibiting high  $\text{Ca}^{2+}$  affinity interacts with the auto-inhibitory region at low  $\text{Ca}^{2+}$  levels to stabilize the structure (Weljie and Vogel, 2004).  $\text{Ca}^{2+}$  binding to the low-affinity N-terminal lobe of the CaM-LD induces a conformational change that releases the auto-inhibition (Harper et al., 2004), resulting in activation of the protein kinase domain. N-variable domains of CDPKs often have a myristoylation and a palmitoylation posttranslational modification, which determines protein subcellular localization and substrate recognition (Asai et al., 2013). Mutations of N-terminal myristoylation and palmitoylation sites in the N-terminal domain eliminated the predominantly plasma membrane localization and the capacity of *St*CDPK5 to activate *St*RBOHB (Respiratory burst oxidase homolog B) *in vivo* (Asai et al., 2013). CPK15 in this study is predicted to have both myristoylation and palmitoylation modifications (Cheng et al., 2002) and could be shown to be localized at the plasma membrane (Figure 27). This localization of CPK15 would facilitate CERK1-interaction to mediate a CERK1-dependent reactive oxygen species (ROS) burst (Figure 25), probably also through association with the NADPH oxidase RBOHD (Respiratory burst oxidase homolog D).

The 34 CDPK members of *Arabidopsis* are cluster into four subgroups (Figure 29). The members in one subgroup often display redundancy along with functional specificity, exemplified by CDPK4/5/6/11 in orchestrating immune gene expression, CDPK1/2/4/11 in ROS production, and CDPK1/2/5/6/ in programmed cell death (PCD) (Gao et al., 2013). The functional specificity of CDPKs is maintained apparently via phosphorylation and activation of different substrates in distinct subcellular compartments. The apparent functional redundancy of closely related CDPKs often challenges genetic investigation of special function. In this study, CDPK15 displayed only a 30-50 % reduction in chitin-

induced ROS accumulation (Figure 23 and 25), which may indicate the presence of functional redundant members such as CDPK21 and CDPK23, the two closest homologs of CDPK15 (Figure 29). It will be interesting to investigate roles of CDPK21 and CDPK23 in chitin-induced signaling.

PAMP perception immediately induces the activation of MAPK and CDPK, leading to expression of defence genes. Unexpectedly, CDPKs and MAPK cascades differentially regulate flg22-induced early genes in at least four regulatory programs (Boudsocq et al., 2010). In this study, CPK15 did not affect MAPK cascades and may thus function independently of MAPK cascades (Figure 26).

Unlike most CDPKs, which are involved in plant immune signaling as positive regulators (Boudsocq et al., 2010), it was reported recently that CPK28 acts as a negative regulator in PTI signaling (Monaghan et al., 2014). CPK28 associates with RBOHD and BIK1, and phosphates the latter, an important convergent substrate of multiple PRR complexes such as CERK1 and FLS2 (Zhang et al., 2010; Kadota et al., 2014). In this study, CPK15 is involved in chitin- but not flg22-induced ROS (Figure 25). Thus we postulate that CPK15 should be placed upstream of BIK1 to specifically act in CERK1-mediated PTI signaling. Indeed, our results showed that CPK15 directly interacts with CERK1 (Figure 28). Further investigation of the possible association between CPK15 and BIK1 or between CPK15 and RBOHD will be very interesting.

Taken together, CPK15 directly targets CERK1 and positively regulates CERK1-mediated PTI signaling in *Arabidopsis*.

## 5. Summary

As one part of a two-tiered pathogen-detection system in plants, PTI is not only sufficient to ward off most microbes, but also contributes to basal immunity during infection.

Although PGN and the LYM1-LYM3-CERK1 receptor complex have been identified as one PAMP-PRR pair in *Arabidopsis*, upstream and downstream events of PGN perception remain elusive. Specifically, it is unclear whether and, if so, how PGN supermolecules are processed prior to perception by the LYM1-LYM3-CERK1 receptor complex. Moreover, the mechanisms linking PGN perception with diverse downstream immune responses are little understood.

In this study, a lysozyme-like hydrolase (lysozyme 1, LYS1) was identified as an enhancer in PGN-induced immunity. Upon bacterial infection or exposure to bacterial patterns, *Arabidopsis* produces LYS1 to release soluble PGN fragments from insoluble bacterial cell walls. LYS1-released soluble PGNs trigger typical immunity-associated responses, such as medium alkalinization and up-regulation of resistance-related genes. Importantly, these immune responses are dependent on the PGN receptor complex. *LYS1* mutants exhibit super-susceptibility to bacterial infection similar to that observed in PGN receptor mutants. We propose that plants employ hydrolytic activities for the decomposition of complex bacterial structures and that the subsequent generation of soluble patterns might aid PRR-mediated immune activation in cell layers adjacent to infection sites.

In addition, we identified the calcium-dependent protein kinase CPK15 as an interactor of CERK1, which is not only involved in PGN perception but also in chitin recognition. CPK15 was shown to interact with CERK1 in the yeast-two-hybrid system and in plant tissue, and *cpk15* mutants displayed reduced ROS accumulation upon chitin treatment. These findings indicate that CPK15 is involved in CERK1-mediated PTI signaling.

Summing up, this study aimed at improving our understanding of PGN- and chitin-triggered immunity by identifying and characterizing critical components of the plant immune system, such as LYS1, involved in upstream events of PGN perception, and CPK15, involved in downstream events of CERK1-mediated glucan perception.

### 6. Zusammenfassung

Als ein Teil eines zweistufigen pflanzlichen Pathogen-Erkennungssystems ist die PAMP-getriggerte Immunität (PTI) nicht nur ausreichend zur Abwehr der meisten Mikroben, sondern trägt auch zur basalen Immunität während der Infektion bei.

Obwohl PGN und der LYM1-LYM3-CERK1 Rezeptorkomplex als ein PAMP/PRR-Paar in *Arabidopsis* identifiziert worden sind, sind sowohl die vor- als auch die nachgeschalteten Ereignisse bei der PGN-Erkennung noch wenig untersucht. Insbesondere ist unklar, ob, und wenn ja, wie PGN-Makromoleküle vor ihrer Perzeption durch den LYM1-LYM3-CERK1 Rezeptorkomplex prozessiert werden. Darüber hinaus ist wenig über die Mechanismen bekannt, die die PGN-Erkennungsproteine mit den verschiedenen nachgeschalteten Immunreaktionen verbindet.

In dieser Studie wurde eine Lysozym-artige Hydrolase (Lysozym 1, LYS1) als Verstärker der PGN-induzierten Immunität identifiziert. Bei bakterieller Infektion oder Behandlung mit bakteriellen PAMPs produziert *Arabidopsis* LYS1, um lösliche PGN-Fragmente aus unlöslichen Bakterienzellwänden freizusetzen. LYS1-generierte lösliche PGNs lösen typische Immunität-assoziierte Reaktionen aus, wie Medium-Alkalisierung und die Hochregulierung von Abwehr-Genen, und zwar abhängig vom PGN-Rezeptorkomplex. *Lys1*-Mutanten zeigen in bakteriellen Infektionen eine erhöhte Anfälligkeit, ähnlich wie es auch in den PGN Rezeptormutanten zu beobachten ist. Wir gehen davon aus, dass Pflanzen hydrolytische Aktivitäten zur Zersetzung komplexer Strukturen aus bakteriellen Zellwände einsetzen, und dass die damit einhergehende Erzeugung von löslichen PAMPs eine PRR-vermittelte Immunaktivierung in den an die Infektionsstelle angrenzenden Zellschichten unterstützen könnte.

Außerdem wurde die Calcium-abhängige Proteinkinase CPK15 identifiziert als ein Interaktor von CERK1, einem Rezeptor der sowohl in der PGN- als auch der Chitin-Erkennung involviert ist. CPK15 konnte mit CERK1 im Hefe-2-Hybrid-System sowie im Pflanzengewebe interagieren, und *cpk15*-Mutanten zeigten eine reduzierte ROS-Akkumulation nach Chitin-Behandlung. Diese Ergebnisse lassen vermuten, dass CPK15 in der CERK1-vermittelten Signalweiterleitung während der PTI beteiligt ist.

Zusammenfassend sollte diese Studie dazu beitragen, unser Verständnis der PGN-ausgelösten Immunität zu verbessern. So wurden hier kritische Komponenten des pflanzlichen Immunsystems identifiziert und charakterisiert, wie zum einen LYS1, welches an der PGN-Wahrnehmung vor Rezeptorbindung beteiligt ist, und zum anderen CPK15, welche wichtig für die durch CERK1 vermittelte Signalweiterleitung nach Glucan-Wahrnehmung ist.

## 7. Reference

- Agrios, G.N.** (2005). *plant pathology*. ( San Diego, California, usa: Elsevier Academic Press).
- Ahuja, I., Kissen, R., and Bones, A.M.** (2012). Phytoalexins in defense against pathogens. *Trends in plant science* **17**, 73-90.
- Aires, A., Mota, V.R., Saavedra, M.J., Monteiro, A.A., Simoes, M., Rosa, E.A., and Bennett, R.N.** (2009). Initial in vitro evaluations of the antibacterial activities of glucosinolate enzymatic hydrolysis products against plant pathogenic bacteria. *Journal of applied microbiology* **106**, 2096-2105.
- Akamatsu, A., Wong, H.L., Fujiwara, M., Okuda, J., Nishide, K., Uno, K., Imai, K., Umemura, K., Kawasaki, T., Kawano, Y., and Shimamoto, K.** (2013). An OsCEBiP/OsCERK1-OsRacGEF1-OsRac1 module is an essential early component of chitin-induced rice immunity. *Cell Host Microbe* **13**, 465-476.
- Akins, R.E., Levin, P.M., and Tuan, R.S.** (1992). Cetyltrimethylammonium bromide discontinuous gel electrophoresis: Mr-based separation of proteins with retention of enzymatic activity. *Analytical biochemistry* **202**, 172-178.
- Akira, S., Uematsu, S., and Takeuchi, O.** (2006). Pathogen recognition and innate immunity. *Cell* **124**, 783-801.
- Antoniw, J.F., Dunkley, A.M., White, R.F., and Wood, J.** (1980). Soluble leaf proteins of virus-infected tobacco (*Nicotiana tabacum*) cultivars [proceedings]. *Biochemical Society transactions* **8**, 70-71.
- Ao, Y., Li, Z., Feng, D., Xiong, F., Liu, J., Li, J.F., Wang, M., Wang, J., Liu, B., and Wang, H.B.** (2014). OsCERK1 and OsRLCK176 play important roles in peptidoglycan and chitin signaling in rice innate immunity. *The Plant journal : for cell and molecular biology* **80**, 1072-1084.
- Apel, K., and Hirt, H.** (2004). Reactive oxygen species: Metabolism, oxidative stress, and signal transduction. *Annual review of plant biology* **55**, 373-399.
- Asai, S., Ichikawa, T., Nomura, H., Kobayashi, M., Kamiyoshihara, Y., Mori, H., Kadota, Y., Zipfel, C., Jones, J.D.G., and Yoshioka, H.** (2013). The Variable Domain of a Plant Calcium-dependent Protein Kinase (CDPK) Confers Subcellular Localization and Substrate Recognition for NADPH Oxidase. *Journal of Biological Chemistry* **288**, 14332-14340.
- Asai, T., Tena, G., Plotnikova, J., Willmann, M.R., Chiu, W.L., Gomez-Gomez, L., Boller, T., Ausubel, F.M., and Sheen, J.** (2002). MAP kinase signalling cascade in Arabidopsis innate immunity. *Nature* **415**, 977-983.
- Audy, P., Benhamou, N., Trudel, J., and Asselin, A.** (1988). Immunocytochemical localization of a wheat germ lysozyme in wheat embryo and coleoptile cells and cytochemical study of its interaction with the cell wall. *Plant physiology* **88**, 1317-1322.
- Ausubel, F.M.** (2005). Are innate immune signaling pathways in plants and animals conserved? *Nat Immunol* **6**, 973-979.
- Bardoel, B.W., van der Ent, S., Pel, M.J., Tommassen, J., Pieterse, C.M., van Kessel, K.P., and van Strijp, J.A.** (2011). *Pseudomonas* evades immune recognition of flagellin in both mammals and plants. *PLoS pathogens* **7**, e1002206.
- Bartel, P.L., and Fields, S.** (1995). Analyzing Protein-Protein Interactions Using 2-Hybrid System. *Method Enzymol* **254**, 241-263.
- Bateman, A., and Bycroft, M.** (2000). The structure of a LysM domain from E-coli membrane-bound lytic murein transglycosylase D (MltD). *Journal of molecular biology* **299**, 1113-1119.
- Bednarek, P.** (2012). Chemical warfare or modulators of defence responses - the function of secondary metabolites in plant immunity. *Curr Opin Plant Biol* **15**, 407-414.
- Beers, E.P., and McDowell, J.M.** (2001). Regulation and execution of programmed cell death in response to pathogens, stress and developmental cues. *Current Opinion in Plant Biology* **4**, 561-567.

- Beintema, J.J., Jekel, P.A., and Hartmann, J.B.H.** (1991). The Primary Structure of Hevamine, an Enzyme with Lysozyme/Chitinase Activity from *Hevea brasiliensis* latex. *European Journal of Biochemistry* **200**, 123-130.
- Belkhadir, Y., Jaillais, Y., Epple, P., Balsemao-Pires, E., Dangl, J.L., and Chory, J.** (2012). Brassinosteroids modulate the efficiency of plant immune responses to microbe-associated molecular patterns. *Proceedings of the National Academy of Sciences of the United States of America* **109**, 297-302.
- Berg, G.** (2009). Plant-microbe interactions promoting plant growth and health: perspectives for controlled use of microorganisms in agriculture. *Applied microbiology and biotechnology* **84**, 11-18.
- Bertsche, U., Mayer, C., Gotz, F., and Gust, A.A.** (2015). Peptidoglycan perception-Sensing bacteria by their common envelope structure. *International journal of medical microbiology : IJMM* **305**, 217-223.
- Bishop, J.G., Dean, A.M., and Mitchell-Olds, T.** (2000). Rapid evolution in plant chitinases: molecular targets of selection in plant-pathogen coevolution. *Proceedings of the National Academy of Sciences of the United States of America* **97**, 5322-5327.
- Bittel, P., and Robatzek, S.** (2007). Microbe-associated molecular patterns (MAMPs) probe plant immunity. *Current Opinion in Plant Biology* **10**, 335-341.
- Böhm, H., Albert, I., Fan, L., Reinhard, A., and Nurnberger, T.** (2014). Immune receptor complexes at the plant cell surface. *Curr Opin Plant Biol* **20**, 47-54.
- Bokma, E., van Koningsveld, G.A., Jeronimus-Stratingh, M., and Beintema, J.J.** (1997). Hevamine, a chitinase from the rubber tree *Hevea brasiliensis*, cleaves peptidoglycan between the C-1 of N-acetylglucosamine and C-4 of N-acetylmuramic acid and therefore is not a lysozyme. *FEBS letters* **411**, 161-163.
- Boller, T.** (1995). Chemoperception of Microbial Signals in Plant-Cells. *Annu Rev Plant Phys* **46**, 189-214.
- Boller, T.** (2005). Peptide signalling in plant development and self/non-self perception. *Curr Opin Cell Biol* **17**, 116-122.
- Boller, T., and Felix, G.** (2009). A renaissance of elicitors: perception of microbe-associated molecular patterns and danger signals by pattern-recognition receptors. *Annual review of plant biology* **60**, 379-406.
- Boudsocq, M., and Sheen, J.** (2013). CDPKs in immune and stress signaling. *Trends in plant science* **18**, 30-40.
- Boudsocq, M., Willmann, M.R., McCormack, M., Lee, H., Shan, L., He, P., Bush, J., Cheng, S.H., and Sheen, J.** (2010). Differential innate immune signalling via Ca(2+) sensor protein kinases. *Nature* **464**, 418-422.
- Bozkurt, T.O., Schornack, S., Banfield, M.J., and Kamoun, S.** (2012). Oomycetes, effectors, and all that jazz. *Current Opinion in Plant Biology* **15**, 483-492.
- Bradford, M.M.** (1976). A rapid and sensitive method for the quantitation of microgram quantities of protein utilizing the principle of protein-dye binding. *Analytical biochemistry* **72**, 248-254.
- Brunner, F., Stintzi, A., Fritig, B., and Legrand, M.** (1998). Substrate specificities of tobacco chitinases. *The Plant journal : for cell and molecular biology* **14**, 225-234.
- Brutus, A., Sicilia, F., Macone, A., Cervone, F., and De Lorenzo, G.** (2010). A domain swap approach reveals a role of the plant wall-associated kinase 1 (WAK1) as a receptor of oligogalacturonides. *Proceedings of the National Academy of Sciences of the United States of America* **107**, 9452-9457.
- Bueter, C.L., Specht, C.A., and Levitz, S.M.** (2013). Innate sensing of chitin and chitosan. *PLoS pathogens* **9**, e1003080.
- Buist, G., Steen, A., Kok, J., and Kuipers, O.P.** (2008). LysM, a widely distributed protein motif for binding to (peptido)glycans. *Molecular microbiology* **68**, 838-847.

- Cabeen, M.T., and Jacobs-Wagner, C.** (2005). Bacterial cell shape. *Nat Rev Microbiol* **3**, 601-610.
- Callewaert, L., and Michiels, C.W.** (2010). Lysozymes in the animal kingdom. *J Biosci* **35**, 127-160.
- Cao, Y., Liang, Y., Tanaka, K., Nguyen, C.T., Jedrzejczak, R.P., Joachimiak, A., and Stacey, G.** (2014). The kinase LYK5 is a major chitin receptor in Arabidopsis and forms a chitin-induced complex with related kinase CERK1. *eLife* **3**.
- Chamaillard, M., Hashimoto, M., Horie, Y., Masumoto, J., Qiu, S., Saab, L., Ogura, Y., Kawasaki, A., Fukase, K., Kusumoto, S., Valvano, M.A., Foster, S.J., Mak, T.W., Nunez, G., and Inohara, N.** (2003). An essential role for NOD1 in host recognition of bacterial peptidoglycan containing diaminopimelic acid. *Nat Immunol* **4**, 702-707.
- Che, Y.Z., Li, Y.R., Zou, H.S., Zou, L.F., Zhang, B., and Chen, G.Y.** (2011). A novel antimicrobial protein for plant protection consisting of a *Xanthomonas oryzae* harpin and active domains of cecropin A and melittin. *Microbial biotechnology* **4**, 777-793.
- Cheng, S.H., Willmann, M.R., Chen, H.C., and Sheen, J.** (2002). Calcium signaling through protein kinases. The Arabidopsis calcium-dependent protein kinase gene family. *Plant physiology* **129**, 469-485.
- Cheong, J.J., Birberg, W., Fugedi, P., Pilotti, A., Garegg, P.J., Hong, N., Ogawa, T., and Hahn, M.G.** (1991). Structure-activity relationships of oligo-beta-glucoside elicitors of phytoalexin accumulation in soybean. *The Plant cell* **3**, 127-136.
- Cheong, Y.H., Chang, H.S., Gupta, R., Wang, X., Zhu, T., and Luan, S.** (2002). Transcriptional profiling reveals novel interactions between wounding, pathogen, abiotic stress, and hormonal responses in Arabidopsis. *Plant physiology* **129**, 661-677.
- Chinchilla, D., Zipfel, C., Robatzek, S., Kemmerling, B., Nurnberger, T., Jones, J.D., Felix, G., and Boller, T.** (2007). A flagellin-induced complex of the receptor FLS2 and BAK1 initiates plant defence. *Nature* **448**, 497-500.
- Cho, J.H., Fraser, I.P., Fukase, K., Kusumoto, S., Fujimoto, Y., Stahl, G.L., and Ezekowitz, R.A.B.** (2005). Human peptidoglycan recognition protein S is an effector of neutrophil-mediated innate immunity. *Blood* **106**, 2551-2558.
- Cho, S., Wang, Q., Swaminathan, C.P., Heseck, D., Lee, M., Boons, G.J., Mobashery, S., and Mariuzza, R.A.** (2007). Structural insights into the bactericidal mechanism of human peptidoglycan recognition proteins. *Proceedings of the National Academy of Sciences of the United States of America* **104**, 8761-8766.
- Choi, J., Tanaka, K., Liang, Y., Cao, Y.R., Lee, S.Y., and Stacey, G.** (2014). Extracellular ATP, a danger signal, is recognized by DORN1 in Arabidopsis. *Biochem J* **463**, 429-437.
- Chomczynski, P., and Sacchi, N.** (1987). Single-step method of RNA isolation by acid guanidinium thiocyanate-phenol-chloroform extraction. *Analytical biochemistry* **162**, 156-159.
- Clough, S.J., and Bent, A.F.** (1998). Floral dip: a simplified method for *Agrobacterium*-mediated transformation of *Arabidopsis thaliana*. *The Plant journal : for cell and molecular biology* **16**, 735-743.
- Cohen-Kupiec, R., and Chet, I.** (1998). The molecular biology of chitin digestion. *Curr Opin Biotech* **9**, 270-277.
- Collinge, D.B., Kragh, K.M., Mikkelsen, J.D., Nielsen, K.K., Rasmussen, U., and Vad, K.** (1993). Plant Chitinases. *Plant Journal* **3**, 31-40.
- Darvill, A.G., and Albersheim, P.** (1984). Phytoalexins and Their Elicitors - a Defense against Microbial Infection in Plants. *Annu Rev Plant Phys* **35**, 243-275.
- Davis, K.M., Nakamura, S., and Weiser, J.N.** (2011). Nod2 sensing of lysozyme-digested peptidoglycan promotes macrophage recruitment and clearance of *S. pneumoniae* colonization in mice. *J Clin Invest* **121**, 3666-3676.

- de Jonge, R., van Esse, H.P., Kombrink, A., Shinya, T., Desaki, Y., Bours, R., van der Krol, S., Shibuya, N., Joosten, M.H., and Thomma, B.P.** (2010). Conserved fungal LysM effector Ecp6 prevents chitin-triggered immunity in plants. *Science* **329**, 953-955.
- den Hartog, M., Verhoef, N., and Munnik, T.** (2003). Nod factor and elicitors activate different phospholipid signaling pathways in suspension-cultured alfalfa cells. *Plant physiology* **132**, 311-317.
- Denance, N., Sanchez-Vallet, A., Goffner, D., and Molina, A.** (2013). Disease resistance or growth: the role of plant hormones in balancing immune responses and fitness costs. *Front Plant Sci* **4**.
- Dixon, R.A., Achnine, L., Kota, P., Liu, C.J., Reddy, M.S., and Wang, L.** (2002). The phenylpropanoid pathway and plant defence—a genomics perspective. *Molecular plant pathology* **3**, 371-390.
- Dodds, P.N., and Rathjen, J.P.** (2010). Plant immunity: towards an integrated view of plant-pathogen interactions. *Nature reviews. Genetics* **11**, 539-548.
- Durrant, W.E., and Dong, X.** (2004). Systemic acquired resistance. *Annual review of phytopathology* **42**, 185-209.
- Dyachok, J.V., Wiweger, M., Kenne, L., and von Arnold, S.** (2002). Endogenous Nod-factor-like signal molecules promote early somatic embryo development in Norway spruce. *Plant physiology* **128**, 523-533.
- Dziarski, R., and Gupta, D.** (2005a). Peptidoglycan recognition in innate immunity. *Journal of endotoxin research* **11**, 304-310.
- Dziarski, R., and Gupta, D.** (2005b). Staphylococcus aureus peptidoglycan is a toll-like receptor 2 activator: a reevaluation. *Infect. Immun.* **73**, 5212-5216.
- Dziarski, R., and Gupta, D.** (2010). Mammalian peptidoglycan recognition proteins (PGRPs) in innate immunity. *Innate immunity* **16**, 168-174.
- Erbs, G., Silipo, A., Aslam, S., De Castro, C., Liparoti, V., Flagiello, A., Pucci, P., Lanzetta, R., Parrilli, M., Molinaro, A., Newman, M.A., and Cooper, R.M.** (2008). Peptidoglycan and muropeptides from pathogens *Agrobacterium* and *Xanthomonas* elicit plant innate immunity: structure and activity. *Chem Biol* **15**, 438-448.
- Faulkner, C., Petutschnig, E., Benitez-Alfonso, Y., Beck, M., Robatzek, S., Lipka, V., and Maule, A.J.** (2013). LYM2-dependent chitin perception limits molecular flux via plasmodesmata. *Proceedings of the National Academy of Sciences of the United States of America* **110**, 9166-9170.
- Felix, G., Regenass, M., and Boller, T.** (1993). Specific perception of subnanomolar concentrations of chitin fragments by tomato cells: induction of extracellular alkalinization, changes in protein phosphorylation, and establishment of a refractory state. *The Plant Journal* **4**, 307-316.
- Felix, G., Duran, J.D., Volko, S., and Boller, T.** (1999). Plants have a sensitive perception system for the most conserved domain of bacterial flagellin. *The Plant journal : for cell and molecular biology* **18**, 265-276.
- Feng, F., and Zhou, J.M.** (2012). Plant-bacterial pathogen interactions mediated by type III effectors. *Current Opinion in Plant Biology* **15**, 469-476.
- Fliegmann, J., Mithofer, A., Wanner, G., and Ebel, J.** (2004). An ancient enzyme domain hidden in the putative beta-glucan elicitor receptor of soybean may play an active part in the perception of pathogen-associated molecular patterns during broad host resistance. *The Journal of biological chemistry* **279**, 1132-1140.
- Flor, H.H.** (1971). Current Status of Gene-for-Gene Concept. *Annual review of phytopathology* **9**, 275-+.
- Fujikawa, T., Kuga, Y., Yano, S., Yoshimi, A., Tachiki, T., Abe, K., and Nishimura, M.** (2009). Dynamics of cell wall components of *Magnaporthe grisea* during infectious structure development. *Molecular microbiology* **73**, 553-570.

- Fujimoto, Y., and Fukase, K.** (2011). Structures, synthesis, and human Nod1 stimulation of immunostimulatory bacterial peptidoglycan fragments in the environment. *Journal of natural products* **74**, 518-525.
- Gao, X., Chen, X., Lin, W., Chen, S., Lu, D., Niu, Y., Li, L., Cheng, C., McCormack, M., Sheen, J., Shan, L., and He, P.** (2013). Bifurcation of Arabidopsis NLR immune signaling via Ca<sup>2+</sup>(+)-dependent protein kinases. *PLoS pathogens* **9**, e1003127.
- Gehrig, H., Schussler, A., and Kluge, M.** (1996). Geosiphon pyriforme, a fungus forming endocytobiosis with Nostoc (cyanobacteria), is an ancestral member of the Glomales: evidence by SSU rRNA analysis. *Journal of molecular evolution* **43**, 71-81.
- Gelius, E., Persson, C., Karlsson, J., and Steiner, H.** (2003). A mammalian peptidoglycan recognition protein with N-acetylmuramoyl-L-alanine amidase activity. *Biochem Biophys Res Commun* **306**, 988-994.
- Girardin, S.E., Boneca, I.G., Viala, J., Chamaillard, M., Labigne, A., Thomas, G., Philpott, D.J., and Sansonetti, P.J.** (2003). Nod2 is a general sensor of peptidoglycan through muramyl dipeptide (MDP) detection. *The Journal of biological chemistry* **278**, 8869-8872.
- Glauner, B., Holtje, J.V., and Schwarz, U.** (1988). The composition of the murein of Escherichia coli. *The Journal of biological chemistry* **263**, 10088-10095.
- Göhre, V., Spallek, T., Haweker, H., Mersmann, S., Mentzel, T., Boller, T., de Torres, M., Mansfield, J.W., and Robatzek, S.** (2008). Plant pattern-recognition receptor FLS2 is directed for degradation by the bacterial ubiquitin ligase AvrPtoB. *Current biology : CB* **18**, 1824-1832.
- Gomez-Gomez, L., and Boller, T.** (2000). FLS2: An LRR receptor-like kinase involved in the perception of the bacterial elicitor flagellin in Arabidopsis. *Mol Cell* **5**, 1003-1011.
- Goodell, E.W., and Schwarz, U.** (1985). Release of cell wall peptides into culture medium by exponentially growing Escherichia coli. *Journal of bacteriology* **162**, 391-397.
- Goormachtig, S., Lievens, S., Van de Velde, W., Van Montagu, M., and Holsters, M.** (1998). Srchi13, a novel early nodulin from Sesbania rostrata, is related to acidic class III chitinases. *The Plant cell* **10**, 905-915.
- Gottwald, T.R., and Graham, J.H.** (1992). A Device for Precise and Nondisruptive Stomatal Inoculation of Leaf Tissue with Bacterial Pathogens. *Phytopathology* **82**, 930-935.
- Grabherr, H.M.** (2011). Characterisation of the role of LysM receptor-like kinases and the CHIA chitinase in the perception of peptidoglycan and in the innate immunity of Arabidopsis thaliana. In *Mathematisch-Naturwissenschaftlichen Fakultät (Tübingen: Eberhard Karls Universität Tübingen)*.
- Graham, L.S., and Sticklen, M.B.** (1994). Plant Chitinases. *Can J Bot* **72**, 1057-1083.
- Grover, A.** (2012). Plant Chitinases: Genetic Diversity and Physiological Roles. *Crit Rev Plant Sci* **31**, 57-73.
- Guan, R., and Mariuzza, R.A.** (2007). Peptidoglycan recognition proteins of the innate immune system. *Trends in microbiology* **15**, 127-134.
- Guan, R., Wang, Q., Sundberg, E.J., and Mariuzza, R.A.** (2005). Crystal structure of human peptidoglycan recognition protein S (PGRP-S) at 1.70 Å resolution. *Journal of molecular biology* **347**, 683-691.
- Gust, A.A., Biswas, R., Lenz, H.D., Rauhut, T., Ranf, S., Kemmerling, B., Gotz, F., Glawischnig, E., Lee, J., Felix, G., and Nürnberger, T.** (2007). Bacteria-derived peptidoglycans constitute pathogen-associated molecular patterns triggering innate immunity in Arabidopsis. *J Biol Chem* **282**, 32338-32348.
- Ham, J.H., Kim, M.G., Lee, S.Y., and Mackey, D.** (2007). Layered basal defenses underlie non-host resistance of Arabidopsis to Pseudomonas syringae pv. phaseolicola. *The Plant journal : for cell and molecular biology* **51**, 604-616.
- Hamid, R., Khan, M.A., Ahmad, M., Ahmad, M.M., Abidin, M.Z., Musarrat, J., and Javed, S.** (2013). Chitinases: An update. *Journal of pharmacy & bioallied sciences* **5**, 21-29.

- Hann, D.R., and Rathjen, J.P.** (2007). Early events in the pathogenicity of *Pseudomonas syringae* on *Nicotiana benthamiana*. *The Plant journal : for cell and molecular biology* **49**, 607-618.
- Harper, J.F., Breton, G., and Harmon, A.** (2004). Decoding Ca<sup>2+</sup> signals through plant protein kinases. *Annual review of plant biology* **55**, 263-288.
- Hayafune, M., Berisio, R., Marchetti, R., Silipo, A., Kayama, M., Desaki, Y., Arima, S., Squeglia, F., Ruggiero, A., Tokuyasu, K., Molinaro, A., Kaku, H., and Shibuya, N.** (2014). Chitin-induced activation of immune signaling by the rice receptor CEBiP relies on a unique sandwich-type dimerization. *Proc Natl Acad Sci U S A* **111**, E404-413.
- Heil, M., and Baldwin, I.T.** (2002). Fitness costs of induced resistance: emerging experimental support for a slippery concept. *Trends in plant science* **7**, 61-67.
- Henrissat, B.** (1991). A classification of glycosyl hydrolases based on amino acid sequence similarities. *Biochem J* **280 ( Pt 2)**, 309-316.
- Henry, G., Thonart, P., and Ongena, M.** (2012). PAMPs, MAMPs, DAMPs and others: an update on the diversity of plant immunity elicitors. *Biotechnol Agron Soc* **16**, 257-268.
- Hogenhout, S.A., Van der Hoorn, R.A.L., Terauchi, R., and Kamoun, S.** (2009). Emerging Concepts in Effector Biology of Plant-Associated Organisms. *Mol Plant Microbe In* **22**, 115-122.
- Huckelhoven, R.** (2007). Cell wall-associated mechanisms of disease resistance and susceptibility. *Annual review of phytopathology* **45**, 101-127.
- Huffaker, A., Pearce, G., and Ryan, C.A.** (2006). An endogenous peptide signal in *Arabidopsis* activates components of the innate immune response. *Proceedings of the National Academy of Sciences of the United States of America* **103**, 10098-10103.
- Inohara, Chamailard, McDonald, C., and Nunez, G.** (2005). NOD-LRR proteins: role in host-microbial interactions and inflammatory disease. *Annual review of biochemistry* **74**, 355-383.
- Jehle, A.K., Lipschis, M., Albert, M., Fallahzadeh-Mamaghani, V., Furst, U., Mueller, K., and Felix, G.** (2013). The Receptor-Like Protein ReMAX of *Arabidopsis* Detects the Microbe-Associated Molecular Pattern eMax from *Xanthomonas*. *The Plant cell* **25**, 2330-2340.
- Jeworutzki, E., Roelfsema, M.R.G., Anschutz, U., Krol, E., Elzenga, J.T.M., Felix, G., Boller, T., Hedrich, R., and Becker, D.** (2010). Early signaling through the *Arabidopsis* pattern recognition receptors FLS2 and EFR involves Ca<sup>2+</sup>-associated opening of plasma membrane anion channels. *Plant Journal* **62**, 367-378.
- Johnsson, N., and Varshavsky, A.** (1994). Split ubiquitin as a sensor of protein interactions in vivo. *Proceedings of the National Academy of Sciences of the United States of America* **91**, 10340-10344.
- Jones, J.D., and Dangl, J.L.** (2006). The plant immune system. *Nature* **444**, 323-329.
- Jovin, T.M.** (1973). Multiphasic zone electrophoresis, IV. Design and analysis of discontinuous buffer systems with a digital computer. *Annals of the New York Academy of Sciences* **209**, 477-496.
- Kadota, Y., Sklenar, J., Derbyshire, P., Stransfeld, L., Asai, S., Ntoukakis, V., Jones, J.D., Shirasu, K., Menke, F., Jones, A., and Zipfel, C.** (2014). Direct regulation of the NADPH oxidase RBOHD by the PRR-associated kinase BIK1 during plant immunity. *Mol Cell* **54**, 43-55.
- Kaku, H., Nishizawa, Y., Ishii-Minami, N., Akimoto-Tomiyama, C., Dohmae, N., Takio, K., Minami, E., and Shibuya, N.** (2006). Plant cells recognize chitin fragments for defense signaling through a plasma membrane receptor. *Proceedings of the National Academy of Sciences of the United States of America* **103**, 11086-11091.
- Kasprzewska, A.** (2003). Plant chitinases - Regulation and function. *Cell Mol Biol Lett* **8**, 809-824.
- Kauss, H., Fauth, M., Merten, A., and Jeblick, W.** (1999). Cucumber hypocotyls respond to cutin monomers via both an inducible and a constitutive H<sub>2</sub>O<sub>2</sub>-generating system. *Plant physiology* **120**, 1175-1182.

- Kelley, L.A., and Sternberg, M.J.E.** (2009). Protein structure prediction on the Web: a case study using the Phyre server. *Nat Protoc* **4**, 363-371.
- Kemmerling, B., Schwedt, A., Rodriguez, P., Mazzotta, S., Frank, M., Qamar, S.A., Mengiste, T., Betsuyaku, S., Parker, J.E., Mussig, C., Thomma, B.P., Albrecht, C., de Vries, S.C., Hirt, H., and Nurnberger, T.** (2007). The BRI1-associated kinase 1, BAK1, has a brassinolide-independent role in plant cell-death control. *Current biology : CB* **17**, 1116-1122.
- Kim, M.S., Byun, M., and Oh, B.H.** (2003). Crystal structure of peptidoglycan recognition protein LB from *Drosophila melanogaster*. *Nat Immunol* **4**, 787-793.
- Kombrink, A., Sanchez-Vallet, A., and Thomma, B.P.** (2011). The role of chitin detection in plant-pathogen interactions. *Microbes and infection / Institut Pasteur* **13**, 1168-1176.
- Kouzai, Y., Mochizuki, S., Nakajima, K., Desaki, Y., Hayafune, M., Miyazaki, H., Yokotani, N., Ozawa, K., Minami, E., Kaku, H., Shibuya, N., and Nishizawa, Y.** (2014). Targeted gene disruption of OsCERK1 reveals its indispensable role in chitin perception and involvement in the peptidoglycan response and immunity in rice. *Molecular plant-microbe interactions : MPMI* **27**, 975-982.
- Kroon, L.P.N.M., Brouwer, H., de Cock, A.W.A.M., and Govers, F.** (2011). The Genus *Phytophthora* Anno 2012. *Phytopathology* **102**, 348-364.
- Kumar, S., Ingle, H., Prasad, D.V., and Kumar, H.** (2013). Recognition of bacterial infection by innate immune sensors. *Crit Rev Microbiol* **39**, 229-246.
- Kurata, S.** (2014). Peptidoglycan recognition proteins in *Drosophila* immunity. *Developmental and comparative immunology* **42**, 36-41.
- Kwon, H.K., Yokoyama, R., and Nishitani, K.** (2005). A proteomic approach to apoplastic proteins involved in cell wall regeneration in protoplasts of *Arabidopsis* suspension-cultured cells. *Plant Cell Physiol* **46**, 843-857.
- Laemmli, U.K.** (1970). Cleavage of structural proteins during the assembly of the head of bacteriophage T4. *Nature* **227**, 680-685.
- Lajunen, H.M.** (2011). Characterisation of the role of LysM receptor-like kinases and the CHIA chitinase in the perception of peptidoglycan and in the innate immunity of *Arabidopsis thaliana*. In *Mathematisch-Naturwissenschaftlichen Fakultät (Tübingen: Eberhard Karls Universität Tübingen)*.
- Lazarovits, G., and Higgins, V.J.** (1976). Histological Comparison of *Cladosporium-Fulvum* Race 1 on Immune, Resistant, and Susceptible Tomato Varieties. *Can J Bot* **54**, 224-234.
- Lecourieux, D., Ranjeva, R., and Pugin, A.** (2006). Calcium in plant defence-signalling pathways. *New Phytol* **171**, 249-269.
- Lee, J., Klusener, B., Tsiamis, G., Stevens, C., Neyt, C., Tampakaki, A.P., Panopoulos, N.J., Noller, J., Weiler, E.W., Cornelis, G.R., Mansfield, J.W., and Nurnberger, T.** (2001). HrpZ(Psph) from the plant pathogen *Pseudomonas syringae* pv. *phaseolicola* binds to lipid bilayers and forms an ion-conducting pore in vitro. *Proceedings of the National Academy of Sciences of the United States of America* **98**, 289-294.
- Li, X., Lin, H., Zhang, W., Zou, Y., Zhang, J., Tang, X., and Zhou, J.M.** (2005). Flagellin induces innate immunity in nonhost interactions that is suppressed by *Pseudomonas syringae* effectors. *Proceedings of the National Academy of Sciences of the United States of America* **102**, 12990-12995.
- Liu, B., Li, J.F., Ao, Y., Qu, J., Li, Z., Su, J., Zhang, Y., Liu, J., Feng, D., Qi, K., He, Y., Wang, J., and Wang, H.B.** (2012a). Lysin motif-containing proteins LYP4 and LYP6 play dual roles in peptidoglycan and chitin perception in rice innate immunity. *The Plant cell* **24**, 3406-3419.
- Liu, T., Liu, Z., Song, C., Hu, Y., Han, Z., She, J., Fan, F., Wang, J., Jin, C., Chang, J., Zhou, J.M., and Chai, J.** (2012b). Chitin-induced dimerization activates a plant immune receptor. *Science* **336**, 1160-1164.

- Liu, X., Grabherr, H.M., Willmann, R., Kolb, D., Brunner, F., Bertsche, U., Kuhner, D., Franz-Wachtel, M., Amin, B., Felix, G., Ongena, M., Nurnberger, T., and Gust, A.A. (2014). Host-induced bacterial cell wall decomposition mediates pattern-triggered immunity in Arabidopsis. *eLife* **3**.
- Livak, K.J., and Schmittgen, T.D. (2001). Analysis of relative gene expression data using real-time quantitative PCR and the 2<sup>-</sup>(Delta Delta C(T)) Method. *Methods* **25**, 402-408.
- Lu, X., Wang, M., Qi, J., Wang, H., Li, X., Gupta, D., and Dziarski, R. (2006). Peptidoglycan recognition proteins are a new class of human bactericidal proteins. *The Journal of biological chemistry* **281**, 5895-5907.
- Macho, A.P., and Zipfel, C. (2014). Plant PRRs and the Activation of Innate Immune Signaling. *Mol Cell* **54**, 263-272.
- Mackey, D., and McFall, A.J. (2006). MAMPs and MIMPs: proposed classifications for inducers of innate immunity. *Molecular microbiology* **61**, 1365-1371.
- Mackowiak, P.A. (1984). Relationship between Growth Temperature and Shedding of Lipopolysaccharides by Gram-Negative Bacilli. *Eur J Clin Microbiol* **3**, 406-410.
- Marshall, R., Kombrink, A., Motteram, J., Loza-Reyes, E., Lucas, J., Hammond-Kosack, K.E., Thomma, B.P., and Rudd, J.J. (2011). Analysis of two in planta expressed LysM effector homologs from the fungus *Mycosphaerella graminicola* reveals novel functional properties and varying contributions to virulence on wheat. *Plant physiology* **156**, 756-769.
- Martin, G.B., Brommonschenkel, S.H., Chunwongse, J., Frary, A., Ganai, M.W., Spivey, R., Wu, T., Earle, E.D., and Tanksley, S.D. (1993). Map-based cloning of a protein kinase gene conferring disease resistance in tomato. *Science* **262**, 1432-1436.
- Martin, M.L., and Busconi, L. (2000). Membrane localization of a rice calcium-dependent protein kinase (CDPK) is mediated by myristoylation and palmitoylation. *The Plant journal : for cell and molecular biology* **24**, 429-435.
- McGuinness, D.H., Dehal, P.K., and Pleass, R.J. (2003). Pattern recognition molecules and innate immunity to parasites. *Trends Parasitol* **19**, 312-319.
- Medzhitov, R., and Janeway, C.A., Jr. (1997). Innate immunity: the virtues of a nonclonal system of recognition. *Cell* **91**, 295-298.
- Medzhitov, R., and Janeway, C.A., Jr. (2002). Decoding the patterns of self and nonself by the innate immune system. *Science* **296**, 298-300.
- Melotto, M., Underwood, W., Koczan, J., Nomura, K., and He, S.Y. (2006). Plant stomata function in innate immunity against bacterial invasion. *Cell* **126**, 969-980.
- Mentlak, T.A., Kombrink, A., Shinya, T., Ryder, L.S., Otomo, I., Saitoh, H., Terauchi, R., Nishizawa, Y., Shibuya, N., Thomma, B.P., and Talbot, N.J. (2012). Effector-Mediated Suppression of Chitin-Triggered Immunity by *Magnaporthe oryzae* Is Necessary for Rice Blast Disease. *The Plant cell* **24**, 322-335.
- Mergaert, P., Van Montagu, M., and Holsters, M. (1997). Molecular mechanisms of Nod factor diversity. *Molecular microbiology* **25**, 811-817.
- Mithöfer, A., Fliegmann, J., Neuhaus-Url, G., Schwarz, H., and Ebel, J. (2000). The hepta-beta-glucoside elicitor-binding proteins from legumes represent a putative receptor family. *Biol Chem* **381**, 705-713.
- Miya, A., Albert, P., Shinya, T., Desaki, Y., Ichimura, K., Shirasu, K., Narusaka, Y., Kawakami, N., Kaku, H., and Shibuya, N. (2007). CERK1, a LysM receptor kinase, is essential for chitin elicitor signaling in Arabidopsis. *Proceedings of the National Academy of Sciences of the United States of America* **104**, 19613-19618.
- Monaghan, J., and Zipfel, C. (2012). Plant pattern recognition receptor complexes at the plasma membrane. *Curr Opin Plant Biol* **15**, 349-357.

- Monaghan, J., Matschi, S., Shorinola, O., Rovenich, H., Matei, A., Segonzac, C., Malinovsky, F.G., Rathjen, J.P., MacLean, D., Romeis, T., and Zipfel, C. (2014). The calcium-dependent protein kinase CPK28 buffers plant immunity and regulates BIK1 turnover. *Cell Host Microbe* **16**, 605-615.
- Muller-Anstett, M.A., Muller, P., Albrecht, T., Nega, M., Wagener, J., Gao, Q., Kaesler, S., Schaller, M., Biedermann, T., and Gotz, F. (2010). Staphylococcal peptidoglycan co-localizes with Nod2 and TLR2 and activates innate immune response via both receptors in primary murine keratinocytes. *PloS one* **5**, e13153.
- Nagpure, A., Choudhary, B., and Gupta, R.K. (2014). Chitinases: in agriculture and human healthcare. *Crit Rev Biotechnol* **34**, 215-232.
- Nakagawa, T., Kurose, T., Hino, T., Tanaka, K., Kawamukai, M., Niwa, Y., Toyooka, K., Matsuoka, K., Jinbo, T., and Kimura, T. (2007). Development of series of gateway binary vectors, pGWBs, for realizing efficient construction of fusion genes for plant transformation. *J Biosci Bioeng* **104**, 34-41.
- Navarro, L., Jay, F., Nomura, K., He, S.Y., and Voinnet, O. (2008). Suppression of the microRNA pathway by bacterial effector proteins. *Science* **321**, 964-967.
- Newman, M.A., Sundelin, T., Nielsen, J.T., and Erbs, G. (2013). MAMP (microbe-associated molecular pattern) triggered immunity in plants. *Front Plant Sci* **4**, 139.
- Nicaise, V., Roux, M., and Zipfel, C. (2009). Recent advances in PAMP-triggered immunity against bacteria: pattern recognition receptors watch over and raise the alarm. *Plant physiology* **150**, 1638-1647.
- Nigro, G., Fazio, L.L., Martino, M.C., Rossi, G., Tattoli, I., Liparoti, V., De Castro, C., Molinaro, A., Philpott, D.J., and Bernardini, M.L. (2008). Muramylpeptide shedding modulates cell sensing of *Shigella flexneri*. *Cell Microbiol* **10**, 682-695.
- Nürnbergger, T. (1999). Signal perception in plant pathogen defense. *Cell Mol Life Sci* **55**, 167-182.
- Nürnbergger, T., and Brunner, F. (2002a). Innate immunity in plants and animals: emerging parallels between the recognition of general elicitors and pathogen-associated molecular patterns. *Curr Opin Plant Biol* **5**, 318-324.
- Nürnbergger, T., and Brunner, F. (2002b). Innate immunity in plants and animals: emerging parallels between the recognition of general elicitors and pathogen-associated molecular patterns. *Curr Opin Plant Biol* **5**, 318-324.
- Nürnbergger, T., and Kemmerling, B. (2009). PAMP-Triggered Basal Immunity in Plants. *Adv Bot Res* **51**, 1-38.
- Nürnbergger, T., Brunner, F., Kemmerling, B., and Piater, L. (2004). Innate immunity in plants and animals: striking similarities and obvious differences. *Immunol Rev* **198**, 249-266.
- Obrdlik, P., El-Bakkoury, M., Hamacher, T., Cappellaro, C., Vilarino, C., Fleischer, C., Ellerbrok, H., Kamuzinzi, R., Ledent, V., Blaudez, D., Sanders, D., Revuelta, J.L., Boles, E., Andre, B., and Frommer, W.B. (2004). K<sup>+</sup> channel interactions detected by a genetic system optimized for systematic studies of membrane protein interactions. *Proceedings of the National Academy of Sciences of the United States of America* **101**, 12242-12247.
- Park, J.T., and Uehara, T. (2008). How bacteria consume their own exoskeletons (turnover and recycling of cell wall peptidoglycan). *Microbiology and molecular biology reviews : MMBR* **72**, 211-227, table of contents.
- Park, S.M., Kim, D.H., Truong, N.H., and Itoh, Y. (2002). Heterologous expression and characterization of class III chitinases from rice (*Oryza sativa* L.) *Enzyme Microb Tech* **30**, 697-702.
- Passarinho, P.A., and de Vries, S.C. (2002). Arabidopsis Chitinases: a Genomic Survey. *The Arabidopsis Book*, e0023.
- Pel, M.J., and Pieterse, C.M. (2013). Microbial recognition and evasion of host immunity. *J Exp Bot* **64**, 1237-1248.

- Ranf, S., Gisch, N., Schaffer, M., Illig, T., Westphal, L., Knirel, Y.A., Sanchez-Carballo, P.M., Zahringer, U., Huckelhoven, R., Lee, J., and Scheel, D. (2015). A lectin S-domain receptor kinase mediates lipopolysaccharide sensing in *Arabidopsis thaliana*. *Nat Immunol* **16**, 426-433.
- Reina-Pinto, J.J., and Yephremov, A. (2009). Surface lipids and plant defenses. *Plant Physiol Bioch* **47**, 540-549.
- Reiser, J.B., Teyton, L., and Wilson, I.A. (2004). Crystal structure of the *Drosophila* peptidoglycan recognition protein (PGRP)-SA at 1.56 Å resolution. *Journal of molecular biology* **340**, 909-917.
- Reith, J., and Mayer, C. (2011). Peptidoglycan turnover and recycling in Gram-positive bacteria. *Applied microbiology and biotechnology* **92**, 1-11.
- Ride, J.P., and Barber, M.S. (1990). Purification and Characterization of Multiple Forms of Endochitinase from Wheat Leaves. *Plant Sci* **71**, 185-197.
- Romeis, T., and Herde, M. (2014). From local to global: CDPKs in systemic defense signaling upon microbial and herbivore attack. *Curr Opin Plant Biol* **20**, 1-10.
- Ronald, P.C., and Beutler, B. (2010). Plant and Animal Sensors of Conserved Microbial Signatures. *Science* **330**, 1061-1064.
- Sakthivel, M., Karthikeyan, N., and Palani, P. (2010). Detection and analysis of lysozyme activity in some tuberous plants and *Calotropis procera*'s latex. *Journal of Phytology* **2**, 65-72.
- Samac, D.A., and Shah, D.M. (1991). Developmental and Pathogen-Induced Activation of the *Arabidopsis* Acidic Chitinase Promoter. *The Plant cell* **3**, 1063-1072.
- Samac, D.A., and Shah, D.M. (1994). Effect of chitinase antisense RNA expression on disease susceptibility of *Arabidopsis* plants. *Plant molecular biology* **25**, 587-596.
- Samac, D.A., Hironaka, C.M., Yallaly, P.E., and Shah, D.M. (1990). Isolation and Characterization of the Genes Encoding Basic and Acidic Chitinase in *Arabidopsis thaliana*. *Plant physiology* **93**, 907-914.
- Sanchez-Vallet, A., Mesters, J.R., and Thomma, B.P. (2015). The battle for chitin recognition in plant-microbe interactions. *Fems Microbiol Rev* **39**, 171-183.
- Sanchez-Vallet, A., Saleem-Batcha, R., Kombrink, A., Hansen, G., Valkenburg, D.J., Thomma, B.P.H.J., and Mesters, J.R. (2013). Fungal effector Ecp6 outcompetes host immune receptor for chitin binding through intrachain LysM dimerization. *eLife* **2**.
- Santos, P., Fortunato, A., Ribeiro, A., and Pawlowski, K. (2008). Chitinases in root nodules. *Plant Biotechnol* **25**, 299-307.
- Schaffler, H., Demircioglu, D.D., Kuhner, D., Menz, S., Bender, A., Autenrieth, I.B., Bodammer, P., Lamprecht, G., Gotz, F., and Frick, J.S. (2014). NOD2 stimulation by *Staphylococcus aureus*-derived peptidoglycan is boosted by Toll-like receptor 2 costimulation with lipoproteins in dendritic cells. *Infection and immunity* **82**, 4681-4688.
- Schenk, P.M., Carvalhais, L.C., and Kazan, K. (2012). Unraveling plant-microbe interactions: can multi-species transcriptomics help? *Trends in biotechnology* **30**, 177-184.
- Schleifer, K.H., and Kandler, O. (1972). Peptidoglycan types of bacterial cell walls and their taxonomic implications. *Bacteriol Rev* **36**, 407-477.
- Schlumbaum, A., Mauch, F., Vögeli, U., and Boller, T. (1886). Plant chitinases are potent inhibitors of fungal growth. *Nature* **324**, 365-367.
- Schwab, R., Ossowski, S., Riester, M., Warthmann, N., and Weigel, D. (2006). Highly specific gene silencing by artificial microRNAs in *Arabidopsis*. *The Plant cell* **18**, 1121-1133.
- Schwab, R., Palatnik, J.F., Riester, M., Schommer, C., Schmid, M., and Weigel, D. (2005). Specific effects of microRNAs on the plant transcriptome. *Dev Cell* **8**, 517-527.
- Senthil-Kumar, M., and Mysore, K.S. (2013). Nonhost resistance against bacterial pathogens: retrospectives and prospects. *Annual review of phytopathology* **51**, 407-427.
- Shahidi, F., and Abuzaytoun, R. (2005). Chitin, chitosan, and co-products: chemistry, production, applications, and health effects. *Advances in food and nutrition research* **49**, 93-135.

- Sharp, J.K., Valent, B., and Albersheim, P. (1984). Host-Pathogen Interactions .26. Purification and Partial Characterization of a Beta-Glucan Fragment That Elicits Phytoalexin Accumulation in Soybean. *Journal of Biological Chemistry* **259**, 1312-1320.
- Shinya, T., Yamaguchi, K., Desaki, Y., Yamada, K., Narisawa, T., Kobayashi, Y., Maeda, K., Suzuki, M., Tanimoto, T., Takeda, J., Nakashima, M., Funama, R., Narusaka, M., Narusaka, Y., Kaku, H., Kawasaki, T., and Shibuya, N. (2014). Selective regulation of the chitin-induced defense response by the Arabidopsis receptor-like cytoplasmic kinase PBL27. *The Plant journal : for cell and molecular biology* **79**, 56-66.
- Sohn, K.H., Saucet, S.B., Clarke, C.R., Vinatzer, B.A., O'Brien, H.E., Guttman, D.S., and Jones, J.D.G. (2012). HopAS1 recognition significantly contributes to Arabidopsis nonhost resistance to *Pseudomonas syringae* pathogens. *New Phytol* **193**, 58-66.
- Stagljar, I., Korostensky, C., Johnsson, N., and te Heesen, S. (1998). A genetic system based on split-ubiquitin for the analysis of interactions between membrane proteins in vivo. *Proceedings of the National Academy of Sciences of the United States of America* **95**, 5187-5192.
- Sun, Y., Li, L., Macho, A.P., Han, Z., Hu, Z., Zipfel, C., Zhou, J.M., and Chai, J. (2013). Structural basis for flg22-induced activation of the Arabidopsis FLS2-BAK1 immune complex. *Science* **342**, 624-628.
- Takenaka, Y., Nakano, S., Tamoi, M., Sakuda, S., and Fukamizo, T. (2009). Chitinase gene expression in response to environmental stresses in Arabidopsis thaliana: chitinase inhibitor allosamidin enhances stress tolerance. *Bioscience, biotechnology, and biochemistry* **73**, 1066-1071.
- Tanabe, T., Kawase, T., Watanabe, T., Uchida, Y., and Mitsutomi, M. (2000). Purification and characterization of a 49-kDa chitinase from *Streptomyces griseus* HUT 6037. *J Biosci Bioeng* **89**, 27-32.
- Tanabe, T., Chamailard, M., Ogura, Y., Zhu, L., Qiu, S., Masumoto, J., Ghosh, P., Moran, A., Predergast, M.M., Tromp, G., Williams, C.J., Inohara, N., and Nunez, G. (2004). Regulatory regions and critical residues of NOD2 involved in muramyl dipeptide recognition. *Embo J* **23**, 1587-1597.
- Teh, O.K., and Moore, I. (2007). An ARF-GEF acting at the Golgi and in selective endocytosis in polarized plant cells. *Nature* **448**, 493-496.
- Tena, G., Boudsocq, M., and Sheen, J. (2011). Protein kinase signaling networks in plant innate immunity. *Curr Opin Plant Biol* **14**, 519-529.
- Terwisscha van Scheltinga, A.C., Kalk, K.H., Beintema, J.J., and Dijkstra, B.W. (1994). Crystal structures of hevamine, a plant defence protein with chitinase and lysozyme activity, and its complex with an inhibitor. *Structure* **2**, 1181-1189.
- Thaler, J.S., Fidantsef, A.L., Duffey, S.S., and Bostock, R.M. (1999). Trade-offs in plant defense against pathogens and herbivores: A field demonstration of chemical elicitors of induced resistance. *Journal of chemical ecology* **25**, 1597-1609.
- Thomma, B.P., Nurnberger, T., and Joosten, M.H. (2011). Of PAMPs and effectors: the blurred PTI-ETI dichotomy. *The Plant cell* **23**, 4-15.
- Tsuji, H., Nishimura, S., Inui, T., Kado, Y., Ishikawa, K., Nakamura, T., and Uegaki, K. (2010). Kinetic and crystallographic analyses of the catalytic domain of chitinase from *Pyrococcus furiosus*- the role of conserved residues in the active site. *The FEBS journal* **277**, 2683-2695.
- Tyler, L., Bragg, J.N., Wu, J.J., Yang, X.H., Tuskan, G.A., and Vogel, J.P. (2010). Annotation and comparative analysis of the glycoside hydrolase genes in *Brachypodium distachyon*. *Bmc Genomics* **11**.
- van den Burg, H.A., Harrison, S.J., Joosten, M.H., Vervoort, J., and de Wit, P.J. (2006). *Cladosporium fulvum* Avr4 protects fungal cell walls against hydrolysis by plant chitinases accumulating during infection. *Molecular plant-microbe interactions : MPMI* **19**, 1420-1430.
- van Loon, L.C., Rep, M., and Pieterse, C.M. (2006). Significance of inducible defense-related proteins in infected plants. *Annual review of phytopathology* **44**, 135-162.

- Voinnet, O., Rivas, S., Mestre, P., and Baulcombe, D. (2003). An enhanced transient expression system in plants based on suppression of gene silencing by the p19 protein of tomato bushy stunt virus. *The Plant journal : for cell and molecular biology* **33**, 949-956.
- von Dach, S.W. (2006). The significance of spiritual values in the peace process in Colombia - An interview with Peter Stirnimann, Caritas Switzerland. *Mt Res Dev* **26**, 310-314.
- Wang, B., Yeun, L.H., Xue, J.Y., Liu, Y., Ane, J.M., and Qiu, Y.L. (2010). Presence of three mycorrhizal genes in the common ancestor of land plants suggests a key role of mycorrhizas in the colonization of land by plants. *New Phytol* **186**, 514-525.
- Wang, L., Weber, A.N., Atilano, M.L., Filipe, S.R., Gay, N.J., and Ligoxygakis, P. (2006). Sensing of Gram-positive bacteria in *Drosophila*: GGBP1 is needed to process and present peptidoglycan to PGRP-SA. *Embo J* **25**, 5005-5014.
- Wang, Z.M., Li, X., Cocklin, R.R., Wang, M., Fukase, K., Inamura, S., Kusumoto, S., Gupta, D., and Dziarski, R. (2003). Human peptidoglycan recognition protein-L is an N-acetylmuramoyl-L-alanine amidase. *The Journal of biological chemistry* **278**, 49044-49052.
- Weidel, W., and Pelzer, H. (1964). Bagshaped Macromolecules--a New Outlook on Bacterial Cell Walls. *Advances in enzymology and related areas of molecular biology* **26**, 193-232.
- Weljie, A.M., and Vogel, H.J. (2004). Unexpected structure of the Ca<sup>2+</sup>-regulatory region from soybean calcium-dependent protein kinase- $\alpha$ . *The Journal of biological chemistry* **279**, 35494-35502.
- Willmann, R., Lajunen, H.M., Erbs, G., Newman, M.A., Kolb, D., Tsuda, K., Katagiri, F., Fliegmann, J., Bono, J.J., Cullimore, J.V., Jehle, A.K., Gotz, F., Kulik, A., Molinaro, A., Lipka, V., Gust, A.A., and Nurnberger, T. (2011). Arabidopsis lysin-motif proteins LYM1 LYM3 CERK1 mediate bacterial peptidoglycan sensing and immunity to bacterial infection. *Proceedings of the National Academy of Sciences of the United States of America* **108**, 19824-19829.
- Xiao, F.M., Goodwin, S.M., Xiao, Y.M., Sun, Z.Y., Baker, D., Tang, X.Y., Jenks, M.A., and Zhou, J.M. (2004). Arabidopsis CYP86A2 represses *Pseudomonas syringae* type III genes and is required for cuticle development. *Embo J* **23**, 2903-2913.
- Yamaguchi, K., Yamada, K., Ishikawa, K., Yoshimura, S., Hayashi, N., Uchihashi, K., Ishihama, N., Kishi-Kaboshi, M., Takahashi, A., Tsuge, S., Ochiai, H., Tada, Y., Shimamoto, K., Yoshioka, H., and Kawasaki, T. (2013). A receptor-like cytoplasmic kinase targeted by a plant pathogen effector is directly phosphorylated by the chitin receptor and mediates rice immunity. *Cell Host Microbe* **13**, 347-357.
- Yokogawa, K., Kawata, S., Takemura, T., and Yoshimura, Y. (1975). Purification and properties of lytic enzymes from *Streptomyces globisporus* 1829. *Agric Biol Chem* **39**, 1533-1543.
- Yoo, S.D., Cho, Y.H., and Sheen, J. (2007). Arabidopsis mesophyll protoplasts: a versatile cell system for transient gene expression analysis. *Nat Protoc* **2**, 1565-1572.
- Zhang, J., Shao, F., Cui, H., Chen, L.J., Li, H.T., Zou, Y., Long, C.Z., Lan, L.F., Chai, J.J., Chen, S., Tang, X.Y., and Zhou, J.M. (2007a). A *Pseudomonas syringae* effector inactivates MAPKs to suppress PAMP-Induced immunity in plants. *Cell Host Microbe* **1**, 175-185.
- Zhang, J., Li, W., Xiang, T., Liu, Z., Laluk, K., Ding, X., Zou, Y., Gao, M., Zhang, X., Chen, S., Mengiste, T., Zhang, Y., and Zhou, J.M. (2010). Receptor-like cytoplasmic kinases integrate signaling from multiple plant immune receptors and are targeted by a *Pseudomonas syringae* effector. *Cell Host Microbe* **7**, 290-301.
- Zhang, L.S., Kars, I., Essenstam, B., Liebrand, T.W.H., Wagemakers, L., Elberse, J., Tagkalaki, P., Tjoitang, D., van den Ackerveken, G., and van Kan, J.A.L. (2014). Fungal Endopolygalacturonases Are Recognized as Microbe-Associated Molecular Patterns by the Arabidopsis Receptor-Like Protein RESPONSIVENESS TO BOTRYTIS POLYGALACTURONASES1. *Plant physiology* **164**, 352-364.
- Zhang, W.G., Fraiture, M., Kolb, D., Loffelhardt, B., Desaki, Y., Boutrot, F.F.G., Tor, M., Zipfel, C., Gust, A.A., and Brunner, F. (2013). Arabidopsis RECEPTOR-LIKE PROTEIN30 and Receptor-Like Kinase

- SUPPRESSOR OF BIR1-1/EVERSHED Mediate Innate Immunity to Necrotrophic Fungi. *The Plant cell* **25**, 4227-4241.
- Zhang, X.C., Wu, X., Findley, S., Wan, J., Libault, M., Nguyen, H.T., Cannon, S.B., and Stacey, G.** (2007b). Molecular evolution of lysin motif-type receptor-like kinases in plants. *Plant physiology* **144**, 623-636.
- Zhang, Z., and Thomma, B.P.H.J.** (2013). Structure-function Aspects of Extracellular Leucine-rich Repeat-containing Cell Surface Receptors in Plants. *J Integr Plant Biol* **55**, 1212-1223.
- Zipfel, C., Robatzek, S., Navarro, L., Oakeley, E.J., Jones, J.D.G., Felix, G., and Boller, T.** (2004). Bacterial disease resistance in Arabidopsis through flagellin perception. *Nature* **428**, 764-767.
- Zipfel, C., Kunze, G., Chinchilla, D., Caniard, A., Jones, J.D.G., Boller, T., and Felix, G.** (2006). Perception of the bacterial PAMP EF-Tu by the receptor EFR restricts Agrobacterium-mediated transformation. *Cell* **125**, 749-760.

## 8. Appendix.

Table 9. Oligonucleotides used in this study

Name	sequences	Tm	gene
EF1a-s	TCA CAT CAA CAT TGT GGT CAT TGG	59,3	<i>At1g07920/30/40</i>
EF1a-as	TTG ATC TGG TCA AGA GCC TAC AG	60,6	<i>At1g07920/30/40</i>
ef1a-100-f	GAGGCAGACTGTTGCAGTCG	61,4	<i>At1g07920/30/40</i>
ef1a-100-r	TCACTTCGCACCCTTCTTGA	57,3	<i>At1g07920/30/40</i>
FRK1-100-f	AGCGGTCAGATTTCAACAGT	55,3	<i>At2g19190</i>
FRK1-100-r	AAGACTATAAACATCACTCT	49,1	<i>At2g19190</i>
A-PRS300	CTG CAA GGC GAT TAA GTT GGG TAA C	63,0	amiRNA
B-PRS300	GCG GAT AAC AAT TTC ACA CAG GAA ACA G	63,7	amiRNA
oligo-dT	TTT TTT TTT TTT TTT TTT TT(AGC)	38,3	reverse transcription
Salk-Lba	TGG TTC ACG TAG TGG GCC ATC G	64,0	T-DNA/SALK line
Gabi-Kat-Lba	CCC ATT TGG ACG TGA ATG TAG ACA C	55,3	T-DNA/Gabi-Kat line
Wisc-Lba(P745)	AAC GTC CGC AAT GTG TTA TTA AGT TGT C	60,0	T-DNA/Wisc line
Sail_Lba	GCTTCCTATTATATCTTCCCAAATTACC	60,7	T-DNA/Sail line
At4g21940miRs-1	GATCTAACGTGTAAGTTTCCCTTCTCTTTTTGTATTCC	68,4	amiRNA of <i>At4g21940</i>
At4g21940miRa-1	AGAAGGGAAACTTTACACGTTAGATCAAAGAGAATCAATGA	67,4	amiRNA of <i>At4g21940</i>
At4g21940miR*s-1	GAAGAGAACTTTACTCGTTAGTTCACAGGTCGTGATATG	69,5	amiRNA of <i>At4g21940</i>
At4g21940miR*a-1	GAACTAACGAGTAAAGTTTCTTCTTACATATATATTCCT	65,3	amiRNA of <i>At4g21940</i>
At4g21940miRs-2	GATTAGTATCTAGTTTACGTCAGTCTCTTTTTGTATTCC	67,4	amiRNA of <i>At4g21940</i>
At4g21940miRa-2	GACTGACGTAAACTAGATACTAATCAAAGAGAATCAATGA	66,4	amiRNA of <i>At4g21940</i>

At4g21940miR*s-2	GACTAACGTAAACTACATACTATTACAGGTCGTGATATG	68,4	amiRNA of At4g21940
At4g21940miR*a-2	GAATAGTATGTAGTTTACGTTAGTCTACATATATATTCCT	64,3	amiRNA of At4g21940
At4g21940+2miRs	GATTTGAGCTATAATCCTACCGATCTCTCTTTTGTATTCC	68,4	amiRNA of At4g21940, At4g04720, At4g04740
At4g21940+2miRa	GATCGGTAGGATTATAGCTCAAATCAAAGAGAATCAATGA	67,4	
At4g21940+2miR*s	GATCAGTAGGATTATTGCTCAATTCACAGGTCGTGATATG	69,5	
At4g21940+2miR* a	GAATTGAGCAATAATCCTACTGATCTACATATATATTCCT	65,3	
Ha-r1	CTAAGCGCTGCACTGAGCAGCG	65,8	HA-tag
10myc-r1	CTAAGCACCGTTCAAGTCTTCC	60,3	myc-tag
gfp-r1	TTACTTGTACAGCTCGTCCATGCCG	64,6	gfp-tag
atrohd-f1	GAATTCATGAAAATGAGACGAGGCAA	60,1	at5g47910
atrohd-r1	GAAGTTCTCTTTGTGGAAGTCAAAC	59,7	at5g47910
atrbohd-r2	CGGAAGAAAGATAAGGAGGTGGTG	62,7	at5g47910
atrbohd-f2	GAGTGGTTCAAGGGAATAATGG	58,4	at5g47910
cpk15-fl-f1	CGCGGATCCATGGGTTGCTTTAGCAGC	69,5	at4g21940
cpk15-gm1-fl-r1	TTGGACTGGAAGAATTTCCCTTG	59,3	at4g21940
cpk15-vk-r1	AAAAGGCCTTTCTCCTCCTCTGATCCA	65,0	at4g21940
cpk15-gm2-fl-r1	GTTTAAGTCAGCAACTCTTTGCAC	59,7	at4g21940
cpk15-q-f1	GTCGATACAGATAACGATGGAAG	58,9	at4g21940
cpk15-q-r1	TTGTTGTGGCAGTGTGATACC	58,9	at4g21940
atrbohd-f	AAGAATTCATGAAAATGAGACGAGGCAA	60,7	at5g47910
atrbohd-r	AAGGATCCCTAGAAGTTCTCTTTGTGGAAGTC	66,9	at5g47910
cerk1-f1	ATGAAGCTAAAGATTTCTCTAATCGC	58,5	at3g61230
cerk1-r1	TAATGCACCATTTGGATCTCTTCC	59,3	at3g61230
Pjet-f	CGACTCACTATAGGGAGAGCGGC	66,0	pJET vector
pjet-r	AAGAACATCGATTTTCCATGGCAG	59,3	pJET vector

### 9 Acknowledgements

This study was carried out at the ZMBP and would never have been possible without help and support from my colleagues, friends and family.

First of all, I would like to thank my supervisor Dr. Andrea Gust for all your guidance and encouragement not only in the academic world but also the world outside. Thank you for providing me with this opportunity for my PhD study, introducing me into this magic world of plant pathology, supervising and supporting me during my PhD study.

Thanks to Prof. Thorsten Nürnberger for your supporting, encouragement and stimulating discussion. Thanks to Dr. Frederic Brunner for your suggestion for purification of active LYS1. Thanks to Prof. Georg Felix for the well-established cell culture system and Dr. Birgit Kemmerling for suggestions and discussions.

I would like to give my sincere appreciations to my colleagues in the biochemistry department and especially to N1 former members (Dr. Roland Willmann, Dr. Heini Grabherr, Dr. Weiguo Zhang, Dr. Eva Haller, Dr. Yoshitake Desaki, Franziska Fellermeier) and current members (Dagmar Kolb, Weilin Wan, Maria Schlöffel, Christina Feiler, Christoph Käsbauer). Thank you for your help, encouragement and advice.

I would express my thanks to collaborators and especially to Dr. Ute Bertsche and Daniel Kühner for HPLC analysis of PGN. Thanks to Dr. Mirita Franz-Wachtel and Prof. Hubert Kalbacher for protein MS analysis.

I also thank ZMBP central facilities for your technical support in microscopy, plant cultivation, and plant transformation. Thanks to Caterina Brancato for protoplast preparation.

I would thank SFB766 for financial support.

Finally, I am grateful to my family for your endless love and unconditional support. I wish to dedicate this thesis to my wife and my twin daughters. I sincerely appreciate my parents, sisters and my grandmother.

**10 Curriculum vitae**

**Name** Xiaokun Liu  
**Date of birth** 12.09.1972  
**Citizenship** P.R.China

**Education experience**

08/2011~present PhD student in Tuebingen University, Germany.  
 09/2010~07/2011 PhD student in Swedish Agriculture University, Sweden.  
 09/1998~07/2001 Master of Science in Zhongshan University, China.  
 09/1991~07/1995 Bachelor of Science in Anhui Normal University, China.

**Professional and Research experience**

08/2011~present PhD student, Tübingen University, Germany.  
 09/2010~07/2011 PhD student, Swedish Agriculture University, Sweden.  
 09/2003~08/2010 Research Officer in National University of Singapore, Singapore.  
 07/2001~09/2003 Project manager in Shanghai, China.  
 09/1998~07/2001 Master, Zhongshan University, China  
 09/1995~07/1998 Teacher, Shuiyang Middle school, China

**Publications**

1. **Liu X**, Grabherr HM, Willmann R, Kolb D, Brunner F, Bertsche U, Kühner D, Franz-Wachtel M, Amin B, Felix G, Ongena M, Nürnberger T, Gust AA.. Host-induced bacterial cell wall decomposition mediates pattern-triggered immunity in Arabidopsis. *Elife*. 2014 Jun 23:e01990
2. Latha Gandla M, Derba-Maceluch M, **Liu X**, Gerber L, Master ER, Mellerowicz EJ, Jönsson LJ Expression of a fungal glucuronoyl esterase in Populus: Effects on wood properties and saccharification efficiency. *Phytochemistry* 2014.06.002.
3. Y Hong and **Liu, XK** : Real time fluorescent PCR by labeled primer with a single fluorescent molecule. 2014, *PCR. Technology Current Innovations* 3rd edition, CRC press.

4. Wang CM<sup>1</sup>, Liu P, Yi C, Gu K, Sun F, Li L, Lo LC, **Liu X**, Feng F, Lin G, Cao S, Hong Y, Yin Z, Yue GH: A first generation microsatellite- and SNP-based linkage map of *Jatropha*. *PloS one*, 2011;6(8):e23632.
5. Yi CX, Zhang SL, **Liu XK**, Hong Y: Does epigenetic polymorphism contribute to phenotypic variances in *Jatropha curcas* L. *BMC Plant Biology* 2010, 10:259.
6. **Liu, XK**, HY Law, YM Tan and Y Hong: High-throughput  $\beta$ -thalassemia carrier screening by allele-specific Q-primer real-time polymerase chain reaction. *Analytical Biochemistry* 404: 97-99 (2010).
7. Yi, CX, J Zhang, KM Chan, **Liu XK** and Y Hong: Quantitative real-time PCR assay to detect transgenic copy number in cotton (*Gossypium hirsutum*). *Analytical Biochemistry* 375: 150-152 (2008).
8. **Liu, XK** and Y Hong: Q-priming PCR: A quantitative real-time PCR system using a self-quenched BODIPY FL-labeled primer. *Analytical Biochemistry* 360: 154-156 (2007).
9. Hong, DYQ, AJ Lau, CL Yeo, **XK Liu**, CR Yang, HL Koh and Y Hong: Genetic diversity and variation of saponin contents in *Panax notoginseng* roots from a single farm. *Journal of Agricultural and Food Chemistry* 53: 8460-8467 (2005).
10. Ao Chen-Qi, **Liu Xiao-Kun**. A simple method for preparing pollen specimen in light microscope. *Chinese Bulletin of Botany*. 18(2):251(2001).